

TR 84084

AD-A156 621

DTIC FILE COPY

UNLIMITED

BR95787  
TR 84084

②

ICAF Doc:

Number ~~1449~~

1441



ROYAL AIRCRAFT ESTABLISHMENT

Technical Report 84084

August 1984

**STANDARDISED FATIGUE LOADING  
SEQUENCES FOR HELICOPTER ROTORS  
(HELIX AND FELIX)**

**PART 1:  
BACKGROUND AND FATIGUE EVALUATION**

Compiled by

P. R. Edwards  
J. Darts

**DTIC**  
**ELECTE**  
JUL 17 1985  
**S** **D**  
**E**

Procurement Executive, Ministry of Defence  
Farnborough, Hants

R O Y A L   A I R C R A F T   E S T A B L I S H M E N T

Technical Report 84084

Received for printing 14 August 1984

STANDARDISED FATIGUE LOADING SEQUENCES FOR HELICOPTER  
ROTORS (HELIX AND FELIX)

PART 1: BACKGROUND AND FATIGUE EVALUATION

compiled by

P. R. Edwards

J. Darts

From work carried out by a Collaborative Group consisting additionally of:

G. Daske	MBB	J.B. de Jonge	NLR
M. Hück	IABG	H.G. Köbler	LBF
F. Och	MBB	D. Schütz	LBF
W. Schütz	IABG	M. Von Tapavicza	MBB
A.A. ten Have	NLR		

SUMMARY

Helix and Felix are standard loading sequences which relate to the main rotors of helicopters with articulated and semi-rigid rotors respectively. The purpose of the loading standards is, first, to provide a convenient tool for providing fatigue data under realistic loading, which can immediately be compared with data obtained by other organisations. Second, loading standards can be used to provide design data. This Report is the first of the two final project reports and describes the background to the definition of Helix and Felix, statistical content according to different counting methods and the results of fatigue tests used to assess them. Full information on generating Helix and Felix is not given in this Report, but is provided in Part 2.

Also published as

NLR Report No. TR 84043U Pt 1  
LBF Report No. FB-167 Pt 1  
IABG Report No. TF-1425/1

Departmental Reference: Materials/Structures 101

Copyright  
©

Controller HMSO London  
1984

# LIST OF CONTENTS

	<u>Page</u>
1 INTRODUCTION	5
2 USES AND CLASSES OF STANDARD SEQUENCES FOR HELICOPTERS	6
3 DESCRIPTION OF HELICOPTERS IN THE STUDY	7
4 ASSESSMENT OF BLADE LOAD SPECTRA TO ASSESS THE FEASIBILITY AND SCOPE OF THE STANDARDS	7
4.1 Introduction	7
4.2 Sea King loading data	8
4.3 CH-53 loading data	9
4.4 Comparison of CH-53 and Sea King loading spectra	9
4.5 Lynx loading data	10
4.6 BO-105 loading data	11
4.7 Comparison of BO-105 and Lynx spectra, between each other and with those for articulated rotors	11
5 METHOD OF GENERATING THE LOADING STANDARDS	12
6 DETAILS OF THE DERIVATION OF HELIX AND FELIX	14
6.1 Mix of sorties	14
6.2 Flight time for a sortie, number of sorties and their sequence	14
6.3 Definition of manoeuvres	15
6.4 Sequence of loads in a manoeuvre	16
6.5 Sequence and mix of manoeuvres in a sortie	16
6.6 Variation in lengths of a sortie	17
6.7 Transition between manoeuvres and magnitudes of ground loads	17
6.8 Shortened versions of Helix and Felix	18
7 STATISTICS OF HELIX AND FELIX	18
7.1 Basic form of the standards	19
7.2 Comparison of Helix and Felix spectra	19
7.3 Comparison of Helix and Felix spectra with operational data	19
7.4 Spectra for Helix and Felix with levels omitted	20
8 OUTLINE AND AIMS OF THE TEST PROGRAMME	21
8.1 Loading sequences used in the tests	21
8.2 Fatigue test specimens and materials	22
8.4 Fatigue test equipment and conditions	23
9 FATIGUE TEST RESULTS AND CUMULATIVE DAMAGE CALCULATIONS	23
9.1 Notched specimens of 3.1354-T3 aluminium alloy	24
9.2 Lug specimens of multidirectional GRP	24
9.3 Shear stress specimens of unidirectional GRP	26
9.4 Notched specimens of titanium alloy 6Al-4V	27
10 ASSESSMENT OF THE TEST RESULTS IN TERMS OF THE PROJECTED USES OF HELIX AND FELIX	28
10.1 Use as tools to obtain comparative fatigue data	28
10.2 Use as design data	29

LIST OF CONTENTS (concluded)

	<u>Page</u>
11 TESTING WITH SHORTENED VERSIONS OF THE STANDARDS	30
11.1 Test sequences	31
11.2 Fatigue test results	31
11.3 Recommendations for the use of shortened sequences	31
12 CONCLUSIONS	32
Appendix A Contributing organisations and acknowledgements	35
Appendix B Derivation of new system of units for Helix and Felix	36
Appendix C Assessment of suitable flight durations and sortie lengths	37
Tables 1 to 46	40
References	77
Illustrations	Figures 1-41
Report documentation page	inside back cover

Accession For	
NTIS GRA&I	<input checked="" type="checkbox"/>
DTIC TAB	<input type="checkbox"/>
Unannounced	<input type="checkbox"/>
Justification	
By	
Distribution/	
Availability Codes	
Dist	Avail and/or Special
A-1	



# 1 INTRODUCTION

A standard loading sequence is a variable amplitude repeated sequence of peak and trough loads to be applied in fatigue and crack propagation tests. Each standard represents loading on a particular class of engineering structure. Two such existing standards are FALSTAFF<sup>1,2</sup> (Fighter Aircraft Loading STandard For Fatigue evaluation) and TWIST<sup>2,3</sup> (Transport WIng Standard) which represent loading on fighter and transport aircraft wings respectively. Their development has arisen from the fact that, often, life prediction methods are not accurate enough to predict fatigue lives or crack rates adequately under service (variable amplitude) loading conditions. Therefore when making a fatigue assessment of, for instance, a new detail, fastening system or method of life improvement, variable amplitude loading has to be used. Often such tests are not tied specifically to any particular project, but are for more general application. In this case a standard sequence, provided a relevant one exists, is often the best choice for the test loading. The advantage of using standard sequences in this situation is that any resulting data can be compared directly with any other obtained using the same standard as well as being capable of being used as design data.

Experience has shown that, following the definition of a standard sequence, a wealth of relevant data accumulates quickly, negating the need for some tests and giving extensive comparative data for others. This can greatly increase the technical value of individual test results and reduce the amount of expensive fatigue testing. Large evaluation programmes using standard sequences can be shared more readily between different organisations and countries because the test results of the programme will be compatible with each organisation's own standard data.

This Report describes the derivation and fatigue assessment of two loading standards for the fatigue evaluation of helicopter rotor materials and components. The work followed an initial feasibility study<sup>3</sup>. The standards were developed as a collaborative study between West Germany, the Netherlands and UK. Details of the contributing organisations are given in Appendix A.

*Additional keywords: Statistical tests.*

As has become the practice the new loading standards have been given identifying names. For these the origin of the word helicopter (helix-spiral, pteron-wing from the Greek) has provided a convenient basis. The new standards are called:

Helix - Loading standard for 'hinged' or articulated rotors;

Felix - Loading standard for 'fixed' or semi-rigid rotors.

The second of the names proves to be particularly appropriate as an early pioneer in helicopter development was Felix Tournachon. Lower case lettering is adopted because the names Helix and Felix are not acronyms.

This Report does not contain full details of the final form of the two standards, only the background to their definition, statistical content according to different counting methods, and results of the fatigue tests used to assess them. A full description of the standards, including details required for their generation is given in Ref 4. It should be noted that Ref 4 and this Report constitute the final complete

summary of the Helix/Felix Project. They supersede Refs 5 and 6, the earlier Project Reports, which defined Helix in what should now be regarded as a provisional form and gave details of ongoing and planned fatigue tests. They supersede also Ref 7, which summarised the statistics and form of Helix and Felix and outlined the fatigue test programme.

The reason why the original published version of Helix should now be regarded as provisional is that, at a late stage in the Project, a simplification was made to Helix and Felix. The number of defined load levels was reduced to 31 for Helix and 33 for Felix, and the maximum load in each sequence was scaled to 100. The differences are described in Appendix B. This change was made in order to simplify analysis and generation of the standards, and to provide a more rational basis for plotting test results. Thus the final defined version of Helix described in this Report and in Ref 4 differs in detail from that published in Ref 5. Also the original versions of the standards were used for the fatigue tests described in this Report. The changes made are small in terms of the predicted effect on fatigue life and should not affect the relevance of the fatigue test results. However the changes are considerable in reducing complication when using the standards, and the earlier versions are now obsolete.

## 2 USES AND CLASSES OF STANDARD SEQUENCES FOR HELICOPTERS

The basis for the use of standard sequences is that they should be representative of loads on a class of engineering structures. As described in section 1 they are primarily a tool for enabling easy comparison of different sets of fatigue data, and it follows that any comparisons in life made using them should be valid over that entire class. Also it should be possible to use any of the data generated for acceptable design life estimates over that class using, for instance, the Relative Miner approach<sup>8</sup>. However they are not intended to be used in tests to validate a component on a specific aircraft. In that case the loading sequence reflecting the usage of that particular aircraft should be used.

Although there may be a considerable variation in the loading experienced by, say, different fighter aircraft or different transport aircraft, there is a degree of commonality between that on aircraft of a particular type. For instance, fighter aircraft wing load spectra are manoeuvre-dominated and asymmetric, whereas transport aircraft wing loads are normally gust-dominated and symmetric. Also in the transport wing case the air-ground-air transition accounts for a far greater share of the fatigue damage than in the fighter case. These differences, and other, justify the use of two different standards for these cases.

In the case of helicopters the loading action on rotor blades is very different from that in the two cases discussed above. Loads are generated by the mechanical rotation of the blades with strong components from both frequency of rotation, (F), and  $F \times$  Number of blades. Cycles having a magnitude of possible significance to fatigue accumulate very much faster than for fixed wing aircraft. Most of these cycles are below the fatigue limit and so, at least according to Miner's Rule, do no damage. Also, the shape

of the load spectrum is very different to that on either fighter or transport aircraft wings, having, at least for helicopters with articulated rotors, a commonly occurring level which is reached at least once every revolution of the blade. It was concluded, then, that the helicopter load spectrum differed sufficiently from those covered by the other standards to justify a new standard loading sequence. However, the question arose as to whether two standards could be justified, one for articulated rotors and one for rigid, or semi-rigid rotors. As described in section 4 this was assessed by comparing blade loads and operational usage patterns mainly on four helicopters, two with articulated rotors and two with semi-rigid rotors.

### 3 DESCRIPTION OF HELICOPTERS IN THE STUDY

Operational and loads data from four helicopters was used in deriving the loading standards. The helicopters concerned were as follows:

#### (a) Westland Helicopters Ltd - Sea King.

A twin-engined aircraft with a maximum take-off weight of 9530 kg, used mainly for anti-submarine warfare operations. The rotor is articulated, 18.9 m diameter, and has five blades. The rotor head material is titanium and steel, and the blade spars are aluminium alloy.

#### (b) Sikorsky - CH-53D/G.

A heavy transport, twin-engined aircraft with a maximum take-off weight of 19050 kg. The rotor construction is similar to that of the Sea King, but there are six blades and the rotor diameter is 22 m.

#### (c) MBB-BO-105.

A twin-engined, multi-purpose aircraft with a maximum take-off weight of 2400 kg. The semi-rigid rotor, 9.8 m diameter, has four blades. The rotor head material is titanium and the blade material is glass-reinforced plastic.

#### (d) Westland Helicopter Ltd - Lynx.

A twin-engined, multi-purpose aircraft with a maximum take-off weight of 4760 kg. The semi-rigid rotor, 12.8 m diameter, has four blades. The rotor head material is titanium and the blade spars are stainless steel.

The two types of helicopters have fundamentally different rotor designs. The Sea King and CH 53 have articulated rotors for which the maximum flapwise bending moments are at about half rotor radius. The Lynx and BO-105 have semi-rigid rotors for which the maximum bending moments are inboard of, or at, the blade root. In the discussion of loading data in the sections which follow, the data for the two rotor designs are considered separately.

### 4. ASSESSMENT OF BLADE LOAD SPECTRA TO ASSESS THE FEASIBILITY AND SCOPE OF THE STANDARDS

#### 4.1 Introduction

Section 4 describes the extent of operational loading data available on mixes of manoeuvres in different roles and on manoeuvre blade loads for the four helicopters in

the study. A comparison of some load spectra for the four cases is presented which was used to answer two questions. First, was there sufficient commonality between spectra, on helicopters having the same type of rotor, to justify a common standard? Second, were differences between the load spectra on the two types of helicopter sufficient to justify two standards?

The helicopter is a multi-role vehicle and in different roles can experience greatly differing sequences of blade loads. For the purposes of this study a sortie was defined as a flight fulfilling a particular role, a flight being the period between take-off and subsequent landing. A survey<sup>10</sup> of UK Service use of helicopters, carried out in 1974, showed that the majority of sorties could be classified under the general headings of Training, Transport, Anti-Submarine Warfare (ASW) and Search And Rescue (SAR).

To perform a defined sortie, a helicopter will need to fly certain characteristic patterns of manoeuvres. For instance, a helicopter in an ASW role involving sonar dunks will go through a transition from cruising speed to hover, deploy and retrieve the sonar buoy, accelerate and manoeuvre to a new search area. By recording this information the average time spent in a manoeuvre can be estimated. With a knowledge of the manoeuvres performed, and the loading on the aircraft for each manoeuvre, a spectrum of loads can be compiled for the sortie. The recording of frequency and duration of manoeuvres during operational sorties is an area of current study<sup>10,11,12</sup>, but from experience mixes of manoeuvres have been defined for use in design and certification of aircraft. Loading spectra synthesised from a design mix of manoeuvres have in most cases compared favourably with measured operational spectra<sup>13,14</sup>.

The loading spectra used for the comparison between the four helicopters were synthesised, where necessary, using the procedure described above. The bases for the derivations were design manoeuvre mixes for selected roles. However, existing measured loading and operational data were not always comprehensive enough for all the requirements of the study. Where possible, measured data was used but sometimes existing estimated data had to be employed or estimates made.

#### 4.2 Sea King loading data

The design mix of manoeuvres for the Sea King in the Transport, ASW and SAR roles is shown in Table 1 in terms of percentage time spent in 24 manoeuvres. The definition of the training role in these terms is difficult because this role can vary from, say, half an hour of handling exercises, to a two hour route - following sortie. Table 1 demonstrates the dependence of the severity of loading on the sortie performed. For example, a Sea King performing an ASW sortie spends about one third of its time hovering, whilst in the Transport role over three quarters of the flight time is occupied by forward flight. Hover is a manoeuvre which generates relatively minor loads whereas the loading in forward flight at 103 kn is significant.

During the Sea King main rotor flight test, stress histories for a number of locations on the rotor were recorded as an aid to fatigue substantiation. The area of interest to the current study was at about half rotor radius, where, in an articulated

rotor system, the maximum flapwise bending moment occurs. At this station the maximum stresses occur on the lower surface of the blade, which is generally under tensile load.

Stress histories were available for the lower rear corner of the blade spar at 55.9% rotor radius for most of the manoeuvres describing a Sea King sortie. These stress histories were measured, by Westland Helicopters Ltd (WHL), using a range-mean-pairs (rainflow) counting method. This gave a mean-alternating matrix for each manoeuvre. An example of this is shown in Fig 1 for normal approach to the hover, one of the manoeuvres which produces the most severe loading. The mean stresses include a contribution due to centrifugal force. As a range-mean pairs (rainflow) counting method was used to analyse the stress histories, the counts recorded in the matrix are whole stress cycles. For each matrix the flight time varied but was generally around 5 s. Examination of two matrices for the same manoeuvre did indicate a considerable variation in the number and magnitudes of the stress cycles in the matrix, and therefore, for each manoeuvre, the matrix considered most damaging was used in the subsequent analyses.

At the time the Sea King transport spectrum was constructed for comparison with that of the CH-53, stress matrices were not available for take-off, forward flight at 20 kn, 30 kn and 40 kn, recovery from rearwards flight, descent, spot turns and landing. Examination of the peak loading in flight suggested that take-off, forward flight at 20 kn and 40 kn and landing, could be simulated by sideways flight to starboard, forward flight at 30 kn by forward flight at 113 kn, recovery from rearwards flight by recovery from sideways flight to starboard, descent by forward flight at 103 kn, and spot turns by rearwards flight. In the final stages of defining the standard loading matrices were available for all the manoeuvres except descent. This latest data confirmed the validity of the earlier assumptions made in the comparison of the two spectra.

#### 4.3 CH-53 loading data

At the time of the study a design mix of manoeuvres was not available for the CH-53.

To determine fatigue load spectra for German Air Force usage of CH-53 helicopters, in-flight measurements of strain were recorded for a number of simulated sorties. The strains were measured at the lower rear corner of the blade spar at about half rotor radius, a position compatible with the Sea King measurements. Out of the total of 26 flights flown, nine flight records were analysed by the range-mean-pairs counting method. Five of these nine flights were Transport sorties and the remainder Training sorties. Only overall loading spectra could be determined from the flight records because the transition from one manoeuvre to another could not be determined accurately, making an analysis on a manoeuvre-by-manoeuve basis difficult. The measured spectra for the Transport and Training sorties are illustrated in Figs 2 and 3 respectively. For ease of presentation the tensile mean stress of the cycles, arising from centrifugal force, has been ignored.

#### 4.4 Comparison of CH-53 and Sea King loading spectra

The similarity of load spectra for different helicopters having articulated rotors was assessed by comparing Sea King and CH-53 data for the transport role. As described

above the CH-53 data was already in the form of an overall spectrum for this sortie, but the spectrum for the Sea King had to be synthesised from loads for the appropriate mix of individual manoeuvres. The results of this synthesis are presented in Fig 4 in the form of a mean-alternating stress matrix. They include the assumptions discussed in section 4.1 on the loads for which data were not available, and used a counting grid twice as coarse as that used (eg Fig 1) when determining loads for individual manoeuvres.

The large number of cycles in the lowest stress amplitude counting interval in Fig 4 were a result of loads accumulating at frequencies higher than the fundamental frequency of rotor revolution. Counts in the other intervals show that the higher stress amplitudes accumulated at about or less than the fundamental frequency.

The Sea King and CH-53 Transport spectra are compared in Fig 5, in which variations in mean stress have been ignored to ease comparison. Both spectra show the characteristic humped shape reported in the literature<sup>15</sup> for helicopters with articulated rotors, and, despite the different data sources, aircraft weights, usage, number of rotor blades and the fact that the spectrum for the Sea King was synthesised, the spectra compare favourably. This is true particularly in the high stress region which is of major importance to blade fatigue life. All cycles in the two spectra are below the plain fatigue limit of titanium alloy, and would require an effective stress concentration of at least three before Miner's Rule predicted any fatigue damage.

The favourable comparison of the CH-53 and Sea King spectra for the transport role led to the conclusion that a standard loading sequence could be defined, and that data from both Sea King and CH-53 could be used in its synthesis.

#### 4.5 Lynx loading data

Table 2 shows the design mix of manoeuvres for the Lynx. This is similar to that for the BO-105 and also to that for published design spectra<sup>16</sup>. Unlike the Sea King manoeuvre mix (Table 1), that for Lynx is for an average sortie. The more frequent of the 43 flight conditions defining this sortie are listed in terms of percentage time spent in a manoeuvre. The less frequent conditions are listed in terms of occurrences per hour.

Mean and alternating flap bending moments at the root of the inner flexible element of the Lynx main rotor hub (3.4% rotor radius) had been estimated by WHL for the fatigue substantiation programme. At this location, the critical rotor section for the Lynx, the loading caused by lag is not significant. These flap bending moments were estimated so as to describe the average sortie (Table 2), rather than the loading caused by individual manoeuvres. The flap bending moments, including the contribution due to centrifugal forces, were converted to mean and alternating strains for the lower surface of the inner flexible element. The resulting spectrum is shown in Fig 6 and includes cycles which occur once per flight and are, therefore, not strictly dependent upon number of hours flown.

#### 4.6 BO-105 loading data

An instrumented BO-105 was flown to the design mix of manoeuvres. As described above the design mix was similar to that of the Lynx (Table 2). Strains were measured on the lower surface of the blade root, the most highly stressed region, for each of these manoeuvres. The record from each flight was then analysed by the rainflow counting technique (generally equivalent to range-mean-pairs counting) to form mean- alternating strain spectra for each manoeuvre. An example of this for one of the most severe manoeuvres in the spectrum, a longitudinal control reversal in autorotation, is illustrated in Fig 7.

#### 4.7 Comparison of BO-105 and Lynx spectra, between each other and with those for articulated rotors

To enable comparison between loading on the BO-105 and the Lynx a spectrum for the BO-105 was constructed corresponding to the mix of manoeuvres shown in Table 2, and used previously to define the Lynx spectrum. The result of this synthesis is shown in Fig 8 and, unlike that shown in Fig 6 for the Lynx, did not include the once per flight loads, since these data were not readily available. The once per flight loads were responsible for the most obvious difference between Figs 6 and 8, namely some cycles having a compressive mean stress in Fig 6 with none in Fig 8.

Spectra for the Lynx and BO-105, corresponding to Figs 6 and 8 respectively, are shown diagrammatically in Fig 9. As for previous plots of load spectra, mean strains were ignored. Also, since for the BO-105 spectrum the once per flight loads were not included, they were removed from that of the Lynx so as to give a more rational basis for comparing them.

Before the spectra for the two helicopters with semi-rigid rotors were compared in detail, a further comparison was made between the spectra for each class of rotor to determine whether a separate standard was necessary for each class. Comparing Fig 9 with Figs 2, 3 and 5, it can be seen that the shapes of the spectra for the two types of rotor were very different. In Fig 9 the characteristic S-shape observed for both the Sea King and the CH-53 was not nearly as evident for either of the semi-rigid rotor helicopters. Particular differences were noted between the spectra in the region from 1-1000 cycles/hour, this region being the most important with regard to fatigue damage. For the helicopters with articulated rotors Fig 5 shows that the stress for a cumulative count of 1000 cycles/hour was about 35 MPa, which is about 70% of the stress reached once per hour. Fig 9 shows, however, that the corresponding percentage for the Lynx was 50%, and that for the BO-105 about 33%. This means that the slopes of the spectra for the two types of helicopter differed on average by a factor of about 2:1 at the upper end. This is a very large difference in fatigue terms. It was concluded, therefore, that the above differences between the spectra justified two standards.

Returning now to the comparison between spectra for the BO-105 and Lynx in Fig 9, it can be seen that although there can, perhaps, be said to be a 'family' resemblance between the shapes of the two spectra compared with those for articulated rotors, there

were significant differences between the two. First the actual levels of strain were very different between the two helicopters. However this was to be expected because of the different materials used in construction; the critical section of the BO-105, the blade root, is made of glass-reinforced plastic, whereas the inner flexible element of the Lynx is of titanium. Factoring the strain level on the Lynx by 2.1 was used to provide a rational basis to compare the shapes of the two spectra. It is apparent from the comparison of the factored Lynx spectrum with the unfactored BO-105 spectrum in Fig 9 that the biggest differences exist at the upper end, that of most concern to fatigue. Comparing the average slopes of the top ends of the spectra as before gives a difference in slope of a factor of 1.4.

The difference in the slope at the upper end of the spectra for the two helicopters with semi-rigid rotors could have been due to a number of factors. First, of course, the differences could be fundamental to the dynamic and aerodynamic design of the two aircraft. However, it may be recalled that the Lynx spectrum was that calculated for design purposes whilst that for the BO-105 was a flight test spectrum from one sample flight. Also there may have been differences in the way that the defined manoeuvres were interpreted. In an effort to investigate this last point the spectrum of the BO-105 was recalculated leaving out the loads for one manoeuvre, that for longitudinal control reversals in autorotation (see Table 1 and Fig 7). The recalculated spectrum is compared with the factored Lynx spectrum in Fig 10, and it can be seen that good agreement was obtained.

The close agreement in Fig 10 between the spectra for the Lynx and BO-105, albeit with one manoeuvre left out of that for the BO-105, shows that there was considerable similarity between the loading on the two helicopters. By comparison it is difficult to see how either the Sea King or CH-53 could be flown to a mix of manoeuvres which would give spectra similar to those in Figs 9 and 10. However the point is made also that changing the manoeuvre mix can give large differences in the loading, at least for helicopters with semi-rigid rotors. Therefore any relevant standard sequence will be used to derive lives applying to spectrum differences at least as great as those shown in Fig 9. It can be said, therefore, that some similarity was demonstrated between the loading on the two semi-rigid rotors, but not to the same extent as on the articulated rotors. It was considered, however, that a standard sequence could be defined for semi-rigid rotors, and should be based mainly on the BO-105 data, which was the most comprehensive set.

## 5 METHOD OF GENERATING THE LOADING STANDARDS

In defining a standard loading history a number of factors should be taken into account. First, the standard should represent as far as possible typical usage of the relevant class of structure. Second, it should be possible to implement easily the generation of the standard on any of the wide range of computers used to control fatigue machines. It should not be over-complicated or excessive in requirements for computer time or storage space. Finally it should not have too fine a resolution of peak and trough values, with a consequent large number of defined turning point magnitudes.

This can create needless complication in, for instance, rainflow-counting the sequence because of the large number of cells required, and may also require more complex generation hardware. It was this last consideration which led to the modifications to Helix and Felix described in Appendix B.

Two main alternative methods of generating the sequence were considered. The first generates the loading, using random draw techniques, from mean-alternating load matrices. This method, which loses the separate identity of manoeuvres, is similar in concept to the well documented<sup>17</sup> methods of generating TWIST and FALSTAFF. The second method defines sorties by fixed logical sequences of manoeuvres, thereby retaining the identity of individual manoeuvres at the expense of a considerable amount of repetition in the sequence. This latter method of generation was used by Critchlow *et al*<sup>18</sup> in 1972. For either generation method an average sortie could be formed to simulate the four sorties defined in section 4.1, or they could be simulated on an individual basis with one or more flight lengths for each sortie. The sequence of sorties could be defined by a random draw algorithm or a predetermined sequence.

As discussed below (a) to (d), the method chosen to generate the loading standards was that using a predefined and repeated sequence of sorties. Logical sequences of manoeuvres defined each sortie, which could have one of three flight lengths. Predefined sequences of loads made up each manoeuvre.

(a) Sorties were defined as logical sequences of manoeuvres so as to simulate more accurately the complex load interactions which influence the fatigue life. A criticism of the earlier standards has been that, during flight, all logical loading sequence is lost.

(b) Variation in the flight lengths of a sortie was chosen because of the need to represent accurately the transition from the ground condition to and from level flight. This transition up to the peak loading in each flight and down again forms one large cycle which can cause a large proportion of the fatigue damage.

(c) Simulation of four separate sorties was chosen in preference to one average sortie because there was considerable variation in loading from sortie to sortie, and for the sequences to be representative this had to be included.

(d) Predetermined sequences of loads in a manoeuvre, and in sequence of sorties, were chosen in preference to random draw algorithms because, in the opinion of the authors, random draw algorithms create unnecessary problems of programming complexity and timing. Experience has shown that, although FALSTAFF is defined using random draw algorithms, many laboratories have avoided these problems by storing the sequence of numbers on disc or in core and using this for generation. However, this method greatly increases storage requirements.

The above method of generating Helix and Felix has resulted in a simply-structured system. This simplicity is illustrated by one application, at RAE, using machine language on a minicomputer, which has given a storage requirement for both program and data of only 1 K of 12-bit words to generate Helix.

## 6 DETAILS OF THE DERIVATION OF HELIX AND FELIX

This section discusses the details of the generation of Helix and Felix. Examples are given of fundamental parts of the standards, but full data for generation appears only in Ref 4. Both standards use the same sequence of sorties and the same three sortie lengths. However, in contrast to the original intention, the sequences of manoeuvres for each sortie, although similar, are not identical for Helix and Felix. Sequences of loads for each manoeuvre are different for the two standards.

### 6.1 Mix of sorties

The 1974 survey<sup>10</sup>, referred to in section 4.1, of UK Service use of helicopters with both types of rotor, included data on Sea King, Gazelle, Scout, Wasp, Wessex, Whirlwind and Puma, and totalled 500 individual aircraft and 7500 flying hours. The results of this survey were considered suitable for this study because other surveys of helicopter usage have generally been limited to one theatre of operations<sup>19</sup>. As stated in section 4.1 it showed that the majority of sorties could be categorised under the general headings of Training, Transport, Anti-Submarine Warfare (ASW) and Search and Rescue (SAR). Table 3 lists the percentage time spent in each of the four sorties for all the helicopters in comparison with the sortie mix for the Sea King only. This comparison demonstrates the above average use of the Sea King in the ASW role.

Despite the survey data being of UK origin only it was found to be a good representation of what was known about Dutch and German helicopter usage. The sortie mix for all aircraft in Table 3 was selected, therefore, as the basis for the standard loading sequences, applying to both types of rotor. It was argued that the loading standards needed to reflect the general usage of helicopters rather than that of one specialised type such as the Sea King, which would be biased heavily in favour of one specific sortie, Anti-Submarine Warfare.

### 6.2 Flight time for a sortie, number of sorties and their sequence

The survey of UK helicopter usage<sup>10</sup> gave information as to lengths of sortie as well as their character. However, the only detailed information in this respect concerned Sea King. This is plotted in Fig 11 for Training and Transport sorties, and in Fig 12 for ASW and SAR sorties. It was considered that representation of flight length variation in the standards was more important than the differences which might exist between Sea King and all-aircraft flight lengths. The sortie lengths for the standard sequences were, therefore, all based on Figs 11 and 12. It is described in Appendix C how the data in Figs 11 and 12 were analysed, considering the occurrence of the most infrequent sortie and flight length combination, related to the required length, in flights, of the standards. It was concluded that the standards should be 140 flights long and that three sortie lengths should be included, namely 0.75, 2.25 and 3.75 hours. Each sortie would be applied in the same three lengths. Table 4 shows the sortie mix for Helix and Felix derived in Appendix C.

The sequence in which the 140 flights are applied in Helix and Felix was defined by a once-and-for-all random draw. The results of this are shown in Table 5.

### 6.3 Definition of manoeuvres

Before the sequence of manoeuvres for each sortie could be defined it was necessary to define individual manoeuvres for each class of helicopter. For articulated rotor helicopters the most comprehensive set of data readily available on blade loads and associated manoeuvres was from the Sea King, and for semi-rigid rotor helicopters the same was true for the BO-105. In view of the similarity demonstrated between loading on helicopters within each class, it was considered reasonable to base Helix on Sea King data and Felix on BO-105 data.

Data available for the Sea King and BO-105 identified 24 and 22 manoeuvres respectively, which were to be placed in sequence in the subsequent definition of the sorties. The data were in the form of mean-alternating stress or strain matrices as, for instance, in Fig 1. These were all non-dimensionalised to express the loads or strains on a scale up to 100 in intervals of four. This scale was deemed to be in 'Helix units' or 'Felix units'. As originally defined Helix<sup>5</sup> and Felix units were on scales up to 74 and had a greater number of defined levels than in the final versions. The differences between the original and, as described here, final versions of the standards are given in Appendix B.

Examination of the mean-alternating stress matrices showed that, for both helicopters, the majority of large amplitude cycles occurred at a common mean stress particular to that manoeuvre (see, for instance, Figs 1 and 8). It was decided therefore that each manoeuvre would have a constant mean stress in Helix and Felix.

Tables 6 and 7 list the defined manoeuvres in Helix and Felix, respectively. Shown also is the loading content of each manoeuvre expressed in Helix/Felix units. As can be seen the definitions of the manoeuvres are similar, but not identical, for the two classes of helicopter. For instance Helix has two manoeuvres, 8 and 9, describing approach to hover, whereas Felix has only one. These differences reflect the different sources of data and different definitions of what at first sight may appear to be the same manoeuvre. The most obvious difference, however, is the inclusion of control reversals in Felix, but not in Helix. These inconsistencies between the two sets of data led, as shown below, to manoeuvre sequences in each sortie which differed in the two standards. However, the longitudinal control reversal in autorotation was not included in Felix since it was not regarded as being representative of normal usage. It may be recalled that omission of this manoeuvre from the BO-105 design mix gave good agreement between the resulting spectrum and that for the Lynx (section 4.7).

For both standards, as for virtually all laboratory loading sequences, an alternating level was selected below which cycles were not included. As can be seen from Tables 6 and 7, the lowest amplitudes included were 20 and 16 for Helix and Felix respectively. The levels of omission from the spectra were below these levels which represented a band of cycles extending both above and below the defined values. The actual omission levels were 20.7 MPa from the Sea King data, and 400 microstrain for the BO-105 data, as can be seen from Figs 5 and 9. It can be seen from Tables 6 and 7 that

the omission of the low level cycles resulted in some manoeuvres having no significant loads. For completeness these manoeuvres were included in the standards but no loads or dwells were applied. Omission of levels from Helix and Felix is discussed further in section 11.

#### 6.4 Sequence of loads in a manoeuvre

The sequence of loads in any manoeuvre was chosen for both standards on the basis of a once-and-for-all random draw. Therefore, every time a particular manoeuvre was performed the sequence of loads was the same. Table 8 shows the first three manoeuvres in the Helix set, as defined for generation. The numbers are all in Helix units. The first number in each list represents the mean stress and each subsequent number represents a complete alternating cycle going tensile first. Many of the manoeuvres defined as in Table 8 are not necessarily complete, and have to be repeated several times in order to carry out their function fully. Full details of manoeuvres for Helix and Felix and their generation can be found in Ref 4.

#### 6.5 Sequence and mix of manoeuvres in a sortie

Describing a sortie by a logical sequence of manoeuvres is a technique which has been used previously<sup>18</sup>. The lack of operational statistics describing manoeuvre sequences led to their synthesis by common sense consideration of the flight profile and the objective of the sortie. In the simplest case the above approach says, for instance, that a helicopter cannot perform a bank turn without first taking off. Tables describing in full the sequence of manoeuvres for each sortie are not given in this Report since they are very lengthy, but are given in full in Ref 4. As referred to earlier<sup>5</sup> the original intention was to use the same sequence of manoeuvres for Helix as Felix. However, in practice it was found that the defined manoeuvres to be included in the standards were not always directly equivalent between Helix and Felix, and so could not always be sequenced in the same way. Therefore the sequences for Helix were derived first, and those for Felix formulated to be as similar as possible. Table 9 shows the equivalence assumed for manoeuvres in Helix and Felix. A discussion follows of the considerations taken into account when synthesising the four sortie sequences.

##### (a) Training

This was the most difficult sortie to define because of the wide ranging operations that are flown. The assumption was made, however, that this sortie should simulate the essential aspects of flight needed to perform other sorties. In addition, a pure training exercise was simulated, in which the helicopter performs manoeuvres to demonstrate handling characteristics. Table 10 shows the first six manoeuvres of the Training sortie for Helix, and Fig 13 shows a trace of these. Note that in Table 10 the column 'matrix applications' refers to the number of times that the defined sequence of loads has to be repeated in order to describe fully the manoeuvre. Details of the transitions between flights and transitions between manoeuvres are given in section 6.7 below.

(b) Transport

This sortie represents take-off and low speed manoeuvres away from the terminal area, flight at cruising speed whilst manoeuvring to take into account terrain and air traffic control restrictions, and finally landing in the terminal area.

(c) ASW

In this sortie, apart from the requirement to move to and from the base area, the helicopter repeatedly decelerates to allow deployment of a sonar buoy, and accelerates to move to a new search area.

(d) SAR

The essential part of this sortie is the flying of low speed manoeuvres in order to execute a rescue.

#### 6.6 Variation in lengths of sortie

In order to define the 0.75 h and 2.25 h flights, it was decided first to define the 3.75 h flights, and then to take fractions of these flights for the other durations. Thus only one sequence of manoeuvres was defined for each sortie, the whole of which was used for the 3.75 h flight. For the flights of 0.75 h and 2.25 h take-off and landing are applied as for the complete sortie, but a selected part or parts is cut out from the rest of the flights. Fig 14 shows how this is done for the Training, Transport and ASW sorties.

Fig 14a shows an altitude profile for a 3.75 h flight. If a 2.25 h flight is to be generated, the loading sequence is applied as before up to the point marked '2.25 h flight marker'. Then a jump is made to the point marked 'landing marker' and the sequence is continued to conclusion from this point. The resulting altitude profile is shown in Fig 14b. If a 0.75 h flight is to be generated then the procedure is identical except that the 0.75 h marker is used instead of the 2.25 h marker. The altitude profile for the 0.75 h flight is shown in Fig 14c.

The procedure for the SAR sortie is slightly more complicated and is described in Fig 15. In this the prime consideration is to ensure that the lengths of the flights to and from the rescue area are related in a logical way. Fig 15a shows the altitude profile for a 3.75 h SAR flight. For a 2.25 h flight a jump is made from the 'First 2.25 h flight marker' to the 'SAR marker'. Generation continues up to the 'Second 2.25 h marker', a jump is made to the 'Landing marker', and landing occurs as before. Fig 15b shows the resulting altitude profile. Fig 15c shows the altitude profile for a 0.75 h flight, which uses the markers for 0.75 h instead of those for 2.25 h.

#### 6.7 Transitions between manoeuvres, and magnitudes of ground loads

Two final pieces of information are needed to complete the definition of Helix and Felix. First is the detail of how to make transitions between manoeuvres, and second how to deal with transitions between flights. These are shown in Fig 16, which gives the transition between landing and take-off for Helix. All manoeuvres, as stated

earlier, consist of a constant mean stress, which, as can be seen from Fig 16, is 72 Helix units for the landing manoeuvre. Each cycle starts going positive so the the first turning point reached by the landing manoeuvre is at  $72 + 28 = 100$  Helix units. It then reverses and reaches its second turning point at  $72 - 28 = 44$  Helix units. The cycle is completed by return to the mean value. Each subsequent cycle starts and finishes in exactly the same way, and the last half cycle in the manoeuvre must return to the mean stress before, either, a transition is made down to the landing load, as at the end of the landing manoeuvre in Fig 16, or a transition is made to the next mean stress. This means that, in the transition from one manoeuvre to another, if the mean stress increases between manoeuvres then the load progresses smoothly from the last half cycle of the first manoeuvre to the first half cycle of the second manoeuvre. This is illustrated in Fig 16 by the dotted transition following the take-off loads. If, on the other hand, the mean stress reduces from manoeuvre to manoeuvre then an extra small cycle is introduced between manoeuvres by the return to the mean at the end of the first manoeuvre. This is illustrated by the full line transition following the take-off.

The measured values used for the ground load transitions are -20 for Helix and -28 for Felix, both values being in Helix/Felix units. It is assumed, for both Helix and Felix, that this ground load transition value is reached at the end of each flight. Thus it is assumed that the rotor comes to a standstill at the end of each flight, so every air-ground-air transition is a start-stop-start transition.

#### 6.8 Shortened versions of Helix and Felix

In section 11.3 below recommendations are made concerning the use of Helix and Felix in shortened forms in order to reduce testing times. This section describes the method of omission of low level cycles in order to obtain the shortened sequences. Section 7 describes the runflow analyses of Helix and Felix in both the full and shortened forms.

The method of omission of cycles is to chose a manoeuvre alternating stress level at and below which cycles are omitted. However, if this is applied rigorously some manoeuvres disappear altogether and there are difficulties in obtaining shortened sequences of the required length (section 11.1). In order to overcome these problems a system of partial omission was adopted, which had the additional advantage of retaining the identity of all manoeuvres. In every manoeuvre which would be omitted in the above system, one alternating cycles is applied at the highest level contained in that manoeuvre. This level is, of course, at or below the nominal level of omission. Additionally some low level cycles occur in the transition from one manoeuvre to another, as described in section 6.7. These low level cycles are retained.

### 7 STATISTICS OF HELIX AND FELIX

In this section are presented the most important statistics, from the point of view of fatigue, of the two standards. Additionally the spectra of Helix and Felix are compared with each other and also with operational data.

### 7.1 Basic form of the standards

The structure of the two standards has already been described in section 6 together with some of the basic data on the form of the sequences. This basic data was presented in Tables 4 to 7 which show the number of flights of each duration for each sortie (Table 4), the sequence of these flights (Table 5) and the load matrices of the component manoeuvres in Helix (Table 6), and Felix (Table 7). Full data on sequence of loads in a manoeuvre and sequence of manoeuvres in a sortie was not presented because of the length of the tables required to give this information, but are given in Ref 3. However, Tables 11 and 12 give the percentage times in each manoeuvre for each full length sortie in Helix and Felix respectively.

### 7.2 Comparison of Helix and Felix spectra

Helix and Felix were analysed by more than one counting method, and the results of these are shown in Tables 13 to 16. Tables 13 and 15 give the results of the rainflow analyses, and Tables 14 and 16 give analyses of peak, trough and levels crossed distributions.

Fig 17 shows a comparison of Helix and Felix spectra using the data obtained from rainflow counting. As in the earlier sections of this paper, mean stresses have been ignored to ease the comparison. However in the earlier comparisons, for instance in Figs 5 and 9, the loads due to the start-stop-start transitions, associated with landing and take-off, were not included. As a consequence Fig 17 shows large steps in both Helix and Felix, at the top end of the spectra, which do not appear in Figs 5 and 9. However, it should be appreciated that the steps are associated with extra loads on the negative side only, and the important peak loads applied in flight are similar to those in Figs 5 and 9. The marked difference in the shapes of the spectra for the flight loads can be seen, with the spectrum for Helix being generally flatter than that for Felix outside the region affected by the start-stop-start transitions.

The difference between the spectra for Helix and Felix are illustrated further in Fig 18 which compares the two on the basis of positive-going levels crossed. Here the differences are more obvious at the high stress end than in the previous figure, because the start-stop-start transitions only affect this plot at the negative stresses. At stresses above 60 Helix/Felix units a much sharper truncation on Helix than Felix can be seen, in line with the comparisons of the loading actions on the two types of helicopters as presented in Figs 5 and 9. Also evident from Fig 18 is that both the top and bottom lines of the Felix spectrum are generally below those for Helix, although the maximum loads have been scaled to be the same in both cases. This indicates a generally lower relative level of mean load for Felix than Helix.

### 7.3 Comparison of Helix and Felix spectra with operational data

It should be appreciated that Helix and Felix were derived for a particular mix of manoeuvres and sorties for which there is no complete comparative set of data. Consequently all the comparisons in this section are for Helix and Felix, representing a

wide ranging mixture of roles, with data for particular helicopters carrying out particular roles. It follows, therefore, that a close similarity between the standards and the operational data would not necessarily be expected. Fig 19 shows the Sea King transport spectrum, from Figs 5 and 9, compared with Helix. The Sea King data was factored so that it represented the same number of flying hours as Helix, and the stresses were multiplied by the same factor as was used to derive Helix units in formulating the standard. As can be seen from Fig 19 there is very good agreement between the two spectra at the low stress end. At the high stress end Helix exhibits the step arising from the air-ground-air transitions which were not included in the Sea King data, so similarity would not be expected in this region.

Fig 20 shows spectra for the Lynx and BO-105 compared with that for Felix. The Lynx and BO-105 spectra were to a design mix of manoeuvres, as described in sections 4.5 to 4.7. For the purpose of the comparison the stresses and numbers of cycle were factored in the same way as was described above for the Sea King. It can be seen from Fig 20 that agreement between Felix and the Lynx spectrum is quite good, except at the upper end where, as in the case of Helix, the Felix spectrum exhibits a step associated with the air-ground-air transitions. Thus as in the case of the Sea King the Lynx flight spectrum compares well with that of the standard. However, in the case of the BO-105, even bearing in mind the fact that air-ground-air transitions were not included in the BO-105 spectrum, agreement with Felix is not good above stresses of 35 Helix units where the BO-105 spectrum curves upwards. At first sight it is, perhaps, a little surprising that the Lynx spectrum agrees better with Felix than that for the BO-105, since Felix was based mainly on BO-105 data. However, it may be recalled that longitudinal control reversals in autorotation were not included in Felix, and, as shown in Fig 10, when this manoeuvre was left out of the design manoeuvre mix, good agreement was found between spectra for the BO-105 and Lynx. In the event the BO-105 spectrum without this manoeuvre compares well with Felix.

It was concluded that both standards had stress spectra which agreed well with operational data despite the differences in mix of manoeuvres.

#### 7.4 Spectra for Helix and Felix with levels omitted

In section 6.7 the method of obtaining short versions of Helix and Felix was described. This is accomplished by removing low level cycles, and enables shorter testing times to be achieved. Section 11.3 below discusses the use of these shortened sequences and makes recommendations. One of these is that the standard shortened sequences should be Helix with the majority of alternating cycles at level 32 and below omitted and Felix with the corresponding omission level of 28. The shortened sequences are known as Helix/32 and Felix/28. Rainflow analyses were carried out on Helix/32 and Felix/28, and the results are presented in Tables 17 and 18 respectively. The spectra of the short and long versions of the two standards are compared in Fig 21 for Helix and Fig 22 for Felix. As can be seen the two short sequences are less than a tenth of the length of the full versions. The actual lengths of the full and shortened sequences are given in Table 19.

## 8 OUTLINE AND AIMS OF FATIGUE TEST PROGRAMME

Standard loading sequences are used for two reasons. First they are a tool for giving an immediate comparison of one set of fatigue data with another. Second they may be used to provide design data. In considering the first point it is clearly an advantage, just from the point of view of convenience, that any test result using a standard loading can immediately be compared with a library of fatigue data without resort to a cumulative damage rule. However a further consideration is whether the use of standard sequences that are as realistic as possible give more valid comparisons than with more simple sequences such as the commonly employed block programme. Thus the question may be asked as to whether the objective of easy comparison can be met by the adoption of a standard in the form of a block programme. Also, if standard block programmes were adopted, would the data generated be better or worse for use in life prediction than the more complex Helix and Felix?

The first part of the fatigue test programme consisted mainly of tests under constant amplitude loading, Helix, Felix and block programmes designed to give fatigue lives similar to those of the two standards. The aim of these tests was to assess whether Helix and Felix, when used either for obtaining comparative fatigue data or design data would give better comparisons or enable more accurate life predictions than those which would be achieved using block programmes or constant amplitude loading. Since Helix and Felix were the most representative of all the loading sequences used, the assumption was made that comparisons using the two standards were the most valid, and assessments were made as to how closely comparisons made under other loadings could repeat them or be used to predict them accurately. The assessment of Helix and Felix as design data was limited to seeing how well other loading actions could be used to predict lives under the two standards (as distinct from comparative lives or comparative fatigue strengths in the earlier assessment). This analysis could at best only identify possible inadequacies in life predictions using the other loading sequences which could possibly be redressed using the more representative Helix and Felix. A full assessment of this would require more fatigue tests under loading spectra for specific design cases on specific helicopters, and is a topic for further study.

The final aim of the test programme was to assess the possibility of using Helix and Felix in a shortened form by omitting some low level cycles. Thus tests were carried out as described in section 11 with a shortened version of one standard, Helix.

The joint test programme consisted of 290 fatigue tests carried out at four different Establishments in three countries, and is summarised in Table 20. Details of the testing are given below and in supplementary reports issued by participating countries<sup>20,21</sup>.

### 8.1 Loading sequences used in the tests

As described in Appendix B, at a late stage in the project Helix and Felix were simplified by reducing the number of defined levels in each sequence to 31 and 33 respectively, and scaling the maximum load in each standard to 100, where previously it was 74. However, this was not decided upon until a late stage in the fatigue test

programme, which was consequently carried out entirely using the original versions of the standards. It is shown in Appendix B that the fatigue performance of the new versions of the standards is likely to differ little from the old. For this reason, in sections 8 to 11 all references to and plots of standards relate to the original versions. However, for ease of comparison both Helix and Felix are plotted on the new scale of 100 representing the maximum load.

Three-level block programmes representing Helix and Felix were derived in two versions each, making four programmes in all, as shown in Fig 23. In the subsequent text the two versions of the block programmes are referred to as V1 and V2 respectively. When testing at high stress levels the number of cycles in each programme was divided throughout by two or four where this was necessary to ensure at least five repetitions of the programme to failure. The first versions were designed by MBB-UD and followed common procedures for substantiation tests at MBB-UD. They used range-pair spectra as a basis and so did not account for the mean loads, the majority of cycles being applied with a minimum load of zero ( $R=0$ ). The results of the subsequent fatigue tests with the first versions of the block programmes, as described later, gave lives that were considerably longer than those under Helix and Felix. Therefore the block programmes were changed to version 2, with the agreement of MBB-UD, by shifting the blocks of amplitude to the mean stresses of the equivalent levels crossed spectra. This is illustrated in Figs 24 and 25, which show the two versions of the block programmes, for Helix and Felix respectively, plotted on top of the levels crossed spectra. The cut-off point at 570080 cycles was chosen arbitrarily by MBB-UD, and is the same for both versions.

## 8.2 Fatigue test specimens and materials

The fatigue test specimens are shown in Figs 26 and 27, with details of the materials used in Tables 21 to 23. Three basic types of specimen were tested. The first of these was a notched (open holed) specimen having a stress concentration factor based on net section of 2.5. The aluminium alloy specimens tested at LBF and IABG were virtually identical to the titanium alloy specimens tested at NLR, the only difference being that the titanium alloy specimens were slightly thicker at 5.5 mm compared with 5 mm for the aluminium alloy specimens. All these specimens were manufactured at LBF. The titanium alloy specimens, manufactured and tested at RAE and used for the tests investigating omission of low level cycles, had test section planform dimensions approximately one half of those of the other specimens. Also their thickness was only 2.2 mm. The stress concentration factor for the RAE specimens was 2.5, the same as for the others described above.

The second type of specimen was a lug, manufactured by MBB-UD, and made out of multidirectional GRP. Details of the layup and material are given in Table 21.

The third and final specimen was a shear stress bend specimen designed to test interlaminar shear strength in fatigue. The form was to a standard MBB-UD specimen and manufacture was out of material taken from a BO-105 helicopter main rotor.

### 8.3 Fatigue test equipment and conditions

Fatigue tests were carried out on a range of servohydraulic and resonant test machines at a wide range of test frequencies. Test frequencies and the types of machine used are given in each table of test results as presented in section 9. All tests were under normal laboratory ambient conditions.

## 9 FATIGUE TEST RESULTS AND CUMULATIVE DAMAGE CALCULATIONS

The fatigue test results are presented in Tables 24 to 45 and Figs 28 to 38. They are grouped in terms of tests on each specimen/material combination, starting in each case with the constant amplitude tests and following with those relating to first, Helix, and second, Felix. Sections 9.1 to 9.4 below discuss each specimen/material combination in turn, apart from the tests investigating omission of low level cycles, which are reported separately in section 11. Sections 9.1 to 9.4 also discuss the cumulative damage behaviour of the respective specimens. Section 10 further discusses the results of section 9 as pertaining to the projected applications of Helix and Felix.

In view of the fact that the block programmes, standards and standards with levels omitted were all of different length in terms of number of cycles, all tests except those under constant amplitude loading have been plotted in terms of number of flights to failure.

On the grounds that no cumulative damage rule has found acceptance as being generally superior to Miner's Rule, only predictions using this Rule are presented here as a basis to the assessment of Helix and Felix. The Rule was applied taking the fatigue limit into account. Variation in calculated damage of individual cycles due to their mean stress being other than that at which constant amplitude tests were carried out was accounted for by interpolating or extrapolating from tests at more than one value of R. This data was either in the form of a set of S-N curves or a Haigh Diagram.

Some assessments were made considering the Relative Miner approach<sup>8,9</sup>, which is the most likely way that data obtained under Helix and Felix would be used to predict life for a component subjected to a loading action in the same class as Helix or Felix. There are a number of variants of this approach, but, as considered here, results of tests under a loading standard are used to adjust stresses and/or lives on relevant existing S-N data, such that application of Miner's Rule to that data would predict accurately the lives obtained under the standard. Miner's Rule is then applied to the adjusted data to predict lives under the required loading action. Clearly there is no advantage to this approach if lives under the standard can be predicted accurately by Miner's Rule because the Relative Miner method would give the same answer as Miner's Rule. However, if Miner's Rule predicts lives that are too long or short for the standard, the Relative Miner Rule compensates for this, assuming in effect that errors in using Miner's Rule directly would be similar for the loading action in question and for the standard.

### 9.1 Notched specimens of 3.1354-T3 aluminium alloy

Fig 28 and Table 24 give fatigue results under constant amplitude axial loading, carried out mainly by LBF. Cross check tests were carried out by IABG which agreed well with those by LBF. All the tests were at a stress ratio  $R = 0.1$  and showed good agreement with those carried out previously by LBF at a range of values of  $R^{22}$ .

A Haigh Diagram derived in the earlier work<sup>22</sup> was used as the basis for the prediction of fatigue life under the standards and related block programmed loading.

Tables 25 to 27 give the results of fatigue tests under Helix and Helix Block V1 and V2, and Tables 28 and 29 give those under Felix and Felix Block V2. The results relating to Helix, together with the predictions using Miner's Rule, are plotted on Fig 29. The corresponding data for Felix is plotted on Fig 30.

Considering first the relative lives under the different loadings on Fig 29, it can be seen that the Helix Block V1 did not give lives comparable with those under Helix. At the highest stresses tested mean lives under block loading were approximately ten times those under Helix, and the fatigue strength under Helix at 1000 flights to failure was 55 per cent higher than under the Block V1. The corresponding fatigue strength of the specimens under Helix Block V2 was similar to that for Helix but there were indications that at higher stresses fatigue lives under Helix Block V2 would be longer than for Helix.

The picture presented by the predictions using Miner's Rule is particularly confusing. Whereas the Miner predictions for Helix Block V2 were good, at least at the lower stress levels, those for Helix predicted a fatigue strength 20 per cent above that realised in practice, and those for Helix Block V1 about 14 per cent below.

Turning now to Felix, it can be seen from Fig 30 that, as for Helix, the block programme V2 fatigue lives were predicted well by Miner's Rule and the lives under the standard, in this case Felix, were overestimated by the Rule. However, this overestimate was not as great as for Helix, the largest overestimate of fatigue strength being about ten per cent in this case compared with 20 per cent for Helix. Also the fatigue strength of the specimens under Felix was generally more than 14 per cent above that for Felix Block V2 whereas for Helix the lives under the standard and the Block V2 were close.

Two conclusions can be drawn from this first set of results. First the block programme V1 was a poor representation of Helix. Second, although the block programme V2 was a better representation, an assessment of aluminium alloy notched specimens for articulated and semi-rigid rotors using block programme V2 would have given lives similar to those predicted by Miner's Rule directly. This means that any predictions using this data and a Relative Miner approach would have predicted lives for Helix and Felix also similar to those of Miner's Rule applied directly. For lives greater than 50 flights to failure this would lead to an overestimate of the fatigue strength under Helix, and presumably a similar overestimate under service loading, of about 20 per cent,

as shown in Fig 29. Relative Miner predictions of Helix lives using the Helix Block VI results would be even more inaccurate since these results imply that specimens should last longer than predicted by Miner's Rule.

By an argument similar to that above, the use of Felix Block V2 data would lead to an overestimate of life under Felix, though the overestimate would be smaller than that for Helix, as indicated by the difference between the predicted and achieved lives under Felix in Fig 30.

## 9.2 Lug specimens of multidirectional GRP

Fig 31 and Table 30 give fatigue results under constant amplitude axial loading at six values of stress ratio  $R$ . A typical failure is shown in Fig 39a. All the tests were carried out by IABG, apart from two cross check tests carried out by LBF, who carried out also all the variable amplitude tests. The check tests agreed well with those by IABG. The results at  $R = 0.1$  were analysed by linear regression analysis and a straight line fitted over most of those data. The data at other  $R$  values were fitted similarly with straight lines having the same slope, an assumption which agreed well with the test results. The fitted straight lines were extrapolated at the high stress end so that the maximum stress was the ultimate value of 153.6 MPa at Cycles = 1. The test results were used to construct a Haigh Diagram which was used for the cumulative damage calculations.

Tables 31 and 32 give the results of the fatigue tests under Felix and Felix Block VI. These results, together with predictions using Miner's Rule, are plotted on Fig 32. As can be seen from Table 30 two batches of specimens were tested in the Felix Block VI tests. The first batch, used for the constant amplitude and Felix tests also, were 10 mm thick. The second batch were only 8 mm thick, but had the same number of layers. Since a realistic comparison between the two batches of specimens would be on the basis of load per layer, the plotted stresses used in Fig 32 were 0.8 of those used in the tests for batch two. As can be seen from Fig 32, lives of the second batch were somewhat below those of the first batch.

As can be seen from Fig 32, Miner's Rule predicted similar lives for Felix and Felix Block VI at the lower stress levels, but predicted lives under Felix to be slightly longer than those under the block loading at the higher stress levels. In contrast the actual fatigue strength under Felix Block VI at the highest stress tested, giving 100 flights to failure, was about 20 per cent higher than that under Felix at the same life, decreasing to about 7 per cent higher at 100 flights to failure. Cumulative damage behaviour was somewhat different for the two loading actions with the achieved fatigue strength under Felix being generally between 10 and 20 per cent below that predicted, and that for the block loading ranging from about 7 per cent below predicted at the lowest stress level tested to 10 per cent above at the highest level tested.

Since the lives for the Felix Block VI tests tended predominantly to last longer than predicted by Miner's Rule, a relative Miner prediction from these would predict for

Felix lives tending to be longer than predicted by Miner's Rule direct and shown in Fig 32. Consequently Relative Miner predictions for Felix would be slightly more in error than those for Miner's Rule applied directly.

### 9.3 Shear stress specimens of unidirectional GRP

Fig 33 and Tables 33 to 34 give fatigue results under constant amplitude loading in bending at a range of values of stress ratio R. The specimens all failed in interlaminar shear, a typical failure being shown in Fig 39b. All stresses plotted and tabulated for these specimens are shear stresses calculated according to the formula:

$$\text{Shear stress} = 0.75 F/A \quad (1)$$

where F = total force applied to the top and bottom of the specimen

A = specimen cross sectional area.

As shown on Fig 33 two batches of specimens were included in the tests. It was found that the second batch of specimens were stronger in fatigue than the first. As a consequence the stresses for batch one specimens were plotted at a stress 20 per cent higher than the actual values so that the test results compared well with those from the first batch.

The curves fitted to the data in Fig 33 were to the Weibull equation with double logarithmic scales. Coefficients in the equation were derived using an IABG-developed five-dimensional regression analysis. The final equation is shown below. For clarity it is expressed in two parts:

$$\text{Lg}(\tau_a) = \text{Lg}(\tau_e) + \text{Lg}\left[\frac{78}{\tau_e} \left(\frac{1-R}{2}\right)\right] \text{Exp} - \left(\frac{\text{Lg}(N)}{4.837}\right)^{2.243} \quad (2a)$$

$$\tau_e = (39.33 - 21.53 R)^{0.7744} \quad (2b)$$

Valid for  $-0.22 < R < 0.55$

where  $\tau_a$  = alternating shear stress

$\tau_e$  = endurance limit (shear stress)

N = number of cycles to failure.

The above equation defines a complete Haigh diagram, which was used for the cumulative damage calculations.

Tables 35 to 37 give the results of fatigue tests under Helix and Helix Block V1 and V2. Tables 38 and 39 give the results of tests under Felix and Felix Block V2. The results relating to Helix, together with the predictions using Miner's Rule are plotted on Fig 34. The corresponding data for Felix is plotted on Fig 35.

Fig 34 may be compared with Fig 29, which shows tests under the same combination of sequences but for aluminium alloy specimens. A similarity between the two diagrams is the relative position of the three curves showing the predictions from Miner's Rule.

However, for the GRP specimens the predictions were much closer together and in all cases Miner's Rule predicted lives that were too long. This is in contrast to the case for aluminium alloy where Miner's Rule predicted lives that were too long for Helix and too short for Helix Block V1. The overall picture in Fig 34 does not suggest that Miner's Rule gives errors in prediction that are markedly different for the three sequences, so there is no evidence that Relative Miner predictions from Helix Blocks V1 or V2 would show substantial errors. However it should be emphasised that the data in Fig 34 are sparse, particularly for Helix (one test point), and firm conclusions cannot be drawn.

Turning now to Fig 35 it can be seen that Felix and Felix Block V2 gave similar lives, the most noteworthy point being that Miner's Rule predicted lives that were too long by a large margin, the difference in predicted and achieved fatigue strength for Felix being more than 20 per cent over the range of test lives. The accuracy of Miner's Rule appeared similar for both Felix and Block V2 but again the data were sparse, and although there was no evidence suggesting that Block V2 Relative Miner predictions would be substantially in error, firm conclusions again cannot be drawn.

#### 9.4 Notched specimens of titanium alloy 6Al-4V

Fig 36 and Table 40 give the results of the axial loading fatigue tests carried out at NLR under constant amplitude loading at two values of stress ratio R. Shown also in Fig 36 are RAE tests under constant amplitude loading, which are discussed in section 11.2.

The curves fitted to the data in Fig 36 were to a form used widely in the helicopter industry<sup>23</sup> viz:

$$S_a = S_e \left( 1 + \frac{A}{N^b} \right) \quad (3)$$

where  $S_a$  = stress amplitude

$S_e$  = endurance limit

$N$  = number of cycles to failure.

A regression analysis was used<sup>24</sup> to evaluate parameters in equation (3) which gave the best fit to the data in Fig 36 so that for  $R = 0.1$ :

$$S_a = 97.1 + \left( \frac{3030}{N^{0.825}} \right) \quad (4)$$

and for  $R = 0.5$ :

$$S_a = 99.4 + \left( \frac{344.7}{N^{0.556}} \right) \quad (5)$$

Most of the cycles in Helix, Felix and the relevant block programmes fall within the range  $R = 0$ , which is close to  $R = 0.1$  as represented in the data on Fig 36, and  $R = 0.5$ . Therefore cumulative damage calculations were carried out by calculating

fatigue damage from S-N curves interpolated between those for  $R = 0.1$  and  $R = 0.5$ , and extrapolated outside where necessary.

Tables 41 and 42 give fatigue test results for Felix and Felix Block V2. These are plotted, together with the relevant Miner's Rule predictions, in Fig 37.

Fig 37 presents a picture not dissimilar to that of Fig 30, which shows a corresponding set of results for aluminium alloy. In both cases the predictions for tests under Felix gave lives that were generally too long (unsafe), with the predictions corresponding approximately to the limit of the achieved scatter band on the long life side. In both cases too, Miner's Rule predicted that life under Felix Block V2 would be shorter than under Felix. However whereas the Miner's Rule predictions were reasonably good for aluminium alloy under Felix Block V2, for titanium alloy, where the scatter was considerably greater and the lives were similar to those under Felix, the predictions followed the low life side of the scatter band. It follows therefore that a Relative Miner prediction of Felix lives from the results of the tests under Felix Block V2 would predict lives longer than those of Miner's Rule applied direct. In fact, Fig 37 shows that the achieved lives were shorter than predicted by Miner's Rule direct. Therefore the Relative Miner prediction would be more in error than Miner's Rule applied direct and, in fact, more unsafe. The amount of extra error would be governed by the difference between the direct Miner predictions for Felix Block V2 and the test results for that loading. This is not easy to assess accurately because of the large scatter, but the results suggest an extra error of 10 per cent on fatigue strength.

Thus it can be concluded that in this case, although the Felix Block V2 tests gave lives similar to those under Felix, the block sequence did not represent Felix well with regard to cumulative damage behaviour, and Relative Miner predictions of Felix from the block tests would be more in error and more unsafe than Miner's Rule applied direct.

#### 10 ASSESSMENT OF THE TEST RESULTS IN TERMS OF THE PROJECTED USES OF HELIX AND FELIX

In sections 9.1 to 9.4 the cumulative damage behaviour of four types of specimen was examined. This assessment was in terms of, first, the accuracy of Miner's Rule applied directly to predict lives under Helix, Felix and the various block programmes. Second was considered the use of a Relative Miner approach to predict lives under the Standards from the block programme data. The discussion continues now to relate this to the projected uses of Helix and Felix.

##### 10.1 Use as tools to obtain comparative fatigue data

The convenience of being able to make a reliable comparison of two sets of fatigue data without resort to cumulative damage rules has already been remarked upon. However it is instructive to examine whether comparisons based on predictions using Miner's Rule would give results significantly different from those using Helix and Felix. Examination of Figs 29, 30, 32, 34, 35 and 37 show that for both Helix and Felix Miner's Rule virtually always predicted lives that were too long. In cases where Miner's Rule overpredicted by the similar amounts, for instance in Figs 30 and 32 for Felix applied to aluminium

alloy and GRP lugs respectively, comparisons were similar to those using Helix and/or Felix. However, there were significant differences in other cases. The largest difference between the two methods of comparison was when comparing aluminium alloy (Fig 30) with unidirectional GRP (Fig 35) for semi-rigid rotor helicopters. Fig 30 shows that the mean fatigue strength under Felix of aluminium alloy specimens was between 0 and 10 per cent less than predicted by the Rule. However in Fig 35 the corresponding factor was between 25 and 30 per cent. Therefore an assessment of the comparative fatigue strength of the two materials based on constant amplitude data would be generally more than 15 per cent in error, assuming of course that the assessment using the more representative Felix was correct.

Consider now the use of block programmed loading for the comparison of fatigue strengths. Helix Block VI appeared to be rather poor in this respect. As can be seen from Fig 29 the fatigue strength for aluminium alloy specimens under this loading was generally more than 50 per cent above that for Helix. However in Fig 34, the only other set of results with either of the Helix block loadings, the fatigue strength agreed well with the one Helix test point and also with the data under Helix Block V2. Helix Block V2 gave much better agreement with Helix for aluminium alloy (Fig 29) particularly at the lower stress levels, and so in this region gave comparative fatigue strengths which were 50 per cent different from those using Helix Block V2.

Felix Block V2 was assessed against Felix in three cases. For aluminium alloys it gave fatigue strengths about 10 per cent below Felix (Fig 30), for unidirectional GRP it gave fatigue strengths similar to Felix (Fig 34), and for titanium alloy specimens, where the scatter was particularly high (Fig 37), it appeared to give fatigue strengths lower than Felix at the higher stresses, and higher than Felix at the lower stresses. Therefore errors in comparative fatigue strengths would be about 10 per cent comparing aluminium alloys with unidirectional GRP, with perhaps some greater errors than that at some stress levels comparing aluminium and titanium alloy. Bearing in mind that few comparisons could be carried out with the block programmes because the coverage was not complete (for instance Felix Block VI was tested on only one type of specimen), there was no reason to suppose from the test results that block programmes would give comparisons more valid than Miner's Rule.

#### 10.2 Use as design data

As shown in section 9 the use of Miner's Rule to predict fatigue lives under Helix and Felix gave some considerable errors, particularly for aluminium alloy under Helix (Fig 29) and unidirectional GRP under Felix (Fig 35) where the fatigue strength was sometimes overestimated by 20 per cent and more. In all cases the Rule predicted lives that were too long. Although these errors can be accounted for in some cases by alternative cumulative damage rules the hope is that Helix and Felix used in conjunction with a Relative Miner approach would give the most reliable predictions. As mentioned in section 9 the present series of tests sought to assess the block programmes as an alternative source of fatigue data to which the Relative Miner approach would be applied in predicting lives for realistic loading sequences as represented by Helix and Felix.

There were no data derived under service loading which could be used to assess Helix and Felix as sources of data to be used in predicting service lives.

The most notable outcome of the test programme was the conclusion that the block programmes did not show the same cumulative damage behaviour as Helix and Felix. Whilst this was most marked in the case of Helix Block V1, which was not regarded as being a good representation of Helix, it was also true of the block programmes V2. This was discussed at length in section 9 and is illustrated particularly in Figs 29 and 37 for aluminium and titanium alloy respectively. In both these cases Miner's Rule predicted lives that were too long for the standard and too short, or relatively inaccurate, for the block programme. However, the Relative Miner approach seeks to minimise errors in Miner's Rule by assuming that cumulative damage behaviour under the waveform for which life is predicted is the same as that under the waveform used to obtain the basic fatigue data. Therefore the use of block programmed loading as the source of basic fatigue data was assessed in section 9 as predicting lives no more accurate than Miner's Rule. In no case was the use of block programmed data likely to predict lives substantially more accurately than Miner's Rule, and for the case of titanium alloy (section 9.4) would predict lives more unsafe as well as less accurate than Miner's Rule. It was concluded from the above that if life prediction more reliable than that provided by Miner's Rule was required it was unlikely to be achieved or substantiated reliably using block programmes. Whilst the possibility of improved life predictions using Helix and Felix as a basis is not proved it is a logical probability and is a promising subject for future research.

It was considered that the conclusion that the block programmes were a poor representation of the cumulative damage behaviour of the more realistic Helix and Felix was the most important finding of the joint test programme.

All the errors assessed above in using block programmes for comparative fatigue data, and life prediction can be said to stem from the lack of correspondence of the cumulative damage behaviour in the two cases. If this lack of correspondence were general, there would be little point in using block programmes of the type assessed, either for fatigue substantiation or life prediction. It is considered that these findings give the strongest possible reasons for adopting more realistic loading in helicopter substantiation procedures, with Helix and Felix playing an important part in this.

#### 11 TESTING WITH SHORTENED VERSIONS OF THE STANDARDS

In their full form Helix and Felix both consist of over 2 million cycles, each sequence representing 140 flights only. Thus a typical test in a servohydraulic machine at 15 Hz to 1500 flights would take about 18 days. There is considerable scope for speeding up tests by using high speed servohydraulic machines; for instance the RAE tests were carried out at 45 Hz, which is three times faster than the example given above. However it was felt that testing times were still formidable and tests were

carried out under sequences with some low level cycles omitted to look at the possibility of further shortening testing times. The tests were on Helix and Helix with levels omitted, on specimens of titanium alloy (section 8.2).

### 11.1 Test sequences

Helix was used as one test sequence. The shortened version was derived by omitting alternating level 20 (old units) and below. This procedure led to 13 out of the 24 manoeuvres in Table 6 disappearing altogether and these were omitted from the sequence. The result was to give a reduction in length of the sequence of 88 per cent. This was the version of the reduced sequence which was used exclusively in the fatigue tests and in this Report is termed Short Helix.

In the subsequent redefinition of Helix and Felix with a reduced number of levels (Appendix B) difficulties were found in defining the shortened version of Helix with a reduction in length similar to that achieved with Short Helix. When omission was employed as before, the omission of level 28 (new units) and below gave only a 44 per cent reduction in length, which was insufficient to give the reduction in testing required. Use of the next level up as the omission level gave a reduction in life of 99 per cent, which was deemed to be excessive. The solution of partial omission adopted is described in sections 6.8 and 7.4, and gave reductions in length of 93 per cent for both Helix and Felix (Table 19). The reduced sequences in the new classification, Helix/32 and Felix/28, were not used in the test programme.

### 11.2 Fatigue test results

Table 43 gives the fatigue test results for constant amplitude loading which are plotted in Fig 36 for comparison with the NLR data. As can be seen the two sets of results did not agree very well. The RAE results showed much greater scatter than the larger NLR specimens and implied a rather higher fatigue limit. Cumulative damage calculations were not therefore carried out for the RAE tests because the S-N data were felt to be inadequate. However, this did not affect the main aim of the tests which was assessment of the performance of the shortened sequence.

Test results under Helix and Short Helix are given in Table 44 and 45 respectively, and plotted in Fig 38. Two peak stress levels only were used in the tests and in both cases the mean life under Short Helix was longer, in terms of number of flights, than under Helix. At the high level the ratio of lives under Short Helix to Helix was 4:1 and at the lower level was 1.8:1. Assuming that Helix gave ideal assessments this represented errors in using Short Helix to assess the fatigue strength of about 4 per cent at the lower stress level and 3 per cent at the higher stress level.

### 11.3 Recommendations for the use of the shortened sequences

In order to reduce testing time in determining fatigue strengths at long lives three approaches can be used. First, the testing frequency can be raised to the limits of valid testing or the limit of the machine, whichever is less. Second, tests can be carried out at a high stress level and the results extrapolated downwards. Third, testing can be carried out using sequences with low levels omitted. The second and third possibilities are the concern of this paper.

The actual results in Fig 38 suggest an error of 4 per cent in using Short Helix to determine the fatigue limit. This is not a particularly large error, and, if validated as a generally applicable result, might well be an acceptable penalty to pay for test lives about one quarter of those for the full standard sequence. A factor based on the results of research work could be used to reduce the errors still further. Alternatively or additionally the results of tests under the full sequence at higher stress levels might be used to deduce the error factor at the fatigue limit, for instance as represented by the tests at the higher stress level in Fig 38 which gave lives under Helix about one tenth of those at the lower stress level.

When low level cycles are removed from a variable amplitude sequence Miner's Rule predicts that, if the S-N curve for the component is a straight line on a Log-Log plot, then the resulting percentage change in life is independent of the overall stress level of the variable amplitude sequence. However, as in Fig 28, S-N curves tend at the bottom to bend towards the long life direction, perhaps forming a fatigue limit, and as a result Miner's Rule predicts that the lowest bank of cycles in, for instance, Helix do some damage at high overall stresses and none, or virtually none, at low overall stress levels. Thus Miner's Rule predicts that the omission of a bank of lowest level cycles will affect life under variable amplitude loading by a larger percentage at high overall stress levels than at low. Although it is generally accepted that cycles below the fatigue limit are more damaging than predicted by Miner's Rule, the above trend is likely still to hold on the grounds that there is still likely to be a damage threshold for small cycles in variable amplitude loading sequences, even if it is somewhat below the constant amplitude fatigue limit. This is supported by the results in Fig 38, where inclusion of low level cycles appeared to be twice as damaging at the higher overall stress level than at the lower.

Nevertheless at present the magnitudes of the errors in using the shortened sequences Helix/32 and Felix/28 are not established and the above results must be regarded as provisional. It is recommended therefore that the shortened sequences should be used with extreme caution. They should be used only at the lower stress levels, close to the fatigue limit where the errors in using them are liable to be less severe as indicated above. Such tests should be supplemented by further tests under the full standard loadings at higher stress levels. Further research is necessary, however, to quantify better the errors in following this procedure, particularly since the data available so far has used Short Helix only.

## 12 CONCLUSIONS

- (1) Two loading standards, Helix and Felix, applying to articulated and semi-rigid rotor helicopters respectively, were defined in both full and shortened forms. The shortened forms of the standards are known as Helix/32 and Felix/28.
- (2) In a fatigue test programme, which included tests on aluminium alloy, titanium alloy and GRP specimens, the use of Helix and Felix was assessed, both from the point of view of tools to provide comparative fatigue data, and as a source of design data.

It was found that Helix and Felix gave comparative fatigue strengths that varied significantly in some cases from those obtained using three-level block programmes, and from those predicted from constant amplitude loading.

It was found also that block programmes designed to be equivalent to Helix and Felix did not represent them well in terms of the accuracy of Miner's Rule in predicting lives under them. The use of data obtained under block programmes and a Relative Miner approach would have led to predictions generally less accurate than those using Miner's Rule applied direct.

(3) It was concluded that the failure of the block programmes to represent the cumulative damage behaviour of the more representative loadings gave the strongest possible reasons for adopting more realistic loading in helicopter substantiation procedures, with Helix and Felix playing an important role in this.

(4) Following tests assessing the effect of omitting low level cycles from Helix, it was recommended provisionally that the shortened versions of the standards should be used with extreme caution, and then only for long life tests to determine the fatigue limit. These tests should be supplemented by tests under the full standards at higher levels.

(5) More research is required into the effect of omitting low level cycles from Helix and Felix, and into the accuracy of the Relative Miner approach using Helix and Felix data as a basis.

Appendix ACONTRIBUTING ORGANISATIONS AND ACKNOWLEDGEMENTSA.1 ORGANISATIONS

LEF: Fraunhofer-Institut für Betriebsfestigkeit

LBF  
Bartningstrasse 47  
D-6100 Darmstadt-Kranichstein  
West Germany

IABG: Industrieanlagen-Betriebsgesellschaft mbH  
Einsteinstrasse 20  
8012 Ottobrun bei München  
West Germany

MBB: Messerschmitt-Bölkow-Blohm GmbH  
Postfach 801140  
8000 München 80  
West Germany

NLR: Nationaal Lucht-en Ruimtevaartlaboratorium  
Voorsterweg 31  
8316 PR Markness E  
NOP  
The Netherlands

RAE: Royal Aircraft Establishment  
Farnborough  
Hampshire GU14 6TD  
UK

A.2 ACKNOWLEDGEMENTS

The support of Westland Helicopters Ltd to this project, particularly Mr A.D. Hall and Mr D. Boocock, is gratefully acknowledged.

Appendix BDERIVATION OF NEW SYSTEM OF UNITS IN HELIX AND FELIX

In the original derivation of Helix and Felix<sup>5</sup> a system of units was used in which the maximum was 74 in both cases. Taking the compressive levels into account also, this gave nearly 100 possible values of range. The actual number of values of range was rather less than this, but there were considerable numbers of ranges in adjacent classes, and so having similar values but rather difficult to identify separately in on-line analysis. A slight error in application accuracy could lead to one range being recorded in the wrong interval. A similar situation existed with regard to peak and trough values. Consequently on-line analysis was rather more complicated than for FALSTAFF and generation mo- difficult because the number of defined levels was greater than the capability of some systems.

It was decided that the number of defined levels was unnecessarily large, so each mean and alternating load value in the two sequences was converted to the new system of units by means of Table 46. The resulting levels crossed spectra are compared with the originals in Figs 40 and 41 for Helix and Felix respectively. As can be seen there was a slight tendency to round up the values of load. It can in fact be seen from Table 46 that this was most marked at the lower stress level. This led to the prediction that the new versions of the standards were somewhat more damaging than the original versions. In an assessment of this using Miner's Rule for the titanium specimens tested at NLR it was predicted that lives under the new versions of the standards would vary between 1 and 0.5 times the lives under the old versions, with the maximum differences at peak levels of about 450 MPa.

It is considered that the above differences do not affect the essential character of Helix and Felix in terms of their planned roles, but some caution should be applied when comparing test results directly with those presented in this Report.

## Appendix C

### ASSESSMENT OF SUITABLE FLIGHT DURATIONS AND SORTIE LENGTHS

#### C.1 GENERAL CONSIDERATIONS

The collection of the Sea King flight durations has been discussed in section 6 and the data presented in graphical form in Figs 11 and 12. For the analysis presented here it is more convenient to have the data in tabular form, Table 45. In this Table for each sortie the number of flights recorded in the initial duration counting interval of 15 min is listed along with the results of using counting intervals of 1 h and 1.5 h. To represent flight durations differing only by 15 min would prove a difficult task and an initial estimate suggested that flight durations differing by 1 h or 1.5 h would be more suitable. The criterion that assesses the suitability of these flight durations is that the most infrequently occurring sortie must occur at least once in the sequence of sorties of the standard. In addition the length of the sequence of sorties should be of the order of 200 sorties long. Details of the analysis follow.

#### C.2 SYMBOLS AND DATA FOR THE ANALYSIS

k	number of counting intervals for the flight length data
m	sortie number m = 1 for Training m = 2 for Transport m = 3 for ASW m = 4 for SAR
$n_{im}$	number of flights of duration $t_i$ for sortie m recorded in Table 45
$NF_{im}$	number of flights of duration $t_i$ for sortie m in the loading standard
$NF_s$	total number of flights in the loading standard
$NFPH_{im}$	number of flights per hour of duration $t_i$ for sortie m in the data
$NFPH_{crit}$	number of flights per hour of duration $t_{crit}$ in the data
$p(t_{im})$	proportion of flights of duration $t_i$ for mission m for the data in Table 45
$p(T_m)$	fraction of 1 hour spent in sortie (all-aircraft sortie mix in Table 2)
$t_i$	mean time of counting interval i for the data in Table 45
$\bar{t}_m$	average flight duration of sortie m in the loading standard
$t_{crit}$	duration of the most infrequent flight in the loading standard.

#### C.3 ANALYSIS

The proportion of flights of duration  $t_i$  for mission m for the data in Table 45 is:

$$p(t_{im}) = \frac{n_{im}}{\sum_{i=1}^k n_{im}}$$

The average flight duration of sortie  $m$  in the loading standard is then:

$$\bar{t}_m = \sum_{i=1}^{i=k} p(t_{im}) t_{im}$$

Using the sortie mix for all aircraft the number of flights per hour of duration  $t_i$  for sortie  $m$  is therefore:

$$NFPH_{im} = \frac{p(t_{im}) p(T_m)}{\bar{t}_m}$$

The criterion has been set that the most infrequent flight must occur once in the loading standard, therefore

$$NF_{im} \geq 1$$

and it follows that

$$NF_{im} = \text{nearest integer value of } \frac{NFPH_{im}}{NFPH_{crit}},$$

and that the length of the loading standard will be:

$$NF_s = \sum_{m=1}^{m=4} \sum_{i=1}^{i=k} NF_{im}$$

with the final constraint that:

$$NF_s \approx 200$$

#### C.4 RESULTS OF ANALYSIS

Three cases were studied using the analysis described above and values of  $NFPH_{im}$ ,  $NF_{im}$  and  $NF_s$  are listed in Table 46 for each case. In the first case to be studied six counting intervals of 1 h were considered, resulting in flight durations of 0.5 to 5.5 h in hourly increments. It can be seen from the data in Table 46 that the critical sortie is a 5.5 h duration ASW mission and for this to occur at least once the sequence of sorties would have to be 6395 flights long. In the second analysis only five counting intervals of an hour were considered, counts recorded between 5 and 6 h being disregarded. Details of the analysis are again presented in Table 46 which indicates that the 4.5 h duration flights for Training, ASW and SAR are the critical sorties that determine the 677 flights of the sortie sequence. In the final analysis presented in

Table 46 the counting interval was increased to 1.5 h and again counts in the longest flight duration region were disregarded. The 3.75 h flights for Training and SAR determine the length of the sortie sequence which at 140 flights was an acceptable length.

Table 1

## MIX OF MANOEUVRES IN SEA KING TRANSPORT, ASW AND SAR SORTIES

Number	Manoeuvre description	Percentage time per hour		
		Transport	ASW	SAR
1	Take-off	0.34	0.12	0.27
2	Forward flight 20 kn	0.40	2.79	0.23
3	Forward flight 30 kn	0.40	2.79	0.23
4	Forward flight 40 kn	0.40	2.79	0.23
5	Forward flight 60 kn	8.49	5.99	25.92
6	Forward flight $V_{NO}$ 103 kn	81.79	35.90	64.82
7	Maximum power climb 70 kn	0.57	1.20	0.44
8	Shallow approach to hover	0.17	-	-
9	Normal approach to hover	-	1.40	0.08
10	Hover	2.83	33.01	4.85
11	Bank turn port 30° $V_{NO}$	0.79	5.51	0.45
12	Bank turn starboard 30° $V_{NO}$	0.79	5.51	0.45
13	Sideways flight to port 30 kn	0.28	0.20	0.22
14	Recovery from 13	0.11	0.08	0.09
15	Sideways flights to starboard 30 kn	0.28	0.20	0.22
16	Recovery from 15	0.11	0.08	0.09
17	Rearwards flight 20 kn	0.28	0.20	0.22
18	Recovery from 17	0.11	0.08	0.09
19	Spot turn port	0.28	0.20	0.22
20	Spot turn starboard	0.28	0.20	0.22
21	Autorotation	0.57	0.40	-
22	Recovery from 21	0.05	0.03	-
23	Descent	0.34	1.20	0.53
24	Landing	0.34	0.12	0.13

Table 2

LYNX DESIGN MISSION MIX

Number	Flight description	Percentage flight time	Number per hour
1	Rapid increase in rpm and engage clutch		5
2	Take-off		5
3	Steady hovering	20	
4	Spot turns		10
5	Low-speed flight control reversals - longitudinal		2.5
6	Low-speed flight control reversals - lateral		2.5
7	Low-speed flight control reversals - yaw		2.5
8	Low-speed flight control reversals - collective		2.5
9	Rearwards flight	0.5	
10	Sideways flight port	0.5	
11	Sideways flight starboard	0.5	
12	Forward flight 0.2 $V_{NE}$	10	
13	Forward flight 0.4 $V_{NE}$	5.4	
14	Forward flight 0.6 $V_{NE}$	6.3	
15	Forward flight 0.8 $V_{NE}$	11.7	
16	Forward flight 0.9 $V_{NE}$ ( $V_{NO}$ )	18	
17	Forward flight 1.0 $V_{NE}$	2.7	
18	Forward flight 1.1 $V_{NE}$	1.0	
19	Cruise turn 0.4 $V_{NE}$	0.6	
20	Cruise turn 0.6 $V_{NE}$	0.7	
21	Cruise turn 0.8 $V_{NE}$	1.3	
22	Cruise turn 0.9 $V_{NE}$	2.0	
23	Cruise turn 1.0 $V_{NE}$	0.3	
24	Transition from hover		7
25	Maximum power climb 70 kn	4	
26	High-speed flight control reversals - longitudinal		2.7
27	High-speed flight control reversals - lateral		2.7
28	High-speed flight control reversals - yaw		2.7
29	High-speed flight control reversals - collective		2.5
30	Descent		7
31	Transition to hover		7
32	Flare		7
33	Entry into autorotation		0.4
34	Recovery from autorotation		0.4
35	Steady flight autorotation	2.5	
36	Control reversals in autorotation - longitudinal	0.1	

Table 2 (concluded)

Number	Flight description	Percentage flight time	Number per hour
37	Control reversals in autorotation - lateral	0.1	0.4
38	Control reversals in autorotation - yaw	0.1	
39	Collective pull up in autorotation		
40	Right turn in autorotation	0.2	
41	Left turn in autorotation	0.2	
42	Single engine flight	3.0	5
43	Landings		

Table 3

PERCENTAGE TIME IN TRAINING, TRANSPORT, ASW AND  
SAR SORTIES FOR UK SERVICE USAGE

Sortie	Percentage time in sortie	
	All aircraft	Sea King
Training	33.0	22.3
Transport	48.5	25.3
ASW	9.0	49.1
SAR	9.5	3.3

Table 4

NUMBER OF FLIGHTS OF EACH SORTIE FOR THE THREE  
FLIGHT DURATIONS IN HELIX AND FELIX

Flight duration (h)	Number of flights			
	Training	Transport	ASW	SAR
0.75	47	38	2	5
2.25	11	20	4	4
3.75	1	5	2	1

Total number of hours represented in each standard = 190.5

Table 5

SEQUENCE OF SORTIES FOR 140 FLIGHT SEQUENCES  
OF HELIX AND FELIX

21, 11, 43, 11, 21, 12, 22, 11, 11, 21, 21, 21, 23, 42, 23, 21, 12, 11, 21, 22, 11,  
 42, 22, 21, 32, 21, 11, 22, 32, 22, 11, 31, 21, 22, 11, 11, 42, 42, 21, 21, 33, 12,  
 31, 22, 22, 11, 11, 11, 11, 11, 21, 21, 11, 41, 11, 12, 22, 22, 22, 11, 21, 11, 21,  
 11, 21, 21, 21, 21, 11, 11, 22, 21, 21, 21, 11, 21, 11, 12, 12, 21, 11, 11, 22, 11,  
 41, 21, 11, 11, 11, 23, 11, 21, 11, 21, 11, 21, 11, 22, 32, 23, 11, 12, 22, 22, 23,  
 12, 21, 11, 22, 11, 11, 41, 33, 22, 32, 21, 11, 21, 21, 22, 21, 21, 12, 21, 11, 21,  
 21, 13, 11, 11, 12, 11, 11, 11, 41, 11, 22, 11, 41, 12.

Key:        Training - 10  
              Transport - 20  
              ASW - 30  
              SAR - 40

Shortest flight duration - 1 (0.75 hour)  
 Middle flight duration - 2 (2.25 hours)  
 Longest flight duration - 3 (3.75 hours)

therefore 23 is a transport flight of the longest duration

Table 6  
LOAD MATRIX FOR HELIX

Alternating stress			20	24	28	32	36	40
No.	Manoeuvre	Mean stress						
1	Take-off	44	2	-	-	-	-	-
2	Forward flight 20 kn	72	13	-	-	-	-	-
3	Forward flight 30 kn	68	-	12	2	-	-	-
4	Forward flight 40 kn	60	4	9	1	-	-	-
5	Forward flight 60 kn	60	11	2	-	-	-	-
6	Forward flight 103 kn	64	2	4	12	-	-	-
7	Maximum power climb 70 kn	68	1	-	-	-	-	-
8	Shallow approach to hover	56	12	5	6	8	4	-
9	Normal approach to hover	60	11	2	4	3	5	1
10	Hover	-	-	-	-	-	-	-
11	Bank turn port 30° $V_{no}$	68	-	1	20	1	-	-
12	Bank turn starboard 30° $V_{no}$	68	-	1	16	1	-	-
13	Sideways flight port, 30 kn	56	3	-	-	-	-	-
14	Recovery from 13	52	11	5	9	1	2	-
15	Sideways flight starboard	60	3	3	3	-	-	-
16	Recovery from 15	52	11	2	3	2	4	1
17	Rearwards flight 20 kn	68	1	-	-	-	-	-
18	Recovery from 17	60	4	-	9	10	1	-
19	Spot turn port	64	30	8	2	-	-	-
20	Spot turn starboard	68	3	-	-	-	-	-
21	Autorotation	60	19	-	-	-	-	-
22	Recovery from 21	60	-	2	10	4	1	-
23	Descent	60	11	2	-	-	-	-
24	Landing	72	1	3	1	-	-	-

All stresses are expressed in Helix units.

Table 7  
LOAD MATRIX FOR FELIX

Alternating stress			16	24	28	32	36	44	48	52	60
No.	Manoeuvre	Mean stress	No. of cycles								
1	Take-off	32	7	13	11	1	-	-	-	-	-
2	Forward flight 0.2 VNE	48	11	2	-	-	-	-	-	-	-
3	Forward flight 0.4 VNE	-	-	-	-	-	-	-	-	-	-
4	Forward flight 0.6 VNE	48	2	-	-	-	-	-	-	-	-
5	Forward flight 0.8 VNE	-	-	-	-	-	-	-	-	-	-
6	Forward flight 0.9 - 1.1 VNE	48	24	1	-	-	-	-	-	-	-
7	Maximum power climb 70 kn	-	-	-	-	-	-	-	-	-	-
8	Transition to hover	40	10	1	-	-	-	-	-	-	-
9	Hover	36	10	1	-	-	-	-	-	-	-
10	Cruise turns 0.4 - 0.8 VNE	60	20	4	-	-	-	-	-	-	-
11	Cruise turns 0.8 - 1.0 VNE	64	14	13	1	-	-	-	-	-	-
12	Sideways flight port	36	11	3	-	-	-	-	-	-	-
13	Sideways flight starboard	36	10	19	13	1	-	-	-	-	-
14	Rearwards	36	10	9	1	-	-	-	-	-	-
15	Spot turns	36	16	2	-	-	-	-	-	-	-
16	Autorotation (AR)	40	32	21	9	3	1	1	-	-	-
17	AR incl large amplitudes	40	32	21	9	3	1	1	3	1	3
18	Recoveries from AR	36	32	2	-	-	-	-	-	-	-
19	Control reversals 0.4 VNE	36	32	12	5	3	1	-	-	-	-
20	Control reversals 0.7 VNE	44	36	13	5	3	2	-	-	-	-
21	Descent	36	-	1	26	2	-	-	-	-	-
22	Landing	8	-	-	-	-	2	-	-	-	-

All stresses are expressed as Felix units.

Table 8

SEQUENCE OF LOADS FOR FIRST THREE OF THE DEFINED HELIX MANOEUVRES

1	Take off 44, 20, 20
2	Forward flight 20 kn 72, 20, 20, 20, 20, 20, 20, 20, 20, 20, 20, 20
3	Forward flight 30 kn 68, 24, 24, 24, 28, 28, 24, 24, 24, 24, 24, 24, 24, 24 etc

Table 9

EQUIVALENCE OF HELIX AND FELIX MANOEUVRES

Helix		Felix		
No.	Manoeuvre	No.	Manoeuvre	Included manoeuvres
1	Take off	1	Take off	Rapid increase rpm take off
2	Forward flight 20 kn	2	Forward flight 0.2 VNE	
3	Forward flight 30 kn	3	Forward flight 0.4 VNE	
4	Forward flight 40 kn	4	Forward flight 0.6 VNE	
5	Forward flight 60 kn	5	Forward flight 0.8 VNE	
6	Forward flight 103 kn	6	Forward flight 0.9 ÷ 1.1 VNE	Fw.fl. 0.9 ÷ 1.0 VNE Fw.fl. 1.1 VNE
7	Maximum power climb 70 kn	7	Maximum power climb 70 kn	
8	Shallow appr. to hover	8	Transition to hover	Transition to hover flare
9	Normal appr. to hover			
10	Hover	9	Hover	Steady hovering transition from hover
11	Bank turn port VNO	10	Cruise turns 0.4 ÷ 0.8 VNE	
12	Bank turn starboard VNO	11	Cruise turns 0.8 ÷ 1.0 VNE	
13	Sideways flight port	12	Sideways flight port	
14	Recovery from 13			
15	Sideways flight starboard	13	Sideways flight starboard	
16	Recovery from 15			

Table 9 (concluded)

Helix		Felix		
No.	Manoeuvre	No.	Manoeuvre	Included manoeuvres
17	Rearwards flight	14	Rearwards	
18	Recovery from 17			
19 20	Spot turn port Spot turn starboard	15	Spot turns	
21	Autorotation	16 (17)	Autorotation (AR) AR incl. large amplitudes)	Entries into AR Steady flight AR Control rev.longit.AR Control rev.lateral AR Control rev.yawing AR Right turn AR Left turn AR Collective pull up AR
22	Recovery from 21	18	Recoveries from AR	
<u>No equivalence</u>		19	Control reversals 0.4 VNE (to be interspersed during) forward flight	Longitudinal Lateral Yawing Collective
<u>No equivalence</u>		20	Control reversals 0.7 VNE (to be interspersed during) forward flights	Longitudinal Lateral Yawing Collective
23	Descent	21	Descent	
24	Landing	22	Landings	

Table 10

FIRST SIX MANOEUVRES IN TRAINING SORTIE OF HELIX

Position No.	Manoeuvre	Manoeuvre No.	Time in manoeuvre	Matrix applications
1	Take off	1	36	6
2	Forward flight 20 kn	2	12	3
3	Forward flight 30 kn	3	12	2
4	Forward flight 40 kn	4	12	3
5	Forward flight 30 kn	3	18	3
6	Forward flight 20 kn	2	20	5

Table 11

PERCENTAGE TIMES IN MANOEUVRES FOR 3.75 h SORTIES IN HELIX

No.	Manoeuvre	Training	Transport	ASW	SAR
1	Take off	0.27	0.27	0.13	0.2
2	Forward flight 20 kn	2.34	0.39	2.79	0.24
3	Forward flight 30 kn	1.69	0.40	2.80	0.22
4	Forward flight 40 kn	1.60	0.41	2.79	0.24
5	Forward flight 60 kn	3.17	8.56	5.96	25.93
6	Forward flight 103 kn	63.04	82.67	35.39	64.93
7	Maximum power climb 70 kn	0.51	0.44	1.33	0.44
8	Shallow appr. to hover	0.07	0.19	0.00	0.00
9	Normal appr. to hover	0.71	0.00	1.39	0.09
10	Hover	19.24	2.86	32.83	4.88
11	Bank turn port VNO	2.22	0.80	5.47	0.44
12	Bank turn starboard VNO	1.78	0.81	5.48	0.44
13	Sideways flight port	0.18	0.24	0.24	0.24
14	Recovery from 13	0.15	0.07	0.07	0.07
15	Sideways flight starboard	0.21	0.23	0.23	0.23
16	Recovery from 15	0.11	0.07	0.07	0.07
17	Rearwards flight	0.30	0.22	0.22	0.22
18	Recovery from 17	0.22	0.09	0.09	0.09
19	Spot turn port	0.67	0.13	0.13	0.13
20	Spot turn starboard	0.40	0.13	0.13	0.13
21	Autorotation	0.44	0.44	0.44	0.00
22	Recovery from 21	0.04	0.04	0.04	0.00
23	Descent	0.52	0.26	1.33	0.56
24	Landing	0.13	0.27	0.13	0.13

Table 12

PERCENTAGE TIMES IN MANOEUVRES FOR 3.75 h SORTIES IN FELIX

No.	Manoeuvre	Training	Transport	ASW	SAR
1	Take off	0.26	0.26	0.12	0.26
2	Forward flight 0.2 VNE	2.25	0.38	2.67	0.22
3	Forward flight 0.4 VNE	1.62	0.38	2.67	0.22
4	Forward flight 0.6 VNE	1.54	0.38	2.67	0.22
5	Forward flight 0.8 VNE	3.04	8.22	5.72	24.89
6	Forward flight 0.9 - 1.1 VNE	60.51	79.22	34.31	62.21
7	Maximum power climb	0.49	0.42	1.28	0.42
8	Transition to hover	0.74	0.16	1.33	0.08
9	Hover	18.74	2.74	31.53	4.67
10	Cruise turns 0.4 - 0.8 VNE	3.07	1.23	8.42	0.69
11	Cruise turns 0.8 - 1.0 VNE	0.77	0.31	2.10	0.17
12	Sideways flight port	0.32	0.30	0.30	0.30
13	Sideways flight starboard	0.31	0.30	0.30	0.30
14	Rearwards	0.50	0.30	0.30	0.30
15	Spot turns	1.03	0.42	0.42	0.42
16/17	Autorotation (AR)	0.42	0.42	0.42	-
18	Recoveries from AR	0.04	0.04	0.04	-
19	Control reversals 0.4 VNE	2.00	2.00	2.00	2.00
20	Control reversals 0.7 VNE	2.00	2.00	2.00	2.00
21	Descent	0.50	0.26	1.28	0.51
22	Landing	0.12	0.26	0.12	0.12

Table 13

HELIX RAINFLOW ANALYSIS

Distribution of the ranges

Range size (Helix units)	Number of ranges	Cumul. number	Average mean (Helix units)
4	5988	4264048	65.5
8	1312	4258060	62.3
12	554	4256748	66.0
16	138	4256194	64.0
20	280	4256056	62.0
24	0	4255776	-
28	554	4255776	66.0
32	0	4255222	-
36	464	4255222	59.2
40	959084	4254758	62.2
44	738	3295674	62.4
48	910654	3294936	63.6
52	7176	2384282	65.4
56	2336362	2377106	64.2
60	4452	40744	65.7
64	20658	36292	61.8
68	542	15634	57.2
72	11796	15092	57.7
76	830	3296	58.4
80	1884	2466	58.5
84	20	582	58.0
88	282	562	56.0
92	0	280	-
96	0	280	-
100	0	280	-
104	0	280	-
108	0	280	-
112	0	280	-
116	0	280	-
120	280	280	40.0

Total number of peaks and troughs in the  
rainflow of Helix = 4264048

Table 14

HELIX ANALYSIS OF PEAKS/TROUGHS AND OF  
POSITIVE LEVEL CROSSINGS

Level (Helix units)	Number peaks	Peaks cumul.	Number troughs	Troughs cumul.	Positive levelcr.
-20	0	2132024	140	140	140
-16	0	2132024	0	140	140
-12	0	2132024	0	140	140
-8	0	2132024	0	140	140
-4	0	2132024	0	140	140
0	0	2132024	0	140	140
4	0	2132024	0	140	140
8	0	2132024	0	140	140
12	0	2132024	281	421	421
16	0	2132024	1688	2109	2109
20	0	2132024	2233	4342	4342
24	0	2132024	10412	14754	14754
28	0	2132024	7093	21847	21847
32	0	2132024	16898	38745	38745
36	0	2132024	1163994	1202739	1202739
40	0	2132024	676930	1879669	1879669
44	0	2132024	210951	2090620	2090620
48	0	2132024	5651	2096271	2096271
52	0	2132024	32039	2128310	2128310
56	141	2132024	88	2128398	2128257
60	160	2131883	1010	2129408	2129107
64	1834	2131723	2283	2131691	2129556
68	2798	2129889	333	2132024	2127091
72	7012	2127091	0	2132024	2120079
76	6346	2120079	0	2132024	2113733
80	248246	2113733	0	2132024	1865487
84	253998	1865487	0	2132024	1611489
88	382222	1611489	0	2132024	1229267
92	1150931	1229267	0	2132024	78336
96	73302	78336	0	2132024	5034
100	5034	5034	0	2132024	0

↑  
Value refers to interval  
between the defined level  
and the one below it.

Table 15

FELIX RAINFLOW ANALYSIS

Distribution of the ranges

Range size (Felix units)	Number of ranges	Cumul. number	Average mean (Felix units)
4	1374	4570144	41.9
8	832	4568770	43.4
12	3682	4567938	50.0
16	2072	4564256	51.9
20	3376	4562184	50.8
24	2462	4558808	49.1
28	1681	4556346	35.3
32	4055804	4554665	47.6
36	1795	498861	39.2
40	10516	497066	49.4
44	960	486550	39.1
48	342776	485590	45.9
52	3184	142814	50.2
56	105036	139630	36.9
60	3930	34594	48.7
64	20528	30664	38.7
68	2158	10136	50.3
72	6756	7978	38.9
76	234	1222	41.9
80	312	988	40.2
84	68	676	41.4
88	50	608	40.0
92	180	558	45.0
96	18	378	40.0
100	16	360	42.0
104	16	344	40.0
108	14	328	34.0
112	13	314	29.8
116	0	301	-
120	285	301	32.9
124	0	16	-
128	16	16	36.0

Total number of peaks and troughs in the  
rainflow of Felix = 4570144

Table 16

FELIX ANALYSIS OF PEAKS/TROUGHS AND OF  
POSITIVE LEVEL CROSSINGS

Level (Felix units)	Number peaks	Peaks cumul.	Number troughs	Troughs cumul.	Positive level cr.
-28	0	2285072	546	546	546
-24	0	2285072	0	546	546
-20	0	2285072	24	570	570
-16	0	2285072	0	570	570
-12	0	2285072	8	578	578
-8	0	2285072	24	602	602
-4	0	2285072	40	642	642
0	0	2285072	1472	2114	2114
4	0	2285072	9442	11556	11556
8	140	2285072	49938	61494	61354
12	0	2284932	55619	117113	116973
16	0	2284932	9146	126259	126119
20	0	2284932	157152	283411	283271
24	0	2284932	81595	365006	364866
28	0	2284932	43200	408206	408066
32	0	2284932	1750246	2158452	2158312
36	140	2284932	17641	2176093	2175813
40	354	2284792	14290	2190383	2189749
44	470	2284438	77633	2268016	2266912
48	3196	2283968	17056	2285072	2280772
52	141552	2280772	0	2285072	2139220
56	8836	2139220	0	2285072	2130384
60	99165	2130384	0	2285072	2031219
64	1796322	2031219	0	2285072	234897
68	22370	234897	0	2285072	212527
72	83615	212527	0	2285072	128912
76	80940	128912	0	2285072	47972
80	17408	47972	0	2285072	30564
84	15500	30564	0	2285072	15064
88	13960	15064	0	2285072	1104
92	1080	1104	0	2285072	24
96	0	24	0	2285072	24
100	24	24	0	2285072	0

↑  
 Value refers to interval  
 between the defined level  
 and the one below it.

Table 17

HELIX/32 RAINFLOW ANALYSIS

(Helix with omission level 32 and below)

Range size (Helix units)	Number of ranges	Cumul. number	Average mean (Helix units)
4	5988	291724	65.5
8	1312	285736	62.3
12	554	284424	66.0
16	138	283870	64.0
20	0	283732	-
24	0	283732	-
28	280	283732	58.0
32	0	283452	-
36	138	283452	70.0
40	15270	283314	65.2
44	0	268044	-
48	40882	268044	60.1
52	732	227162	62.8
56	190524	226430	64.0
60	142	35906	58.0
64	20130	35764	61.8
68	542	15634	57.2
72	11796	15092	57.7
76	830	3296	58.4
80	1884	2466	58.5
84	20	582	58.0
88	282	562	56.0
92	0	280	-
96	0	280	-
100	0	280	-
104	0	280	-
108	0	280	-
112	0	280	-
116	0	280	-
120	280	280	40.0
124	0	0	-
128	0	0	-
132	0	0	-

Total number of peaks and troughs in the  
rainflow matrix of Helix/32 = 291724

Table 18

FELIX/28 RAINFLOW ANALYSIS

(Felix with omission level 28 and below).

Range size (Felix units)	Number of ranges	Cumul. number	Average mean (Felix units)
4	1374	322068	41.9
8	832	320694	43.4
12	3682	319862	50.0
16	1628	316180	56.0
20	4	314552	50.0
24	436	314548	32.6
28	459	314112	16.0
32	4118	313653	48.0
36	4381	309535	52.2
40	1664	305154	44.0
44	692	303490	38.0
48	162666	302798	47.3
52	872	140132	37.3
56	104666	139260	36.9
60	3930	34594	48.7
64	20528	30664	38.7
68	2158	10136	50.3
72	6756	7978	38.9
76	234	1222	41.9
80	312	988	40.2
84	68	676	41.4
88	50	608	40.0
92	180	558	45.0
96	18	378	40.0
100	16	360	42.0
104	16	344	40.0
108	14	328	34.0
112	13	314	29.8
116	0	301	-
120	285	301	32.9
124	0	16	-
128	16	16	36.0
132	0	0	-

Total number of peaks and troughs in the  
rainflow matrix of Felix/28 = 322068

Table 19

NUMBERS OF FULL CYCLES IN HELIX AND FELIX  
BOTH IN FULL AND SHORTENED FORM

Sequence	Number of whole cycles
Helix	2132024
Helix/32	145862
Felix	2285072
Felix/28	161034

Table 20

## SURVEY OF THE JOINT TEST PROGRAMME

Material	Ti 6Al 4V	Al Cu Mg 2 (eq. 2024)	Unidir. GRP	Multidirectional GRP
Specimen type	Open hole, $K_t = 2.5$	Open hole, $K_t = 2.5$	Unnotched	Lugs, 10 mm hole dia.
Thickness	2.2 mm 5.5 mm	5 mm	10 mm	10 (2nd delivery: 8)
Loading type	Axial	Axial	4-point bending	Axial
Laboratory	RAE NLR	IABG LBF	IABG	IABG LBF
Testing type	Number of tests			
Constant amplitude	5 15	5 25	38	45 2
Helix standard	14	21	1	
Helix reduced	14			
Helix block		5 11	9	
Felix standard	11	17	7	18
Felix block	8	5	3	11

Table 21

DETAILS OF MATERIALS USED IN LBF AND IABG TESTSMaterials

Al-alloy 3.1354.5 (equivalent to 2024-T3, unclad),

fabricated by

Vereinigte Aluminium-Werke AG, Bonn.

Chemical composition in per cent:

Cu	Si	Mn	Mg	Fe	Zn
4.72	0.17	0.65	1.65	0.30	<0.03

Mechanical properties:

Sy = 378 MPa

Su = 486 MPa

$\delta_5$  = 17.3 per cent

mean values of five  
static tests each

Glass fibre reinforced plastics (GRP)

Prepeg EHG 275/68/38 (8.4331.1/8.4568.6 Werkstoffleistungsblatt der Deutschen Luftfahrt).

Epoxy reinforced by tissue of glass fibres (fibre content about 55 per cent of volume).

36 layers with the following fibre orientations.

0° layers No. 1, 5, 9, 13, 17, 20, 24, 28, 32, 36

+45° layers No. 2, 6, 10, 14, 18, 19, 23, 27, 31, 35

-45° layers No. 4, 8, 12, 16, 21, 25, 29, 33

90° layers No. 3, 7, 11, 15, 22, 26, 30, 34

valid for multi-  
directional  
GRP-lugs only

Two batches have been tested which differ in thickness but not in number of layers. The laminate build-up is the same in both cases.

Mean static strength of lugs based on net area stresses = 153.6 MPa.

GRP-shear-specimens.

Unidirectional textile roving EC 9 - 756 - K 43 - (68) HF Resin System:

LY 556 / HT 972.

The material was taken out of rotor blades of the MBB BO 105 helicopter. Two batches have been delivered from MBB-UD which differed considerably in fatigue strength.

Table 22

DETAILS OF MATERIAL USED IN NLR TESTS

Titanium alloy Ti-6Al-4V, mill annealed.

German material designation : 3.716.4.1

Tensile strength \* 1073 MPa

0.2 yield strength\* 1052 MPa

Elongation \* 11.3 per cent

\*Average of five tensile test results on prismatic bars according to DIN 50125, taken from the same sheet (in rolling direction).

Chemical composition (per cent).

Fe	C	O <sub>2</sub>	N <sub>2</sub>	H <sub>2</sub>	Al	V	Ti
0.14	0.018	0.18	0.01	0.012	63	4.0	Balance

Table 23

DETAILS OF MATERIAL USED IN THE RAE TESTS

Titanium alloy Ti 318/TA10 annealed.

## Measured mechanical properties

UTS MPa	0.2% PS MPa	% Elongation 50 mm
987	922	12.5

## Measured chemical composition %

Fe	Al	V	O <sub>2</sub>	N <sub>2</sub>
0.09	6.0	4.2	0.14	0.011

Table 24

TEST RESULTS - CONSTANT AMPLITUDE

Material: 3.1354-T3 (eq. 2024-T3)

All tests by LBF except  
where statedNotched specimens  $K_t = 2.5$ ;  $R = 0.1$ 

Machine: Amsler Vibrophore resonant

Specimen No.	Alternating stress (MPa)	Cycles to failure	Frequency Hz	Remarks
A1.2	113	23,000	140	Tests conducted by IABG for comparison of the testing equipment used by LBF and IABG.
A2.9	113	25,000	140	
A2.11	113	27,000	140	
A1.14	113	27,000	140	
A2.7	83	113,000	140	
A2.15	83	112,000	140	
A3.10	83	164,000	140	
A4.7	83	149,000	140	
1.01	83	111,300	32	
2.01	83	293,390	32	
3.01	83	138,470	32	
4.01	83	168,050	32	
5.01	83	128,730	32	
Stair case tests				
A2.5	66	452,000	140	Runout in parenthesis at high level
A4.5	66	535,000	140	
A3.2	60	5,363,000	140	
A2.3	60	6,949,000	140	
A4.15	60(96)	10 <sup>7</sup> (63,000)	140	
A1.16	60	2,350,000	140	
A4.19	60	261,000	140	
A5.20	60	898,000	140	
A5.2	54(96)	10 <sup>7</sup> (46,000)	140	
A1.18	54(96)	10 <sup>7</sup> (58,000)	140	
A4.17	54(96)	10 <sup>7</sup> (57,000)	140	Runout
A5.21	54(96)	10 <sup>7</sup> (63,000)	140	Runout

Table 25

TEST RESULTS - HELIX STANDARD

Material: 3.1354-T3 (eq. 2024-T3)

LBF tests

Notched specimens  $K_t = 2.5$ 

Machine: Servohydraulic with Schenck electronics.

Specimen No.	Peak stress (MPa)	Cycles to failure	Flights to failure	Frequency Hz.	Remarks
A1.6	550	6,000	0.7	25	
A1.10	383	55,000	2.8	25	
A5.18	306	75,000	4.5	25	
A5.10	250	174,900	12.1	35	
xA5.16	250	158,300	10.4	35	Retest at high level
A4.9	200	743,000	43.1	35	
A4.13	200	537,600	29.8	35	
A5.4	200	417,800	22.6	35	
xA4.11	200	484,000	27.5	35	Retest at high level
A1.8	185	904,000	56.1	35	
A3.20	185	513,000	28.1	35	
A3.8	185	778,400	44.4	35	
xA4.1	185	880,000	55.0	35	Retest at high level
A2.20	175	833,800	49.3	35	
A4.20	175	10,536,800	692.5	35	
A3.6	175	693,000	40.4	35	
A3.14	165	4,073,200	267.1	35	
A4.3	165	2,111,700	139.3	35	
xA5.16	165	$28 \times 10^6$	1,800	35	Runout
xA4.11	155	$26 \times 10^6$	1,700	35	Runout
xA4.1	150	$33 \times 10^6$	2,100	35	Runout

Table 26

## TEST RESULTS - HELIX BLOCK FIRST VERSION

Material: 3.1354-T3 (eq. 2024-T3)

LBF tests

Notched specimen  $K_t = 2.5$ 

Machine: Servohydraulic with Schenck electronics

Specimen No.	Peak stress (MPa)	Cycles to failure	Flights to failure	Frequency Hz	Remarks
A4.16	383	122,400	30.0	35	Retest at high level  Only one side cracked
A3.16	383	88,700	21.8	35	
A3.21	306	366,900	90.1	35	
A2.17	306	264,200	64.9	35	
xA3.12	306	24,400	6.0	35	
A5.14	275	2,776,900	681.9	35	
A1.2	275	325,600	80.0	35	
A5.5	275	1,832,500	450.0	35	
A3.4	250	4,625,200	1,135.9	35	
A2.1	250	2,907,500	714.0	35	
xA3.12	200	14,727,900 →	3,600 →	35	Runout

Table 27

## TEST RESULTS - HELIX BLOCK SECOND VERSION

Material: 3.1354-T3 (eq. 2024-T3)

IABG tests

Notched specimens  $K_t = 2.5$ 

Frequency = 30 Hz

Machine: Schenck resonant

Specimen No.	Maximum stress in spectrum (MPa)	Cycles to failure	Flights to failure	Remarks
5	230	855,190	210	Runout
3	200	762,550	187	
4	185	1,458,270	358	
1	170	2,544,290	625	
2	150	16,532,300 →	4,060 →	

Table 28

TEST RESULTS - FELIX STANDARD

Material: 3.1354-T3 (eq. 2024-T3)

IABG tests

Notched specimen  $K_t = 2.5$ 

Test frequency = 25 Hz

Machine: Servohydraulic with Schenck electronics

Specimen No.	Maximum stress in spectrum (MPa)	Cycles to failure	Flights to failure	Remarks
18	300	950,000	60	
22	300	740,000	47	
23	280	1,900,000	120	
17	270	1,250,000	79	
24	260	3,400,000	215	
12	250	2,710,000	172	
13	250	2,100,000	133	
14	250	2,930,000	186	
21	240	2,290,000	145	
A4.18	238	6,100,000	386	
20	230	13,200,000	836	
15	230	3,930,000	249	
A4.4	224	5,670,000	359	
A4.12	224	3,650,000	231	
19	220	19,120,000	1211	
25	220	15,300,000 →	969 →	Runout
16	200	45,000,000 →	2851 →	Runout

Table 29

TEST RESULTS - FELIX BLOCK SECOND VERSION

Material: 3.1354-T3 (eq. 2024-T3)

IABG tests

Notched specimen  $K_t = 2.5$ 

Test frequency: 30 Hz

Machine: Schenck resonant

Specimen No.	Maximum stress in spectrum (MPa)	Cycles to failure	Flights to failure	Remarks
1	300	102,470	25	Retest
2	260	231,070	56	
3	210	967,600	238	
4	190	2,565,360	630	
5	170	23,984,100 →	5,890 →	Runout

Table 30

TEST RESULTS - CONSTANT AMPLITUDE

Material: GRP Multidirectional

All tests by IABG except  
where stated

Specimen: Lug

Frequency: 30-70 Hz

Machine: Schenck resonant

Stress amplitude (MPa)	$R = \left( \frac{S_{\min}}{S_{\max}} \right)$	Cycles to failure	Remarks
50.0	-0.33	344,500	
40.0	-0.33	2,894,100	
32.0	-0.33	14,744,200	
45.0	-0.22	233,900	Lug oval
40.0	-0.22	3,170,000	
35.0	-0.22	5,644,300	Lug oval
30.0	-0.22	19,463,000	
45.0	0.1	25,000	
45.0	0.1	22,800	
43.0	0.1	46,000	
43.0	0.1	66,800	
42.0	0.1	72,830	LBF
40.0	0.1	136,800	
40.0	0.1	176,500	
40.0	0.1	231,800	
37.0	0.1	830,200	
37.0	0.1	397,600	
35.0	0.1	1,140,000	LBF
35.0	0.1	718,000	
34.0	0.1	1,625,200	
34.0	0.1	1,555,500	
32.0	0.1	2,643,700	
31.5	0.1	3,221,800	
31.5	0.1	2,348,000	
29.0	0.1	11,563,000	
29.0	0.1	4,033,000	
29.0	0.1	4,868,500	
29.0	0.1	8,489,600	

Table 30 (concluded)

Stress amplitude (MPa)	$R = \left( \frac{S_{\min}}{S_{\max}} \right)$	Cycles to failure	Remarks
29.0	0.1	$10^7$ →	Runout
26.7	0.1	$10^7$ →	Runout
26.7	0.1	$10^7$ →	Runout
26.7	0.1	$10^7$ →	Runout
26.7	0.1	19,594,800	
25.0	0.1	24,580,000	
25.0	0.1	47,438,200	
40.0	0.2	48,700	
35.0	0.2	432,800	
30.0	0.2	1,841,000	
25.0	0.2	11,532,100	
40.0	0.4	5,000	
30.0	0.4	135,600	
25.0	0.4	825,200	
20.0	0.4	11,561,600	
28.0	0.55	41,000	
23.0	0.55	151,600	
20.0	0.55	785,200	
16.0	0.55	26,296,400	

Table 31

TEST RESULTS - FELIX STANDARD

Material: Multidirectional GRP

LBF tests

Specimen: Lug

Machine: Servohydraulic with Schenck electronics

Specimen No.	Peak stress (MPa)	Cycles to failure	Flights to failure	Frequency Hz	Remarks
10	130	314,100	16.3	35	Retest at high level
7	130	326,900	16.8	35	
x15	130	96,800	5.9	35	
x22	130	83,200	5.8	35	
16	110	1,835,900	110.5	35	
13	110	1,531,800	98.1	35	
4	110	1,968,600	119.0	35	
9	102	3,234,300	195.4	35	
14	102	1,975,600	119.3	35	
17	102	3,361,700	201.6	35	
11	102	4,457,400	272.5	35	
1	95	3,627,400	223.9	35	
20	95	11,495,200	705.6	35	
3	95	9,261,100	567.7	35	
8	95	6,672,000	407.9	35	
25	91	20,314,900	1,302.1	35	
x22	87	$31 \times 10^6$ →	2,000 →	35	Runout
x15	80	$30 \times 10^6$ →	2,000 →	35	Runout

Table 32

TEST RESULTS - FELIX BLOCK FIRST VERSION

Material: Multidirectional GRP

LBF tests

Specimen: Lug

Machine: Servohydraulic with Schenck electronics

Specimen No.	Peak stress (MPa)	Cycles to failure	Flights to failure	Frequency Hz	Remarks
23	130	361,900	88.8	35	Batch 1 about 10 mm thick
24	130	569,800	139.8	35	
6	110	2,278,700	559.2	35	
18	110	2,107,900	517.3	35	
2	102	3,135,500	769.5	35	
19	95	5,700,700	1,399.0	35	
26	130	828,700	203.5	35	Batch 2 about 8 mm thick
28	110	3,418,000	839.4	35	
27	102	4,560,700	1,120.0	35	
29	95	6,270,900	1,540.0	35	
30	91	9,121,300	2,240.0	35	

Note: Plotted stresses reduced by 20% to give comparison on the basis of the same load per layer.

Table 33

TEST RESULTS - CONSTANT AMPLITUDE LOADING

Material: Unidirectional GRP (first batch)

IABG tests

Specimen: 4 point bend

Specimen No.	Minimum shear stress	Maximum shear stress	Stress amplitude (MPa)	$R = \left( \frac{\tau_{\min}}{\tau_{\max}} \right)$	Cycles to failure	Remarks
1.	5.2	47.2	20.5	0.11	7,000	Amsler F ~ 55 Hz
2	4.8	43.6	19.0	0.11	10,000	
22	4.5	41.3	17.9	0.11	74,500	
21	4.5	41.3	17.9	0.11	52,300	
31	4.5	41.3	17.9	0.11	86,800	
32	4.3	38.9	16.9	0.11	152,900	
33	4.2	37.8	16.4	0.11	160,200	
25	4.1	37.1	16.1	0.11	1,751,000	
34	3.9	35.5	15.4	0.11	2,666,200	
3	3.6	33.0	14.4	0.11	1,914,200	
4	3.6	33.0	14.1	0.11	12,712,000	
12	5.2	47.2	21.00	0.11	6,200	Schenck Reson F ~ 33 Hz
16	4.9	44.9	20.00	0.11	29,400	
29	4.7	42.7	19.00	0.11	56,900	
14	4.4	40.4	18.00	0.11	108,100	
1.12	4.4	40.4	18.00	0.11	25,900	
39	4.3	39.3	17.50	0.11	457,200	
1.6	4.2	38.2	17.00	0.11	48,900	
38	4.0	36.5	16.25	0.11	439,000	
26	4.00	36.0	16.00	0.11	952,500	
41	3.7	33.7	15.00	0.11	7,351,000	
9	4.9	44.9	20.00	0.11	41,120	Servohydr F ~ 25 Hz
10	4.9	44.9	20.00	0.11	9,780	
15	4.9	44.9	20.00	0.11	16,700	
36	5.6	50.6	22.50	0.11	3,910	Servohydr F ~ 5 Hz
5	4.9	44.9	20.00	0.11	11,250	
37	4.6	41.6	18.50	0.11	81,800	

Table 34

## TEST RESULTS - CONSTANT AMPLITUDE LOADING

Material: Unidirectional GRP (second batch)

IABG tests

Specimen: 4 point bend

Specimen No.	Minimum shear stress	Maximum shear stress	Stress amplitude (MPa)	$R = \left( \frac{\tau_{\min}}{\tau_{\max}} \right)$	Cycles to failure	Remarks
U1.17	10.1	45.9	28.00	-0.22	23,800	Servohydr
01.10	9.4	42.6	26.00	-0.22	50,200	F ~ 25 Hz
U1.5	8.7	39.4	24.00	-0.22	447,100	
U1.15	5.9	53.9	24.00	0.11	16,600	Servohydr
01.12	5.4	49.4	22.00	0.11	34,200	F ~ 25 Hz
01.13	5.2	47.2	21.00	0.11	138,800	
01.3	5.0	45.0	20.00	0.11	10,200,000	Runout
7	4.3	39.3	17.50	0.11	2,345,380	
U1.3	4.2	38.2	17.00	0.11	11,339,000	Runout
01.11	24.0	60.0	18.00	0.4	3,300	Schenck Res F ~ 33 Hz
01.8	20.0	50.0	15.00	0.4	12,965,600	Servohydr F ~ 25 Hz

Table 35TEST RESULTS - HELIX STANDARD

Material: Unidirectional GRP (second batch)

IABG tests

Specimen: 4 point bend

Machine: Servohydraulic with Schenck electronics

Specimen No.	Maximum shear stress in spectrum (MPa)	Cycles to failure	Flights to failure	Remarks
28	48.0	1,900,000	120	

Table 36TEST RESULTS - HELIX BLOCK FIRST VERSION

Material: Unidirectional GRP (first batch)

IABG tests

Specimen: 4 point bend

Frequency: 30 Hz

Machine: Schenck resonant

Specimen No.	Maximum shear stress in spectrum (MPa)	Cycles to failure	Flights to failure	Remarks
U1.13	42.0	11,997,480	2,946	Runout
43	42.0	3,419,416	840	
45	37.8	2,292,700	563	
46	37.8	5,691,020	1,398	
42	37.8	59,461,700	14,602	Runout

Table 37TEST RESULTS - HELIX BLOCK SECOND VERSION

Material: Unidirectional GRP (second batch)

IABG tests

Specimen: 4 point bend

Frequency: 30 Hz

Machine: Schenck resonant

Specimen No.	Maximum shear stress in spectrum (MPa)	Cycles to failure	Flights to failure	Remarks
U1.8	50.82	285,178	70	
1.7	50.82	1,538,300	378	
U1.11	46.20	9,693,400	2380	
01.6	44.00	13,259,000	3256	

Table 38TEST RESULTS - FELIX STANDARD

Material: Unidirectional GRP (second batch)

IABG tests

Specimen: 4 point bend

Specimen No.	Maximum shear stress in spectrum (MPa)	Cycles to failure	Flights to failure	Remarks
1.18/0	50.82	5,720,000	362	
7.1/4	50.82	3,070,000	194	
1.14/0	50.82	770,000	49	
1.10/U	50.82	2,070,000	131	
1.5/U	48.28	8,240,000	522	
1.15/0	48.28	7,850,000	497	
1.17/0	47.10	33,230,000	2106	

Table 39

TEST RESULTS - FELIX BLOCK SECOND VERSION

Material: Unidirectional GRP (second batch)

IABG tests

Specimen: 4 point bend

Frequency: 30. Hz

Machine: Schenck resonant

Specimen No.	Maximum shear stress in spectrum (MPa)	Cycles to failure	Flights to failure	Remarks
01.6	50	3,025,770	245	Cancelled
U1.11	50			
01.15	45	17,957,590	4418	
U1.10	45	438,510	105	

Table 40

TEST RESULTS - CONSTANT AMPLITUDE LOADING

Material: Titanium alloy 6Al-4V

NLR tests

Specimen: Notched  $K_t = 2.5$ 

Frequency: 15 Hz

Machine: Amsler pulsator

R	Specimen No.	(1) $S_{max}$ (MPa)	(1) $S_{min}$ (MPa)	(1) $S_a$ (MPa)	Cycles to failure	Remarks
0.5	15	700	350	175.0	32,000	
	42	700	350	175.0	20,300	
	4	600	300	150.0	31,600	
	6	550	275	137.5	39,900	
	2	500	250	125.0	69,200	
	5	450	225	112.5	157,300	
	17	400	200	100.0	1,415,800	
0.1	8	600	60	270.0	12,200	
	9	500	50	225.0	27,600	
	10	450	45	202.5	42,500	
	11	400	40	180.0	56,000	
	14	350	35	157.5	111,100	
	38	300	30	135.0	124,300	
	44	300	30	135.0	192,600	
	43	260	30	115.0	1,583,800	

(1) NOTE: Stresses refer to net section of specimen.

Table 41

TEST RESULTS - FELIX STANDARD

Material: Titanium alloy 6Al-4V  
 Specimen: Notched  $K_t = 2.5$   
 Frequency: 12.5 Hz  
 Machine: Amsler servohydraulic

NLR tests

Specimen No.	$S_{max}$ (MPa)	Life (flights)	Remarks
20	650	42	Re-test at high level
52	650	19	
24	650	37	
25	550	74	
18	500	164	
26	450	275	
55	400	201	
48	400	276	
66	400	161	
68	375	1711	Runout
52	350	1500 →	

Table 42

TEST RESULTS FELIX BLOCK PROGRAMME - SECOND VERSION

Material: Titanium alloy 6Al-4V  
 Specimen: Notched  $K_t = 2.5$   
 Frequency: 7.5 Hz  
 Machine: Amsler servohydraulic

NLR tests

Specimen No.	$S_{max}$ (MPa)	Life (flights)	Remarks
51	600	32	Re-test at high level
53	500	31	
50	500	416	
47	500	106	
56	450	53	
45	450	1502	
54	425	794	
50	400	1478 →	Runout

Table 43

CONSTANT AMPLITUDE TEST RESULTS

Material: Titanium alloy 6Al-4V

RAE tests

Specimen: Notched 2.5 K<sub>t</sub>

Frequency: 45 Hz

R = 0.1

Machine: Instron servohydraulic

Specimen No.	Alternating stress (MPa)	Cycles to failure
D33	157	4,523,570
D34	191	2,960,310
D35	191	2,112,450
D36	191	73,260
D37	191	51,280

Table 44

TEST RESULTS FOR HELIX

Material: Titanium alloy 6Al-4V

RAE tests

Specimen: Notched 2.5 K<sub>t</sub>

Frequency: 45 Hz

Machine: Instron servohydraulic

Specimen No.	Peak stress (MPa)	Cycles to failure	Flights to failure
D3	459	779,127	44
D4	459	431,137	23
D13	459	224,644	13
D14	459	2,126,913	139
D15	459	1,156,619	76
D16	459	4,689,455	303
D17	459	1,344,595	89
D18	459	584,384	33
D24	383	27,947,751	1834
D25	383	21,295,087	1401
D26	383	15,602,008	1019
D29	383	19,828,814	1299
D30	383	27,490,083	1807
D32	383	30,717,791	2016

Table 45

TEST RESULTS FOR SHORT HELIX

Material: Titanium alloy 6Al-4V  
Specimen: Notched 2.5 K<sub>t</sub>  
Frequency: 45 Hz  
Machine: Instron servohydraulic

RAE tests

Specimen No.	Peak stress (MPa)	Cycles to failure	Flights to failure
D1	459	177,093	101
D2	459	99,178	51
D7	459	235,616	131
D8	459	202,410	112
D9	459	1,422,872	803
D10	459	158,247	93
D11	459	1,225,678	689
D12	459	2,181,961	1228
D19	383	4,214,441	2373
D20	383	16,353,950	9212
D21	383	5,094,533	2870
D22	383	3,644,262	2085
D23	383	877,975	497
D27	383	9,308,860	5238

Table 46

EQUIVALENCE OF OLD AND NEW UNITS IN HELIX AND FELIX

	Number of class	Range of old units	New units
	1	73-75	100
	2	70-72	96
	3	67-69	92
	4	64-66	88
	5	61-63	84
	6	58-60	80
	7	55-57	76
	8	52-54	72
	9	49-51	68
	10	46-48	64
	11	43-45	60
	12	40-42	56
	13	37-39	52
	14	34-36	48
	15	31-33	44
	16	28-30	40
	17	25-27	36
	18	22-24	32
	19	19-21	28
	20	16-18	24
	21	13-15	20
	22	10-12	16
	23	7-9	12
	24	4-6	8
	25	1-3	4
	26	-2-0	0
	27	-5- -3	-4
	28	-8- -6	-8
	29	-11- -9	-12
	30	-14- -12	-16
Helix	31	-17- -15	-20
	32	-20- -18	-24
Felix	33	-23- -21	-28

REFERENCES

- | <u>No.</u> | <u>Author</u>                                        | <u>Title, etc</u>                                                                                                                                                                                                  |
|------------|------------------------------------------------------|--------------------------------------------------------------------------------------------------------------------------------------------------------------------------------------------------------------------|
| 1          | Various authors                                      | FALSTAFF. A description of a Fighter Aircraft Loading<br>STANDARD For Fatigue evaluation.<br>Joint publication by F+W (Switzerland), LBF and IABG (Germany)<br>and NLR (Netherlands) (1976)                        |
| 2          | J.B. de Jonge<br>D. Schütz<br>H. Lowak<br>J. Schijve | A standardised load sequence for flight simulation tests on<br>transport wing structures.<br>NLR TR 73029 U, LBF Bericht FB-106 (1973)                                                                             |
| 3          | Various authors                                      | Standard load sequences for helicopter rotor parts. -<br>feasibility study.<br>IABG Report No.893 (1972)                                                                                                           |
| 4          | P.R. Edwards<br>J. Darts                             | Standardised fatigue loading sequences for helicopter rotors<br>(Helix and Felix). Part 2 : Final definition of Helix and<br>Felix.<br>RAE TR 84085, NLR TR 84043 U Pt.2, LBF FB 167 Pt.2 IABG TF<br>1425/2 (1984) |
| 5          | J. Darts<br>D. Schütz                                | Development of standardised fatigue test load histories for<br>helicopter rotors - basic considerations and definition of<br>Helix and Felix.<br>In 'Helicopter fatigue life assessment', AGARD CP-297 (1980)      |
| 6          | D. Schütz<br>H.G Köbler<br>W. Schütz<br>M. Hück      | Development of standardised fatigue test load histories for<br>helicopter rotors - fatigue test programme and test results.<br>In 'Helicopter fatigue life assessment', AGARD CP-297 (1980)                        |
| 7          | A.A. ten Have                                        | Helix and Felix: loading standards for use in the fatigue<br>evaluation of helicopter rotor components.<br>NLR MP 82041U, also in AGARDograph 'Helicopter fatigue design<br>guide' (1983)                          |
| 8          | D. Schütz<br>H. Lowak                                | Zur Verwendung von Bemessungsunterlagen aus Versuchen mit<br>betriebsähnlichen Lastfolgen zur Lebensdauerabschätzung.<br>Fraunhofer-Institut für Betriebsfestigkeit, Darmstadt LBF-<br>Bericht No.FB 109 (1976)    |
| 9          | W. Schütz                                            | The fatigue life under three different load spectra - tests<br>and calculations.<br>AGARD-CP-118 Symposium on random loading fatigue, Lyngby,<br>Denmark (1972)                                                    |
| 10         | A.D. Hall                                            | Helicopter design mission load spectra.<br>In : 'Helicopter design mission load spectra', AGARD-CP-206,<br>pp 3-1 to 3-5 (1976)                                                                                    |

REFERENCES (continued)

<u>No.</u>	<u>Author</u>	<u>Title, etc</u>
11	P.B. Hovell D.A. Webber	Operational flight data from a helicopter in the training role. RAE Technical Report 78014 (1978)
12	T.L. Cox F.J. Giessler	Acquisition of operational data during NOE missions. USARTL-TR-78-3 (1978)
13	T.L. Cox R.B. Johnson S.W. Russell	Dynamic loads and structural criteria. USAAMRDL-TR-75-9 (1975)
14	R. Boocock L.L. Erle J.F. Needham G.D. Roeck H.G. Smith	OH-6A design and operational flight loads study. USAAMRDL-TR-73-21 (1974)
15	R. Prinz	Die Ermittlung der Lebensdauer von Hubschrauberbauteilen. DLR Mitt 69-26 (also as 'Determination of the life of helicopter structural members', RAE Library Translation 1520 (1972))
16	J.E. Dougherty H.E. Spicer	Helicopter fatigue substantiation procedures for civil aircraft. In 'Symposium on fatigue tests of aircraft structures - low cycle, full scale and helicopters'. ASTM STP 338 (1963)
17	J.H. Argyris W. Aicher H.J. Ertelt	Analyse und Synthese von Betriebsbelastungen. ISD Report 193 (also as 'Analysis and synthesis of operational loads', RAE Library Translation 2008 (1979))
18	W.J. Critchlow C.J. Buzzetti J. Fairchild	The fatigue and fail-safe program for the certification of the Lockheed model 286 rigid rotor helicopter. In 'Aircraft fatigue-design, operation and economic aspects'. Proc 5th ICAF Symposium Melbourne, published Pergamon (1972)
19	J.D. Porterfield P.F. Maloney	Correlation and evaluation of CH-47A flight spectra data from combat missions in Vietnam. USA AVLABS-TR-69-77 (1970)
20	W. Schütz J. Bergmann M. Hück	Helix-Felix. Standard load sequences for the evaluation of helicopter rotor parts - tests and results. IABG TF-1397 (1983)
21	J.B. de Jonge A. Nederveen A.A. ten Have	Fatigue tests on notched titanium specimens under the helicopter test load spectrum Felix. NLR TR 82046 L (1983)
22	H. Lowak	Ergänzende Untersuchungen zur Zeitfestigkeit gekerbter Flachstäbe aus 3.1354.5. LBF TM 75/75

REFERENCES (concluded)

<u>No.</u>	<u>Author</u>	<u>Title, etc</u>
23	Various authors	Helicopter fatigue - a review of current requirements and substantiation procedures. AGARD Report No.294 (1979)
24	R. Noback	State of the art and statistical aspects of helicopter fatigue substantiation procedures. In 'Helicopter fatigue life assessment', AGARD CP-297 (1980)

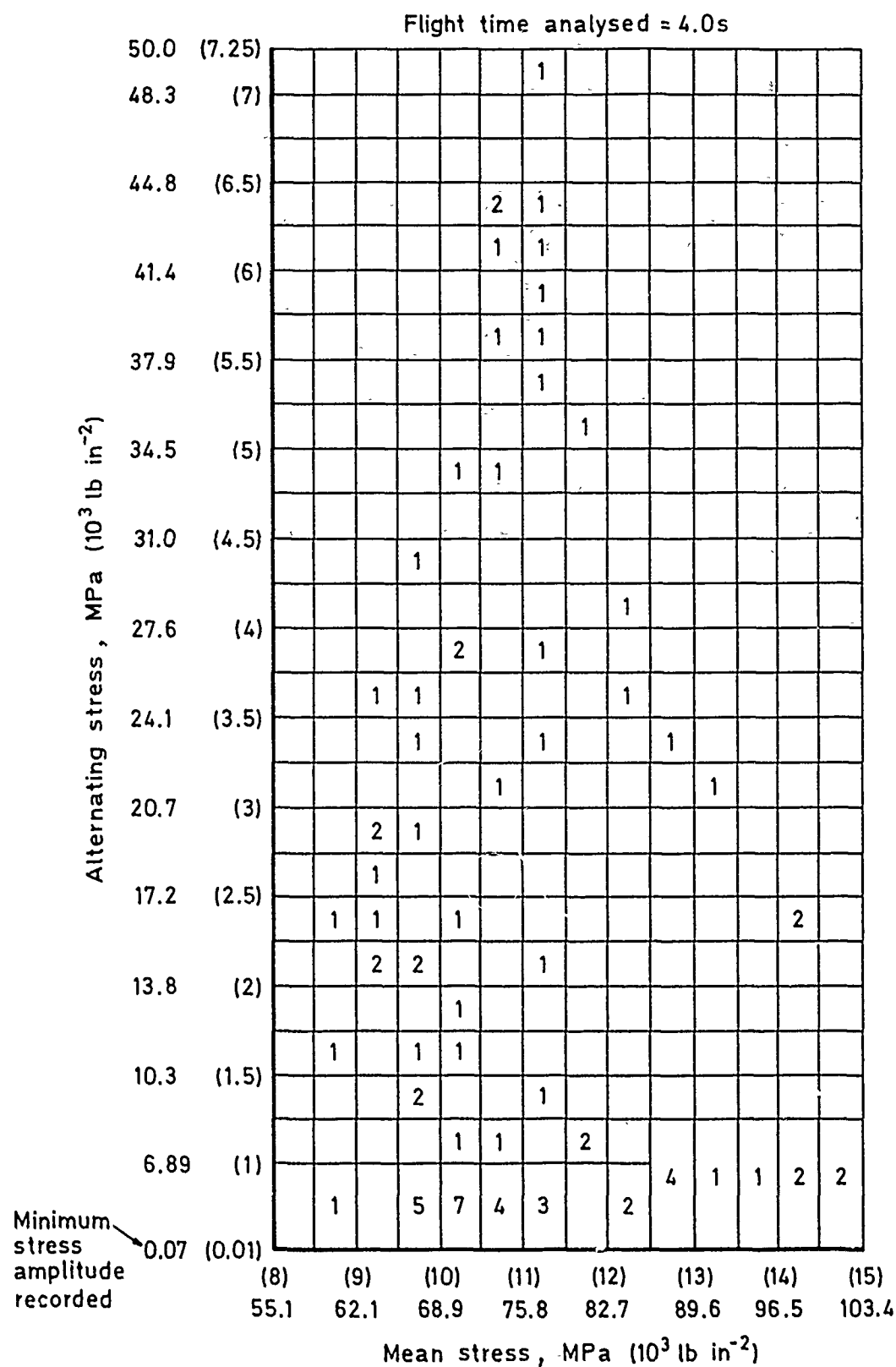


Fig 1 Stress spectrum at the bottom rear corner of Sea King blade spar at half rotor radius for a normal approach to hover

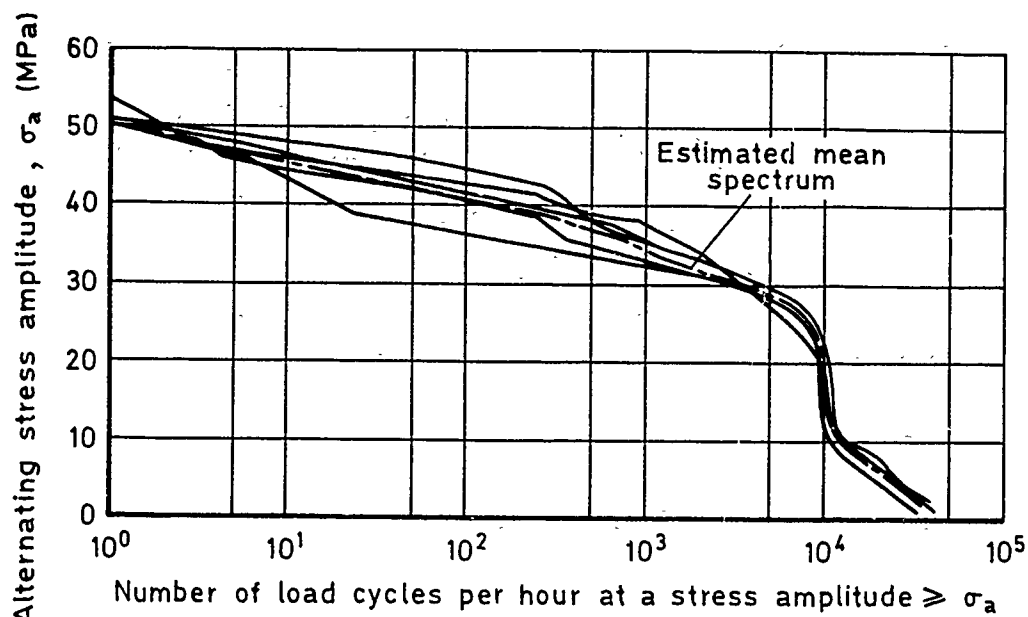


Fig 2 Stress spectra for five CH 53 transport flights

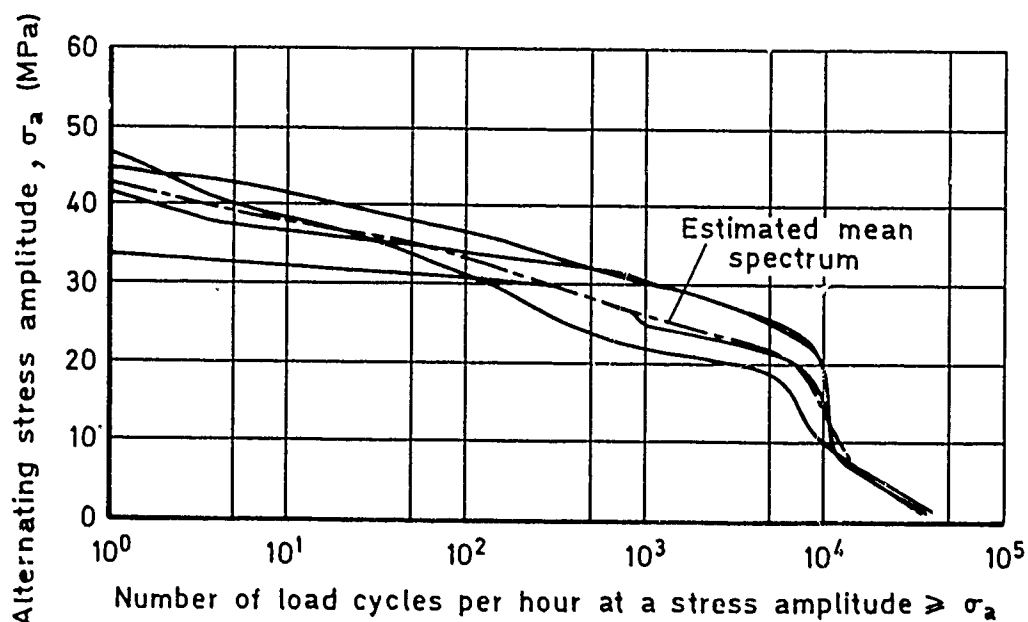
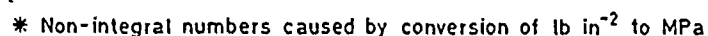
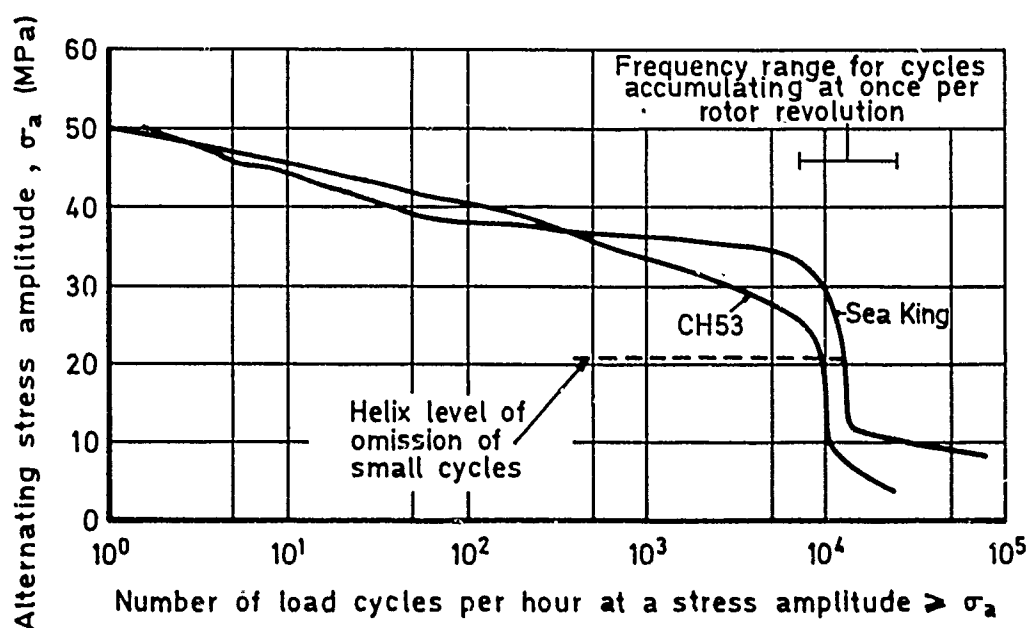


Fig 3 Stress spectra for four CH 53 training flights



**Fig 4** Synthesised stress spectrum for Sea King blade at half rotor radius for the transport role



**Fig 5 Comparison of stress spectra at half rotor radius for CH 53 and Sea King transport sorties**

Numbers in boxes are the number of cycles per hour

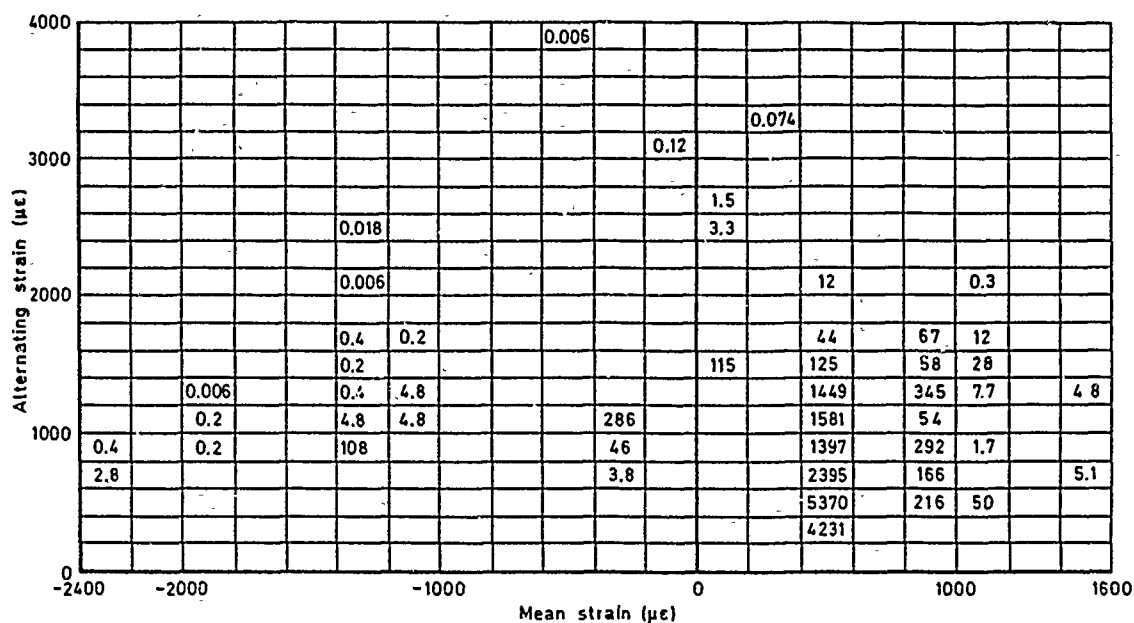


Fig 6 Synthesised Lynx strain spectrum for low surface of inner flexible element at 3.4% rotor radius

Matrix for 3.6s of flight

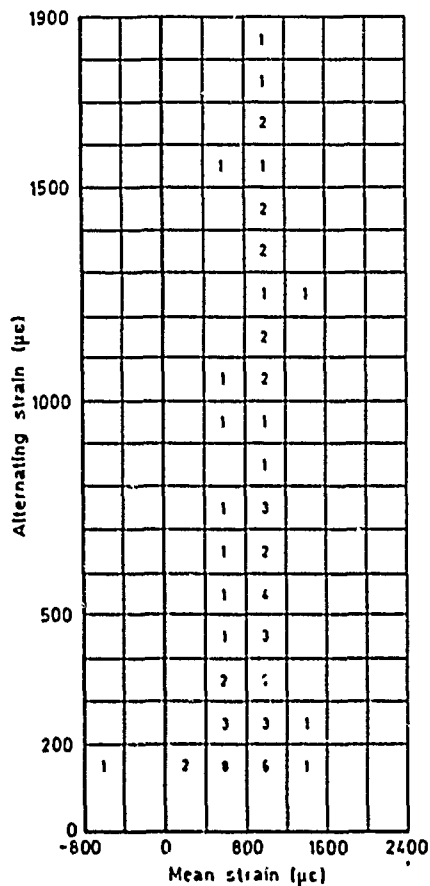


Fig 7 Strain spectrum for the lower surface of BO-105 blade root for a longitudinal control reversal in autorotation

Numbers in boxes are the number of cycles per hour

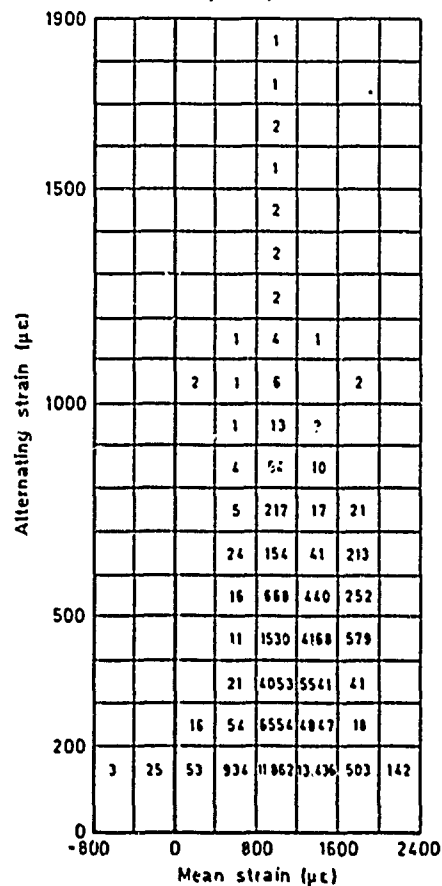


Fig 8 Strain spectrum for lower surface of BO-105 blade root

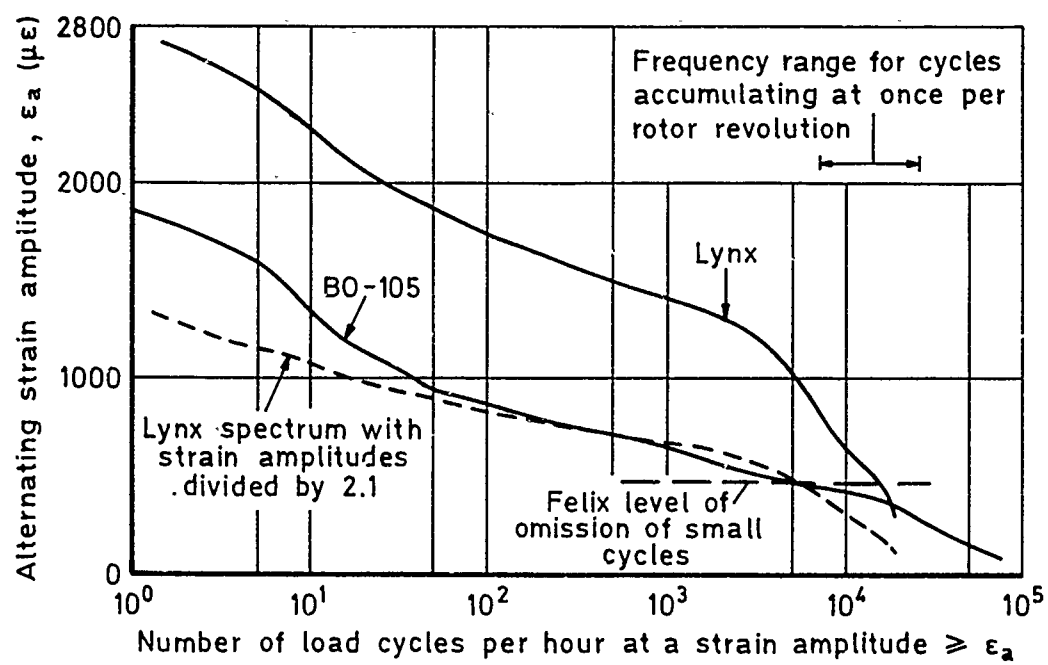


Fig 9 Comparison of strain spectra for BO-105 and Lynx design sortie

Fig 10

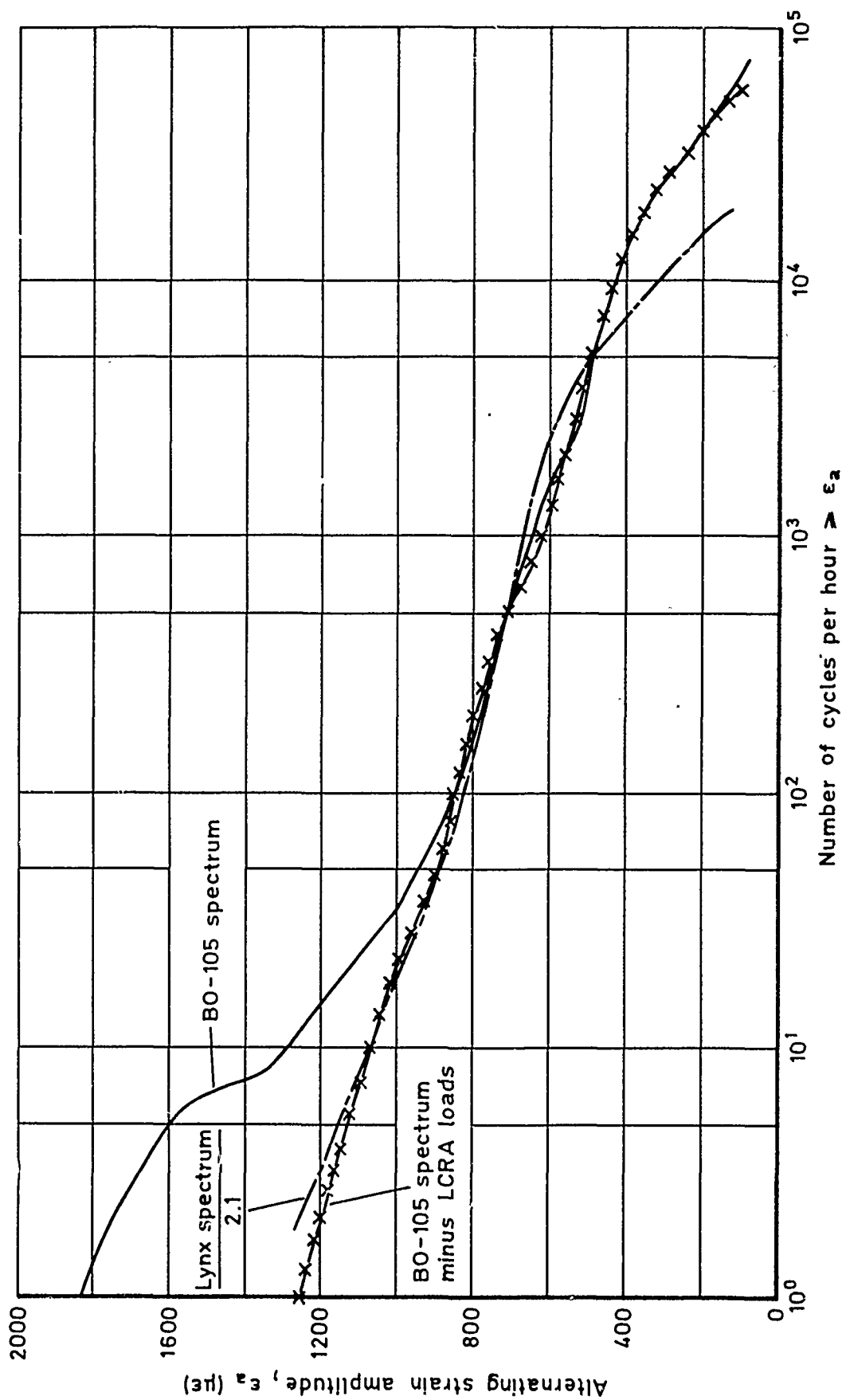


Fig 10 Comparison of factored Lynx spectrum with BO-105 spectrum minus longitudinal control reversal in autorotation loads

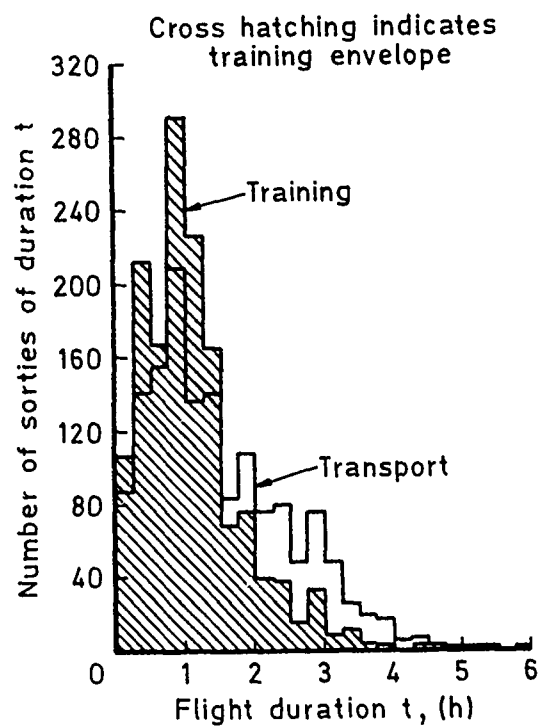


Fig 11 Variation of flight duration for Sea King training and transport sorties

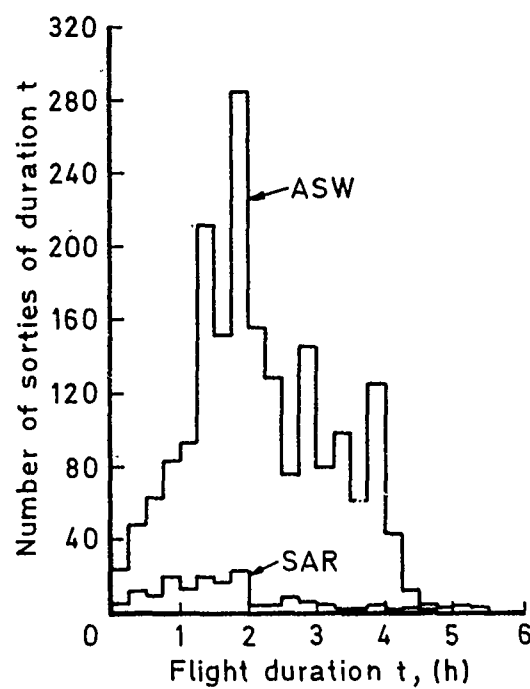
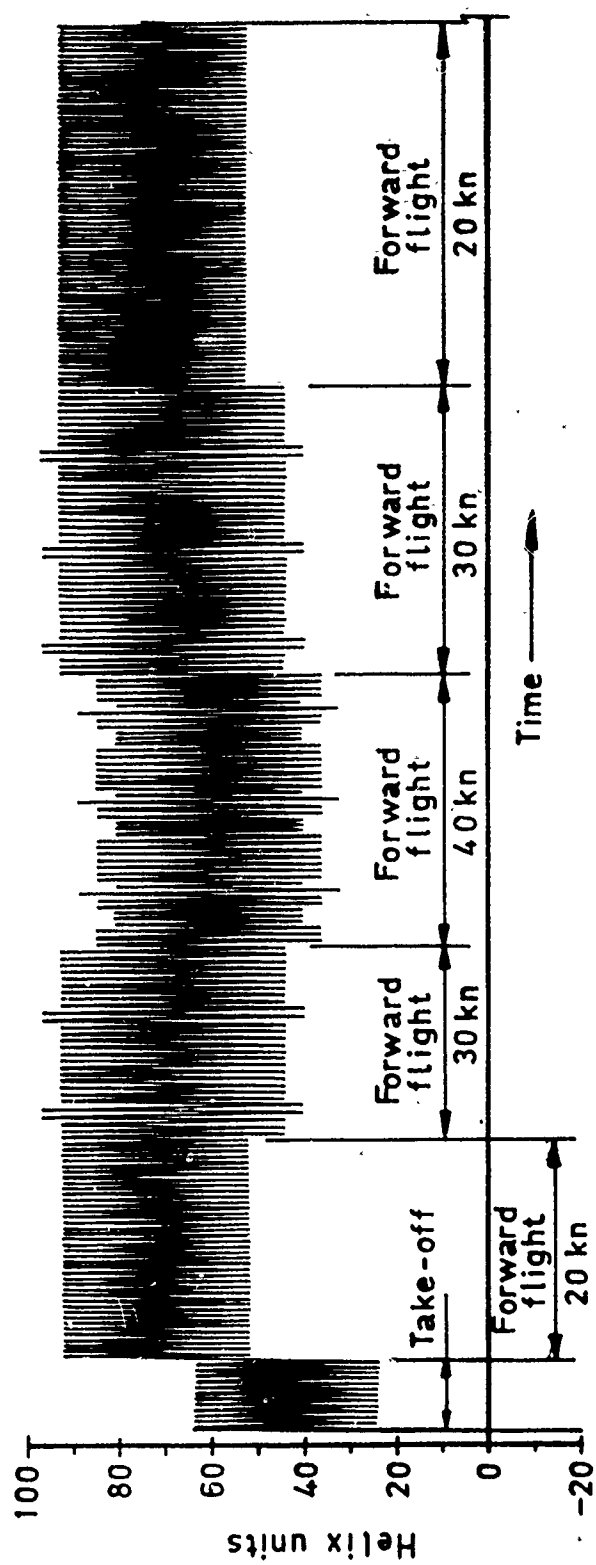
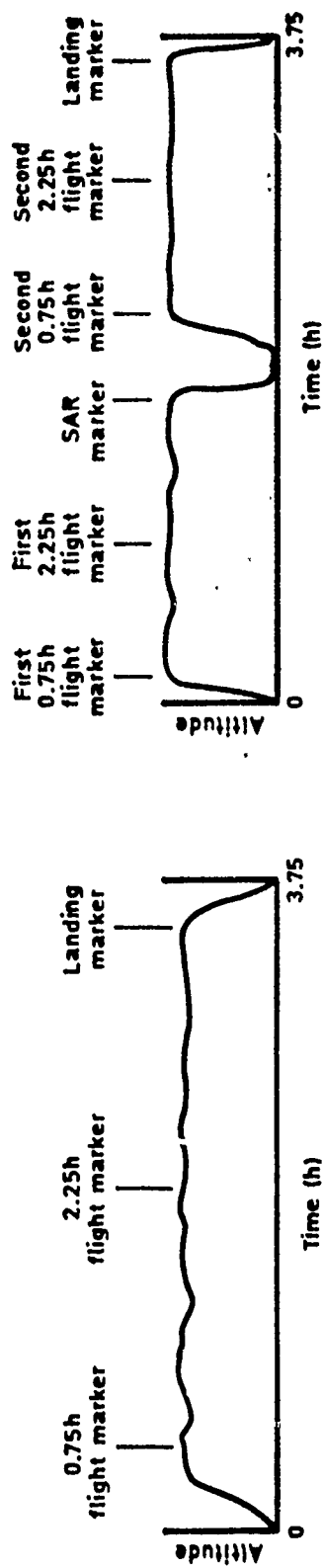


Fig 12 Variation of flight duration for Sea King ASW and SAR sorties

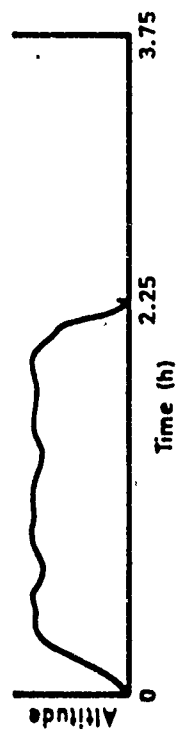
**Fig 13**



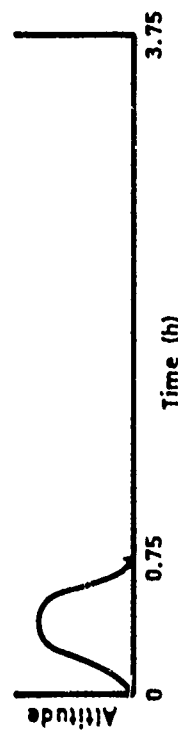
**Fig 13 Example of the load time history for the first phase of a training flight in Helix**



a Altitude profile for 3.75h flight

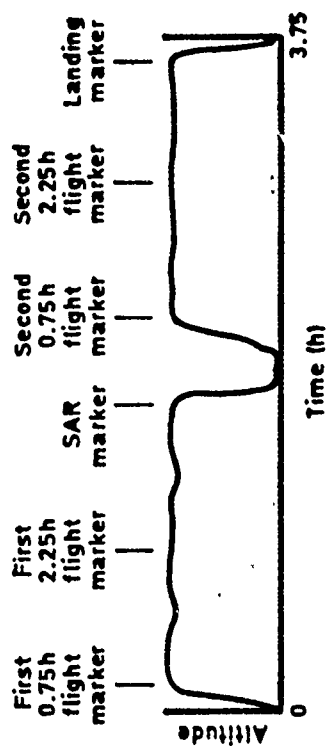


b Altitude profile for 2.25h flight

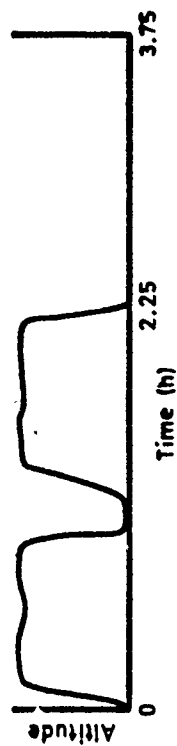


c Altitude profile for 0.75h flight

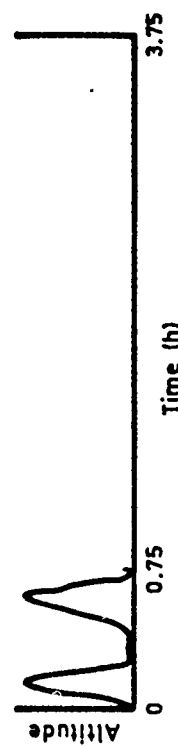
Fig 14 Example of the construction of the 0.75h and 2.25h transport training and ASW flights



a Altitude profile for 3.75h SAR flight



b Altitude profile for 2.25h SAR flight



c Altitude profile for 0.75h SAR flight

Fig 15 Example of the construction of the 0.75h and 2.25h SAR flights

Fig 16

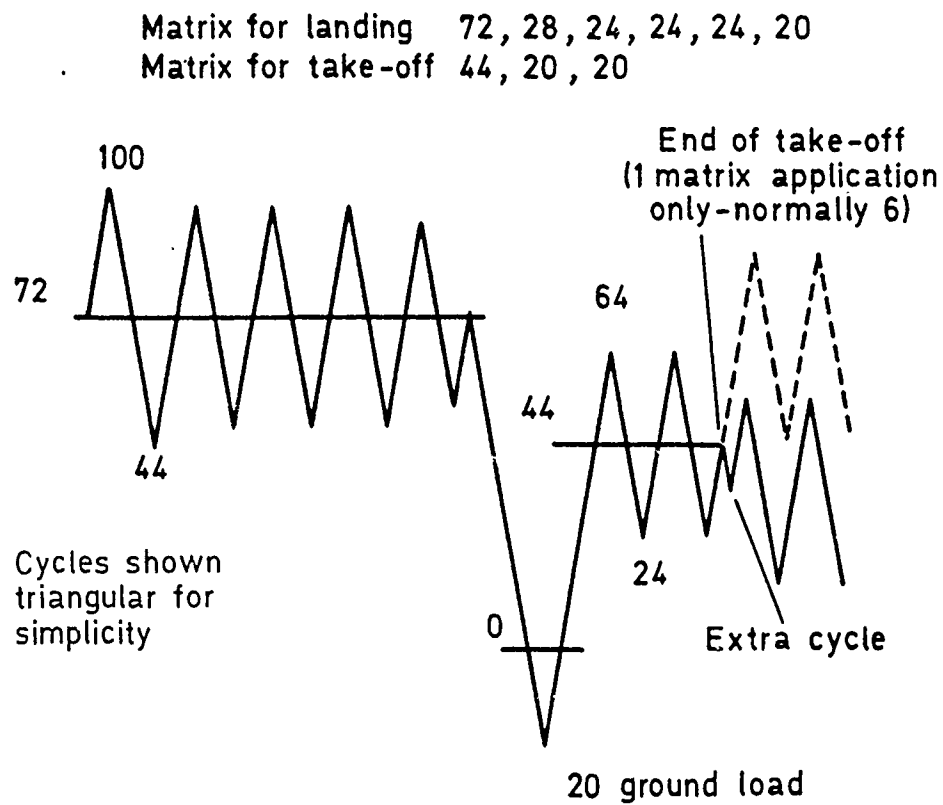


Fig 16 Landing/take-off sequence with alternative following loads

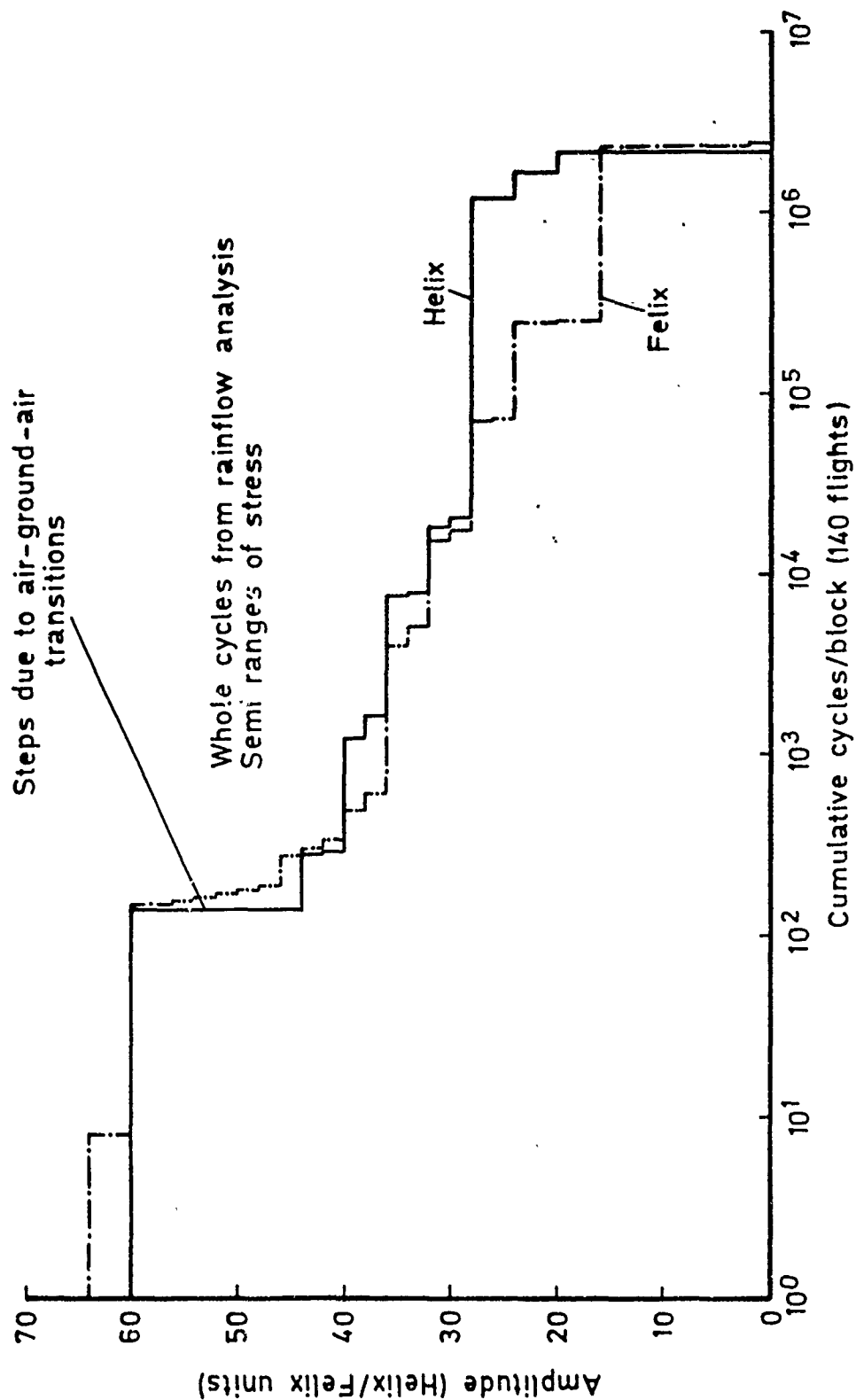


Fig 17 Comparison of Helix and Felix — whole cycles from rainflow analysis

Fig 18

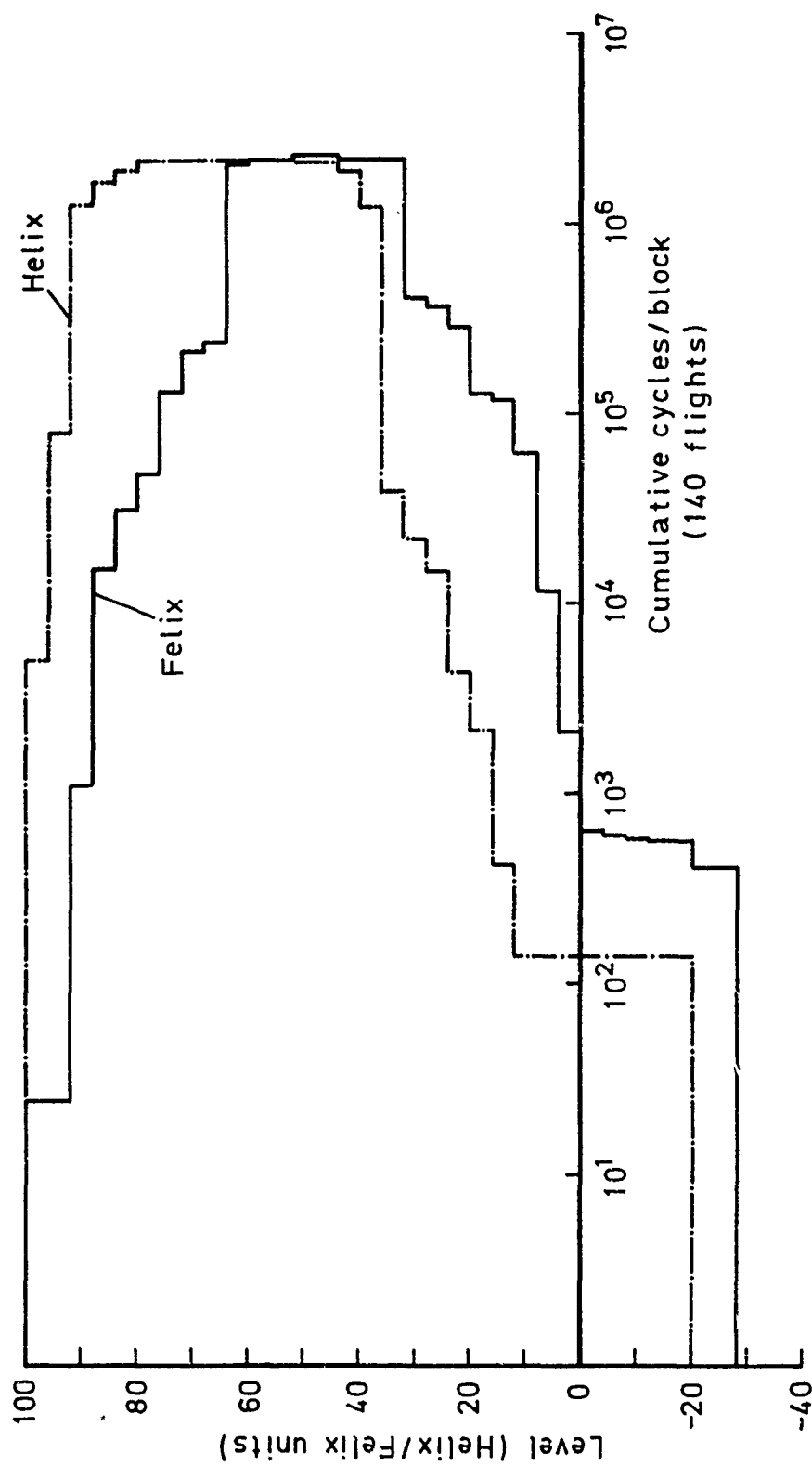


Fig 18 Comparison of Helix and Felix spectra — positive — going levels crossed

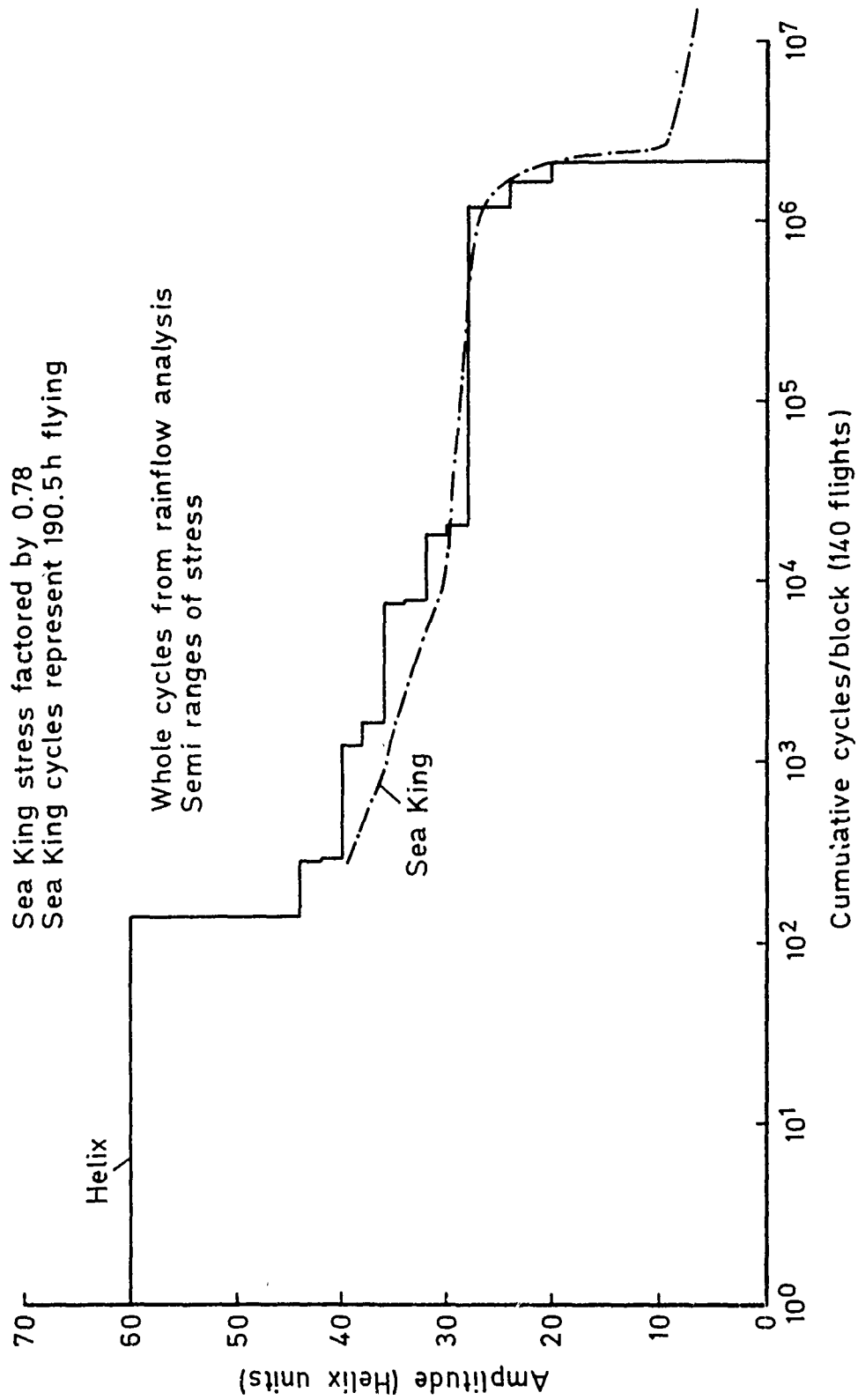


Fig 19 Comparison of Sea King transport spectrum with Helix

Fig 20

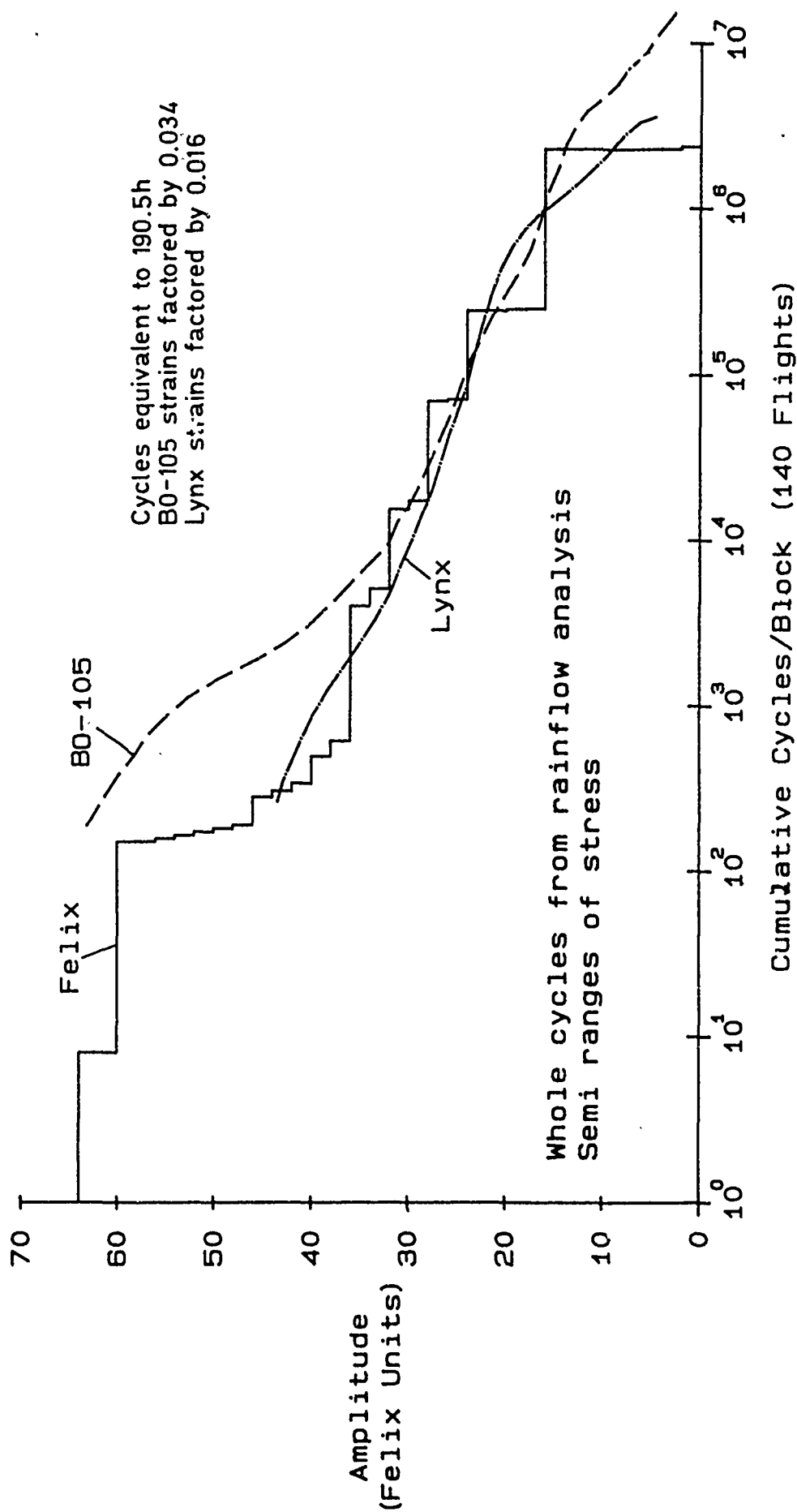


Fig 20 Comparison of Felix spectrum with those for BO-105 and Lynx

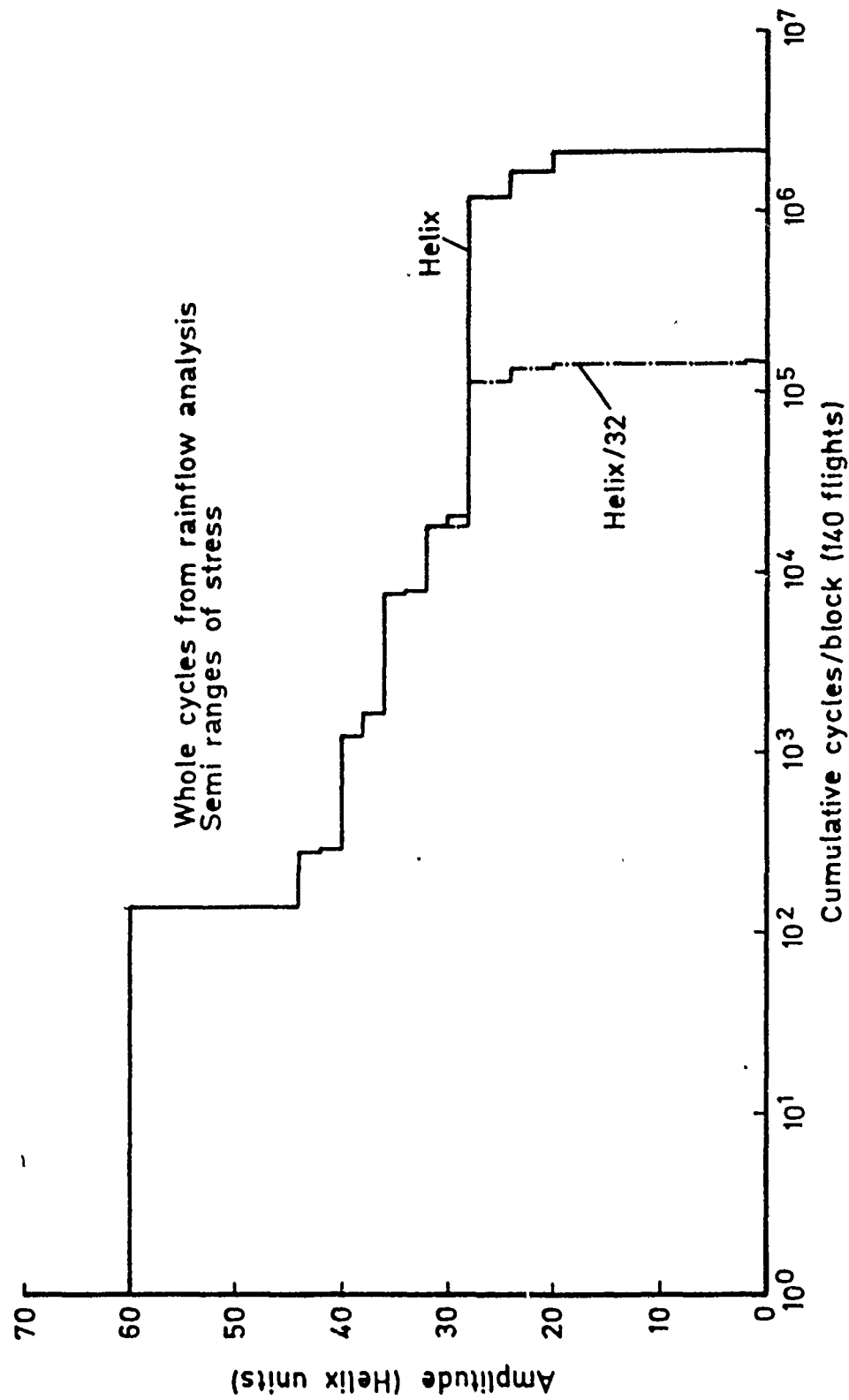


Fig 21 Comparison of spectra of Helix and Helix with omission level 32

Fig 22

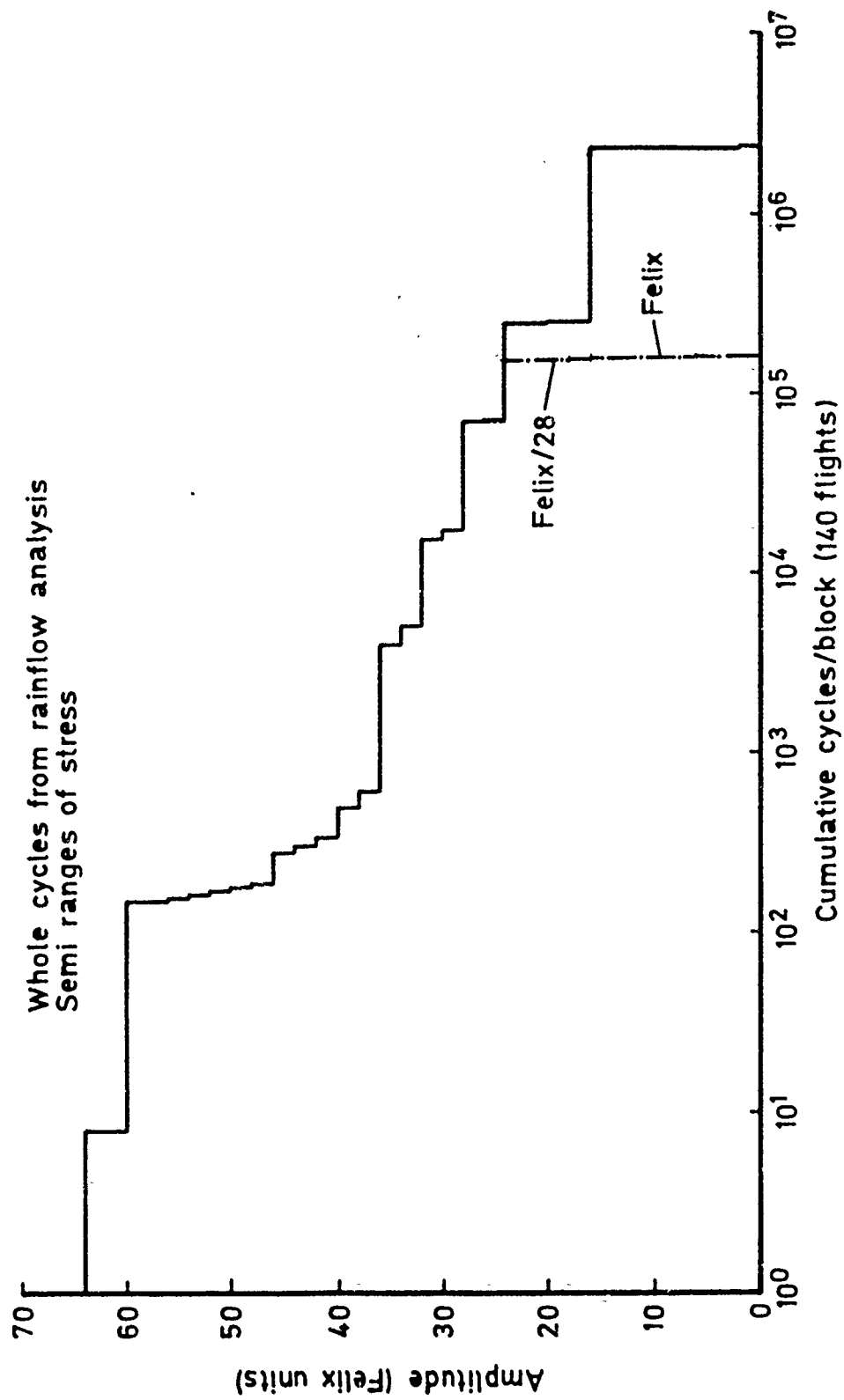
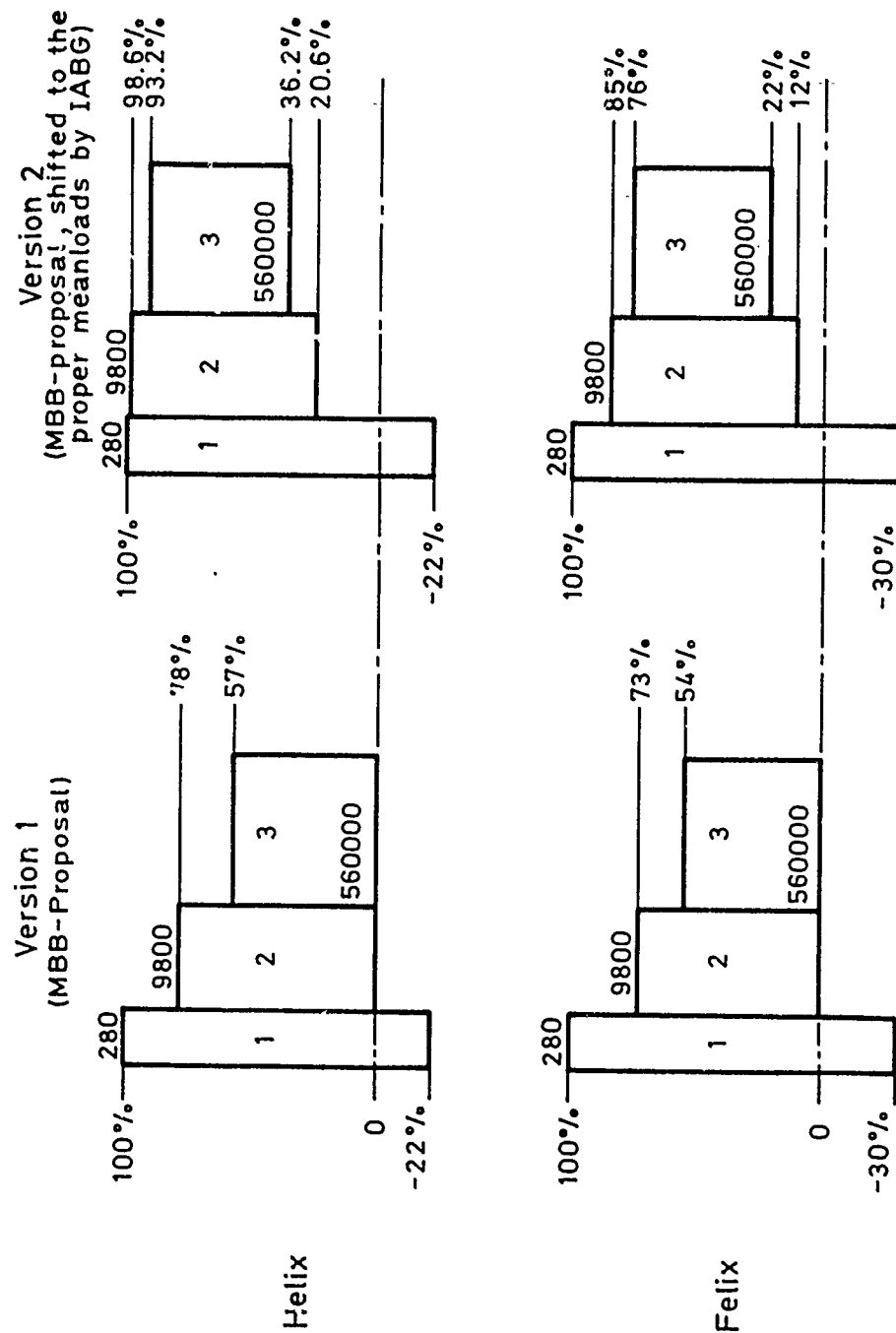


Fig 22 Comparison of spectra for Felix and Felix with omission level 28



Sequence 1-2-3-3-2-1-1-2 etc

Fig 23 Three level block — programmes — 140 flights each

Fig 24.

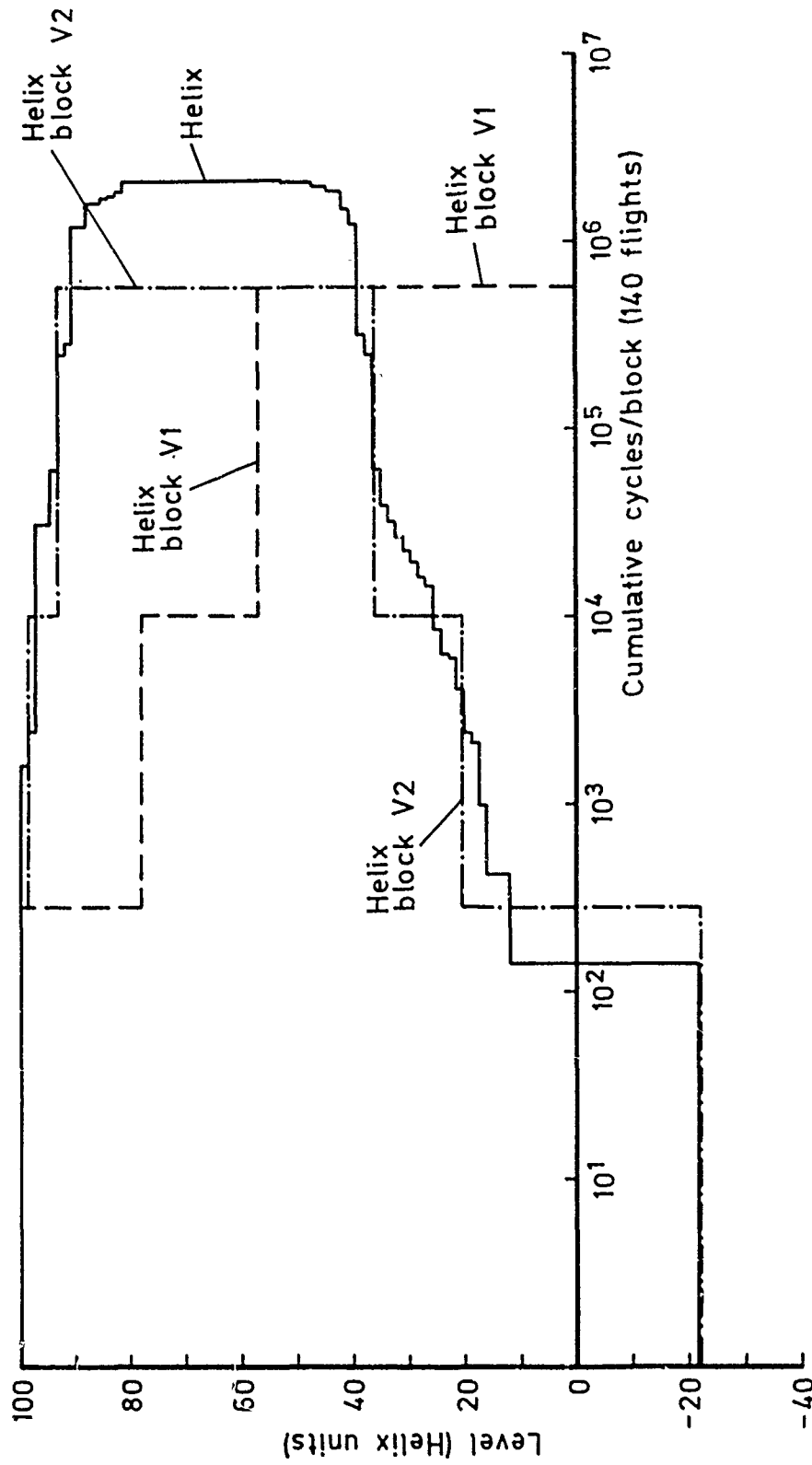


Fig 24 Comparison of Helix with Helix blocks V1 and V2 — positive going levels crossed

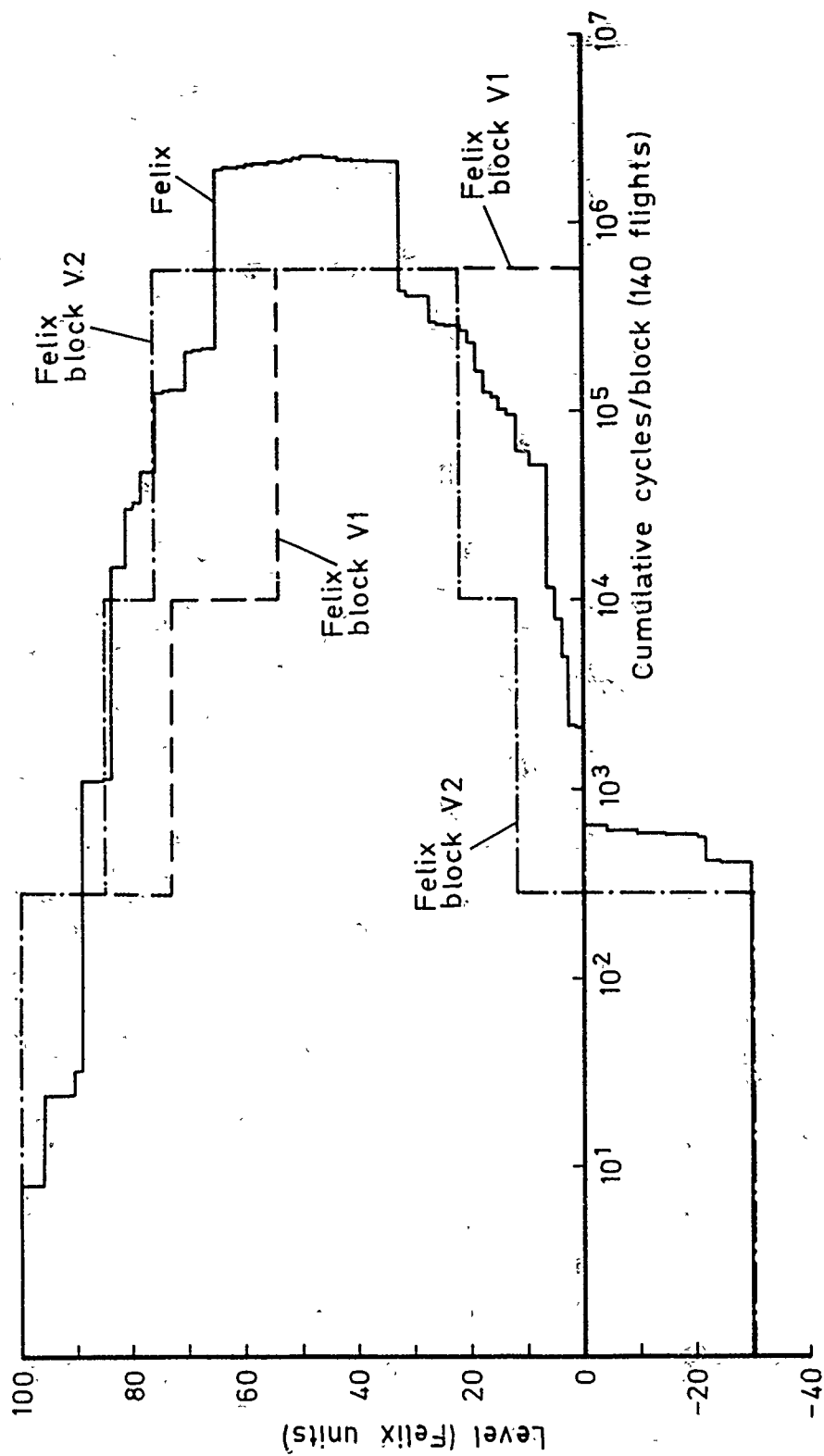
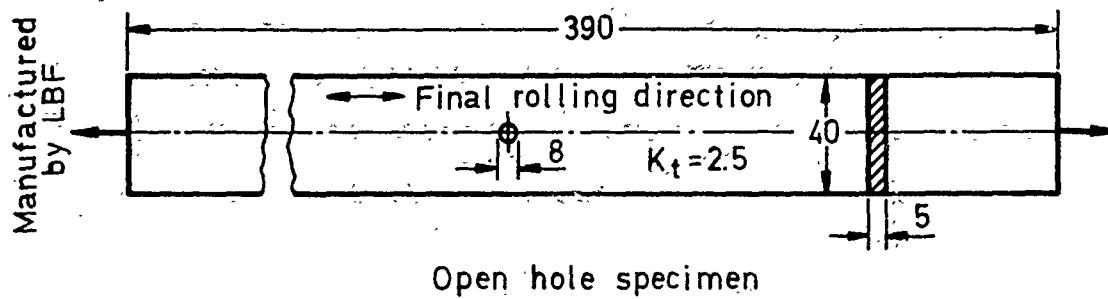


Fig 25 Comparison of Felix with Felix blocks V1 and V2 — positive going levels crossed

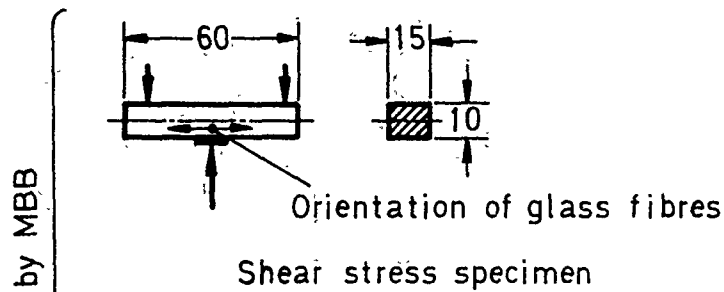
Fig 26a-c

Material: Al Cu Mg2 (Equivalent to 2024)



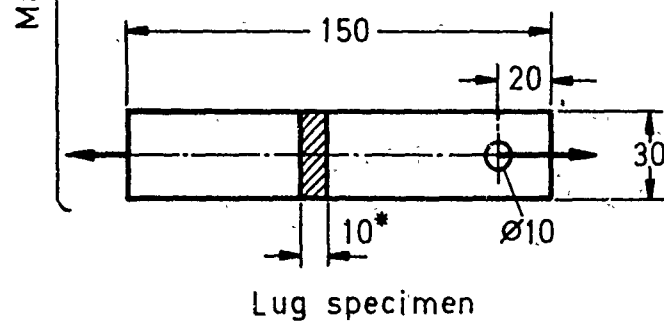
a)

Material: Unidirectional GRP



b)

Material: Multidirectional GRP



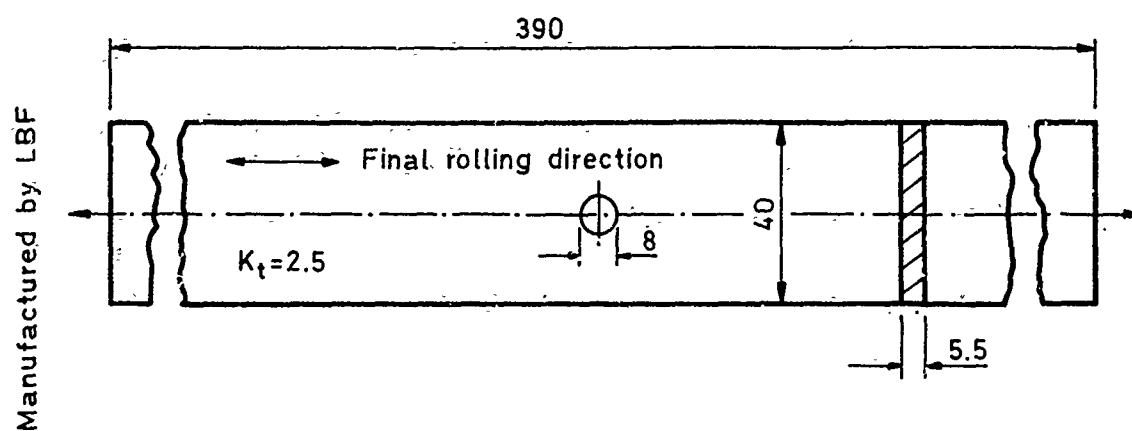
c)

Dimensions in mm

\* Second delivery: 8mm, but the same number of layers

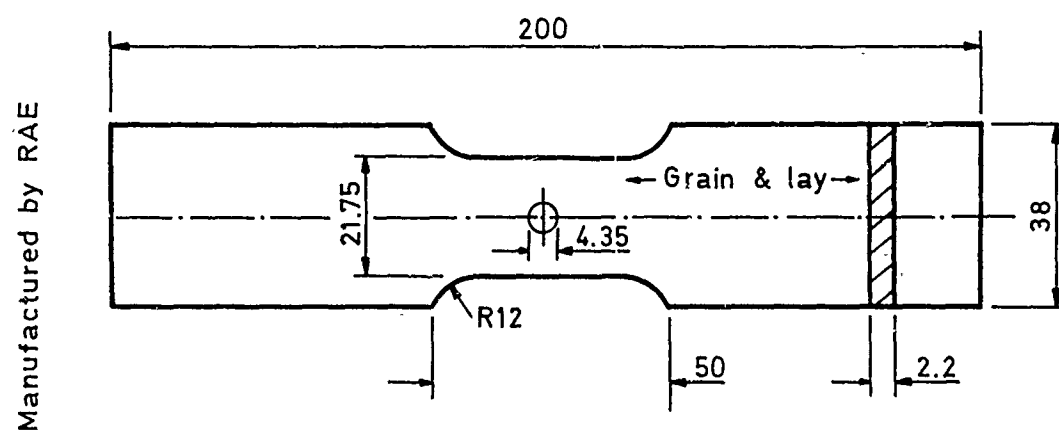
Fig 26a-c Test specimens used by IABG and LBF

Material Ti-6Al-4V



a) NLR specimens

Material Ti-6Al-4V



b) RAE specimens

Dimensions in mm

Fig 27a&amp;b Test specimens used by NLR and RAE

Fig 28

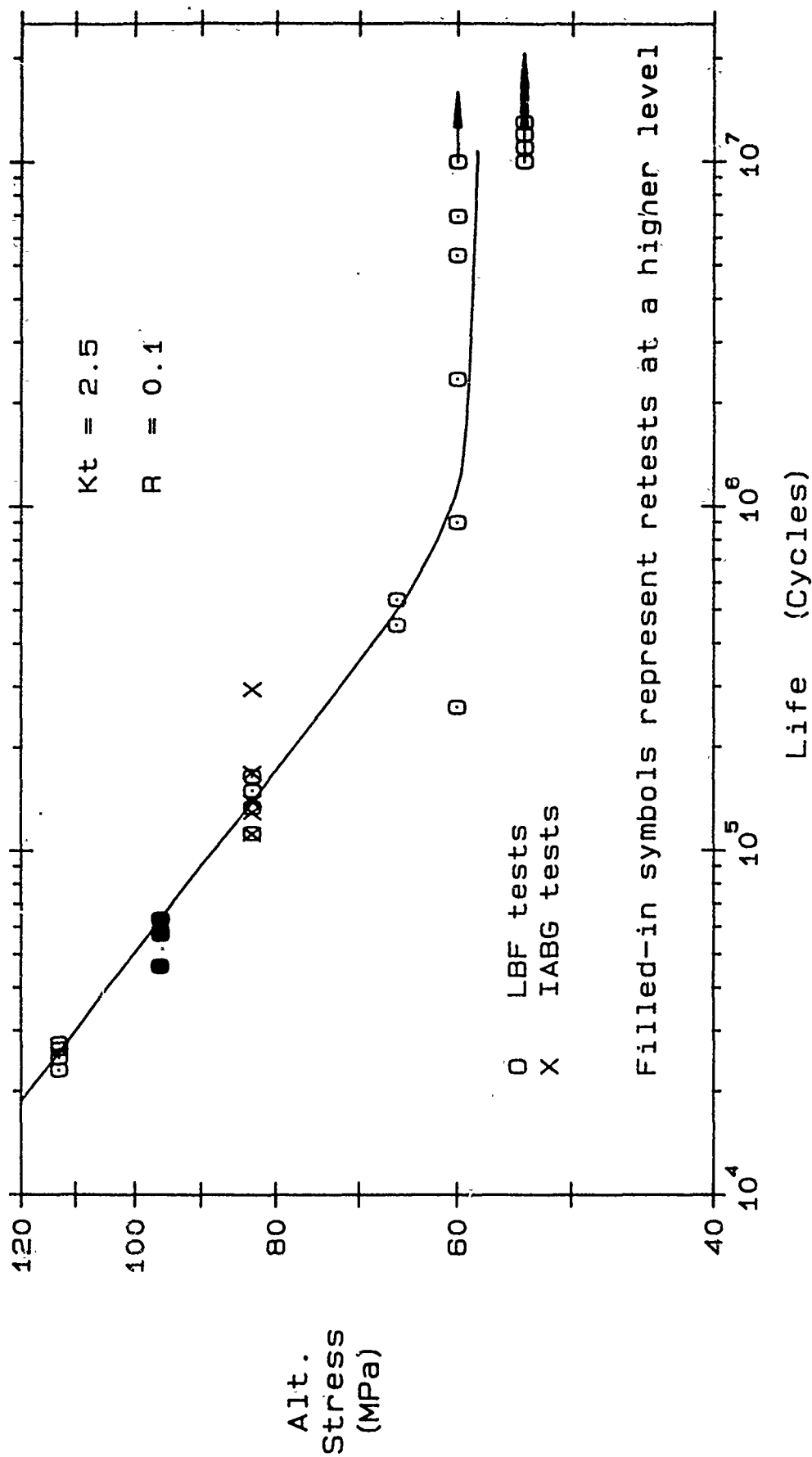


Fig 28 Constant amplitude tests on 3.1354-T3 aluminium alloy notched specimens

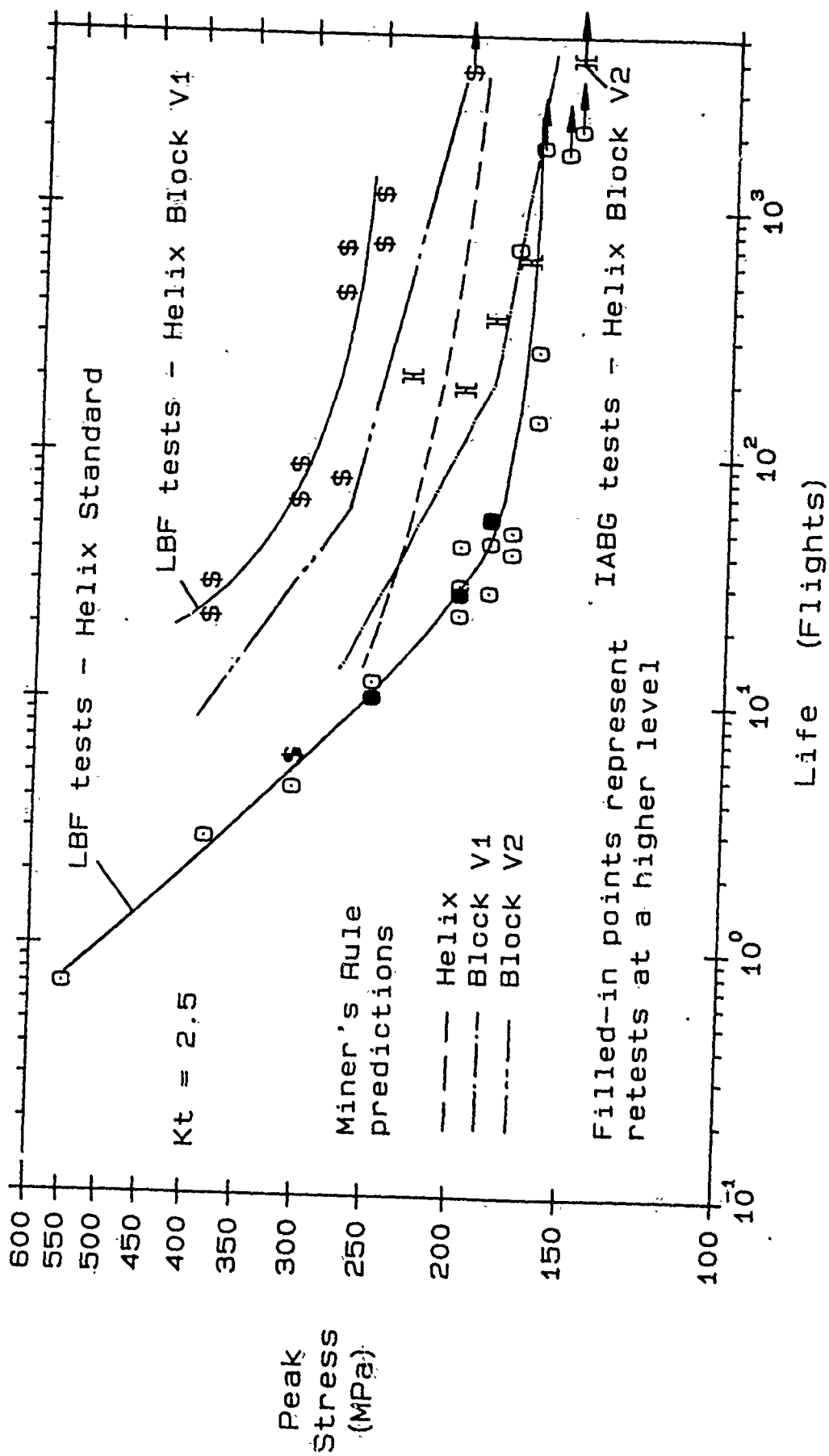


Fig 29 Helix and Helix block tests on 3.1354-T3 aluminium alloy notched specimens

Fig 30

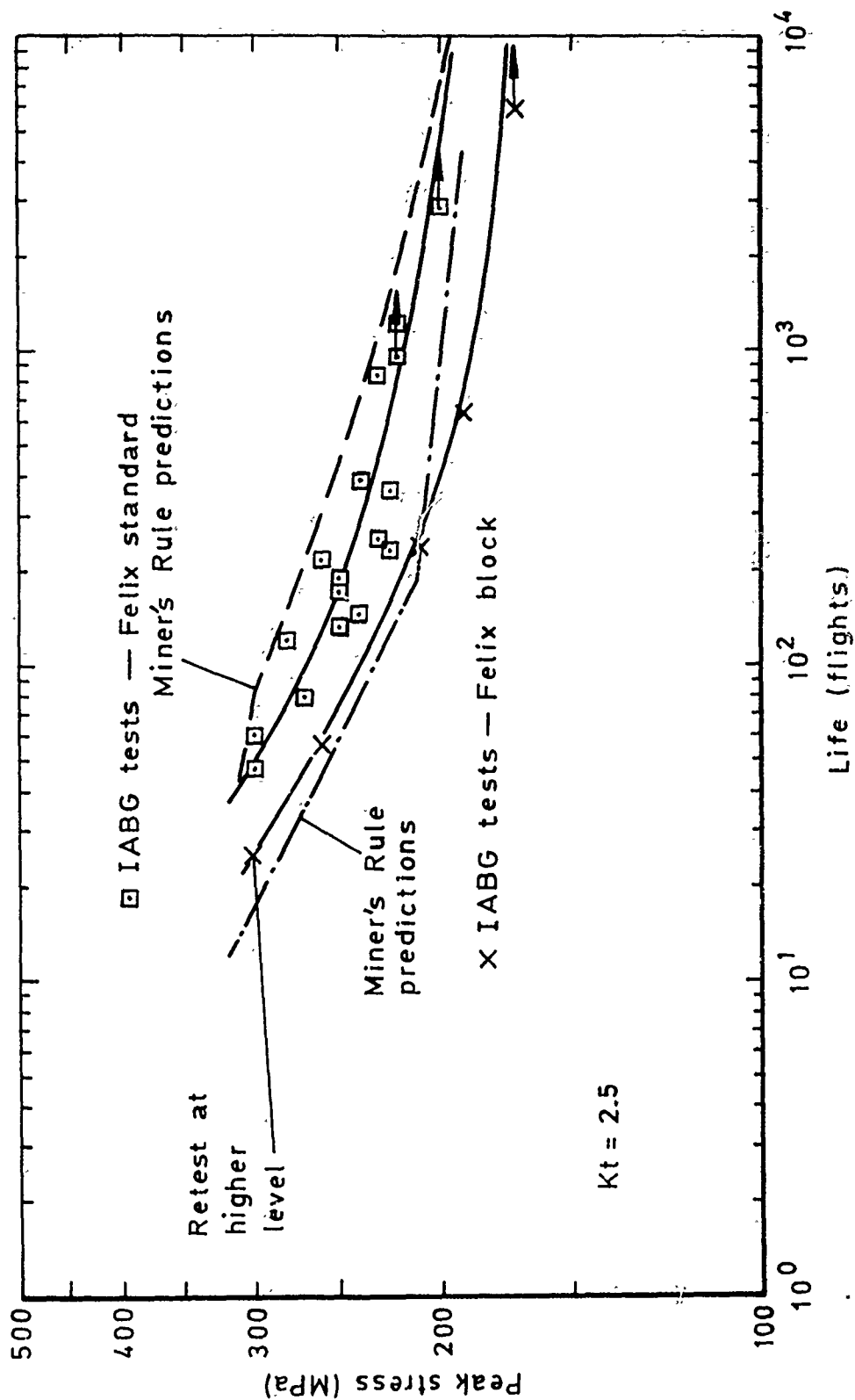


Fig 30 Felix and Felix block tests on 3.1354-T3 aluminium alloy notched specimens

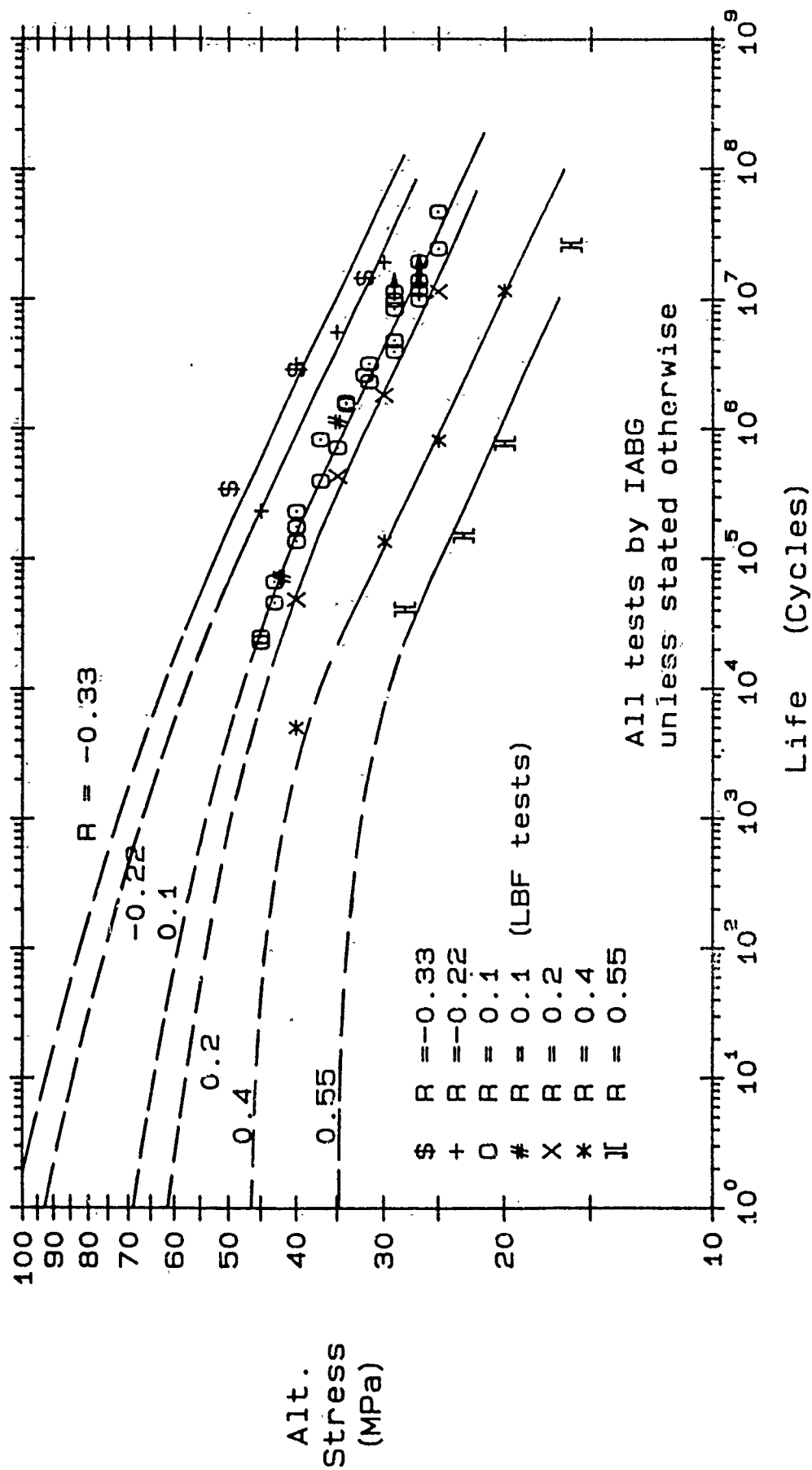


Fig 31 Constant amplitude tests on multidirectional GRP lug specimens

Fig 32

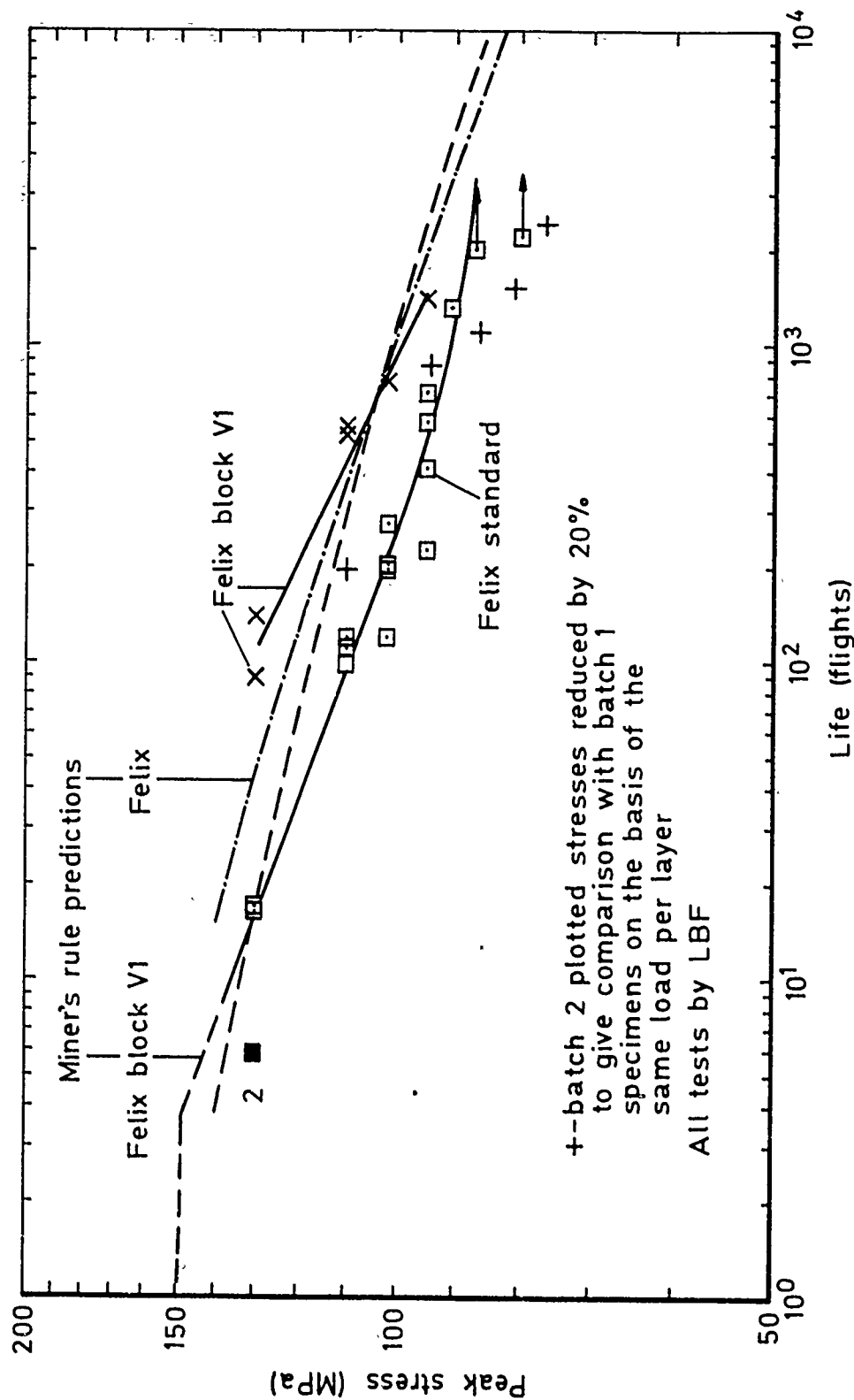


Fig 32 Felix and Felix block V1 tests on multidirectional GRP lug specimens

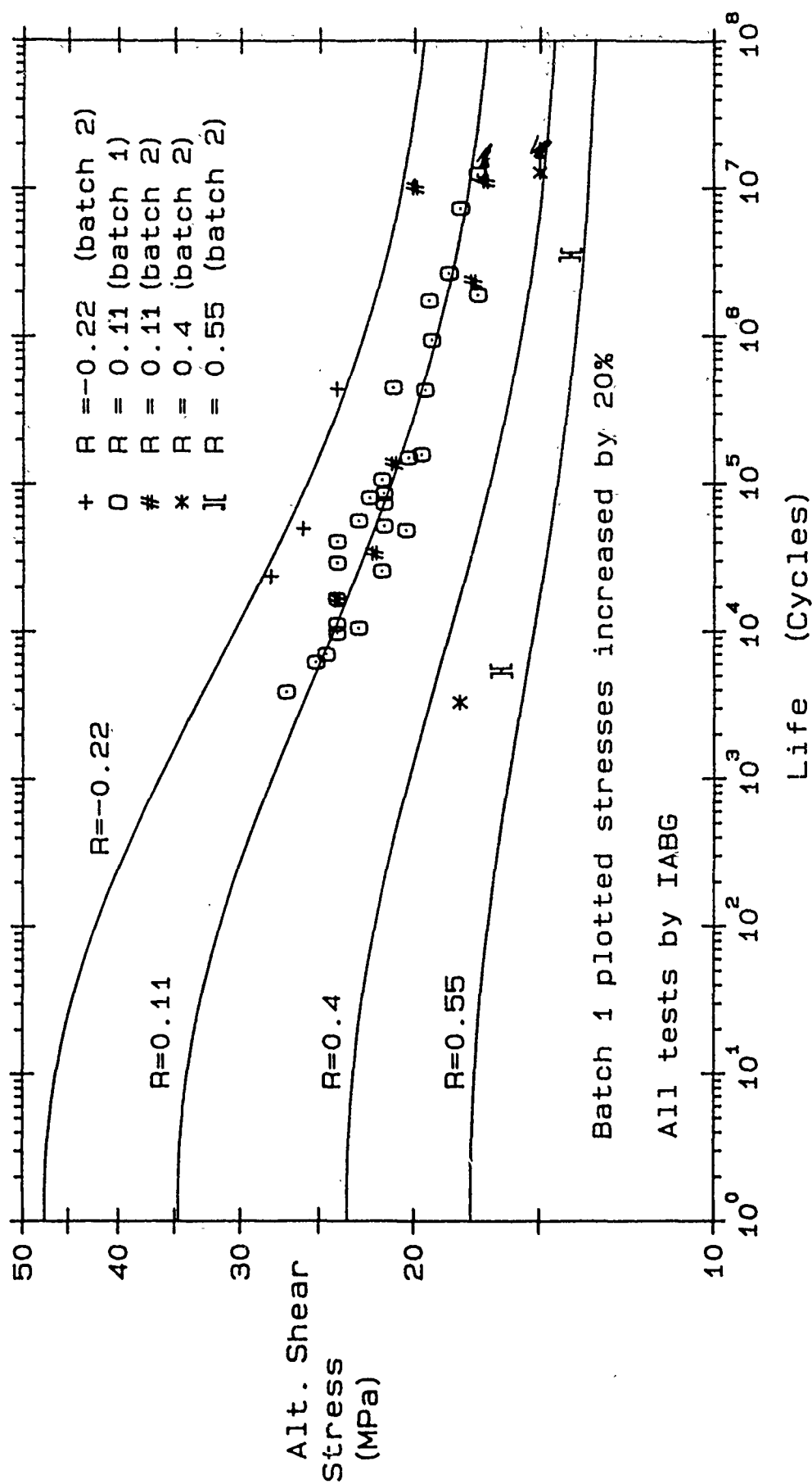


Fig 33 Constant amplitude tests on unidirectional GRP bend specimens

Fig 34

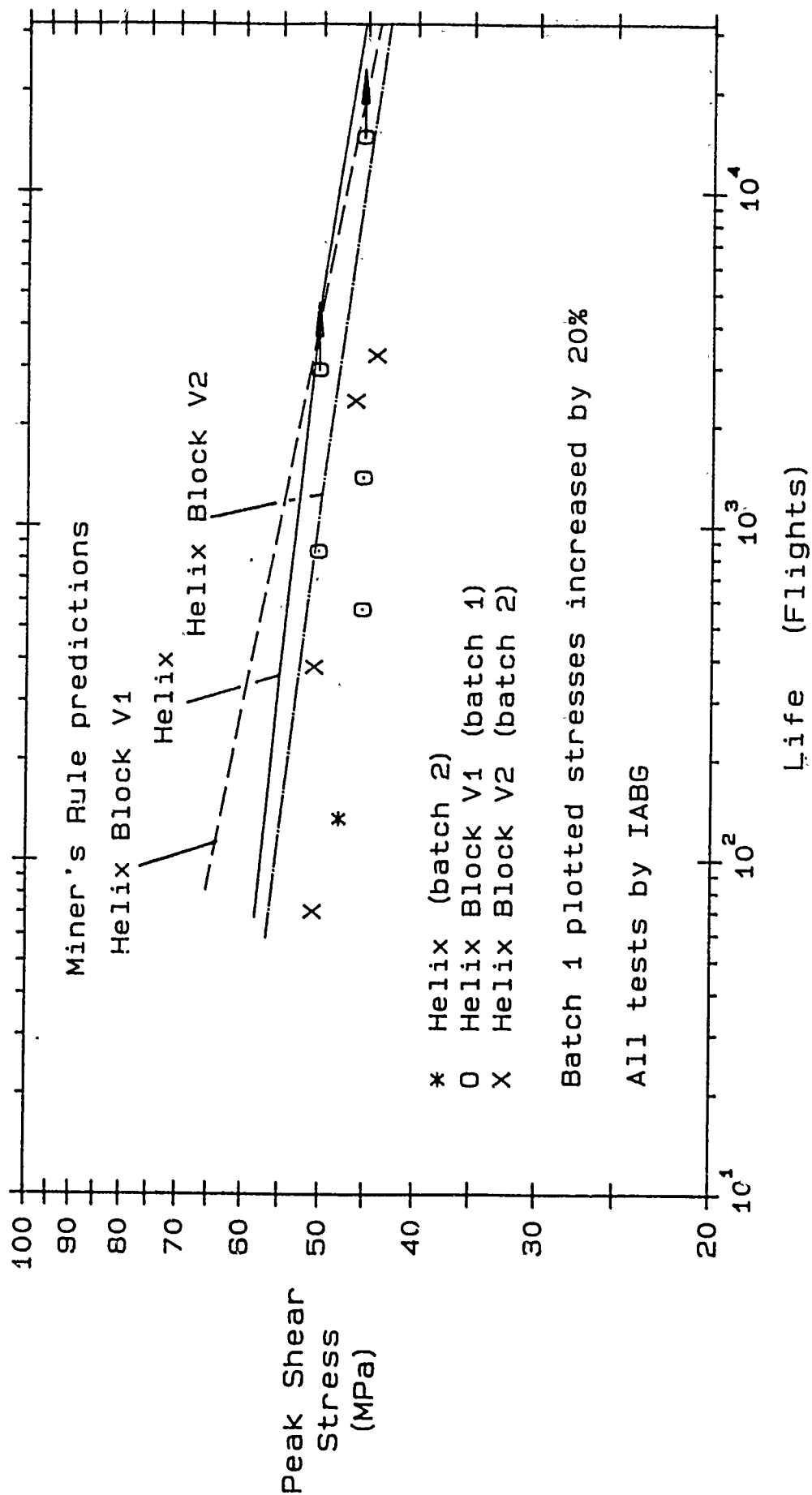


Fig 34 Helix and Helix block tests on unidirectional GRP bend specimens

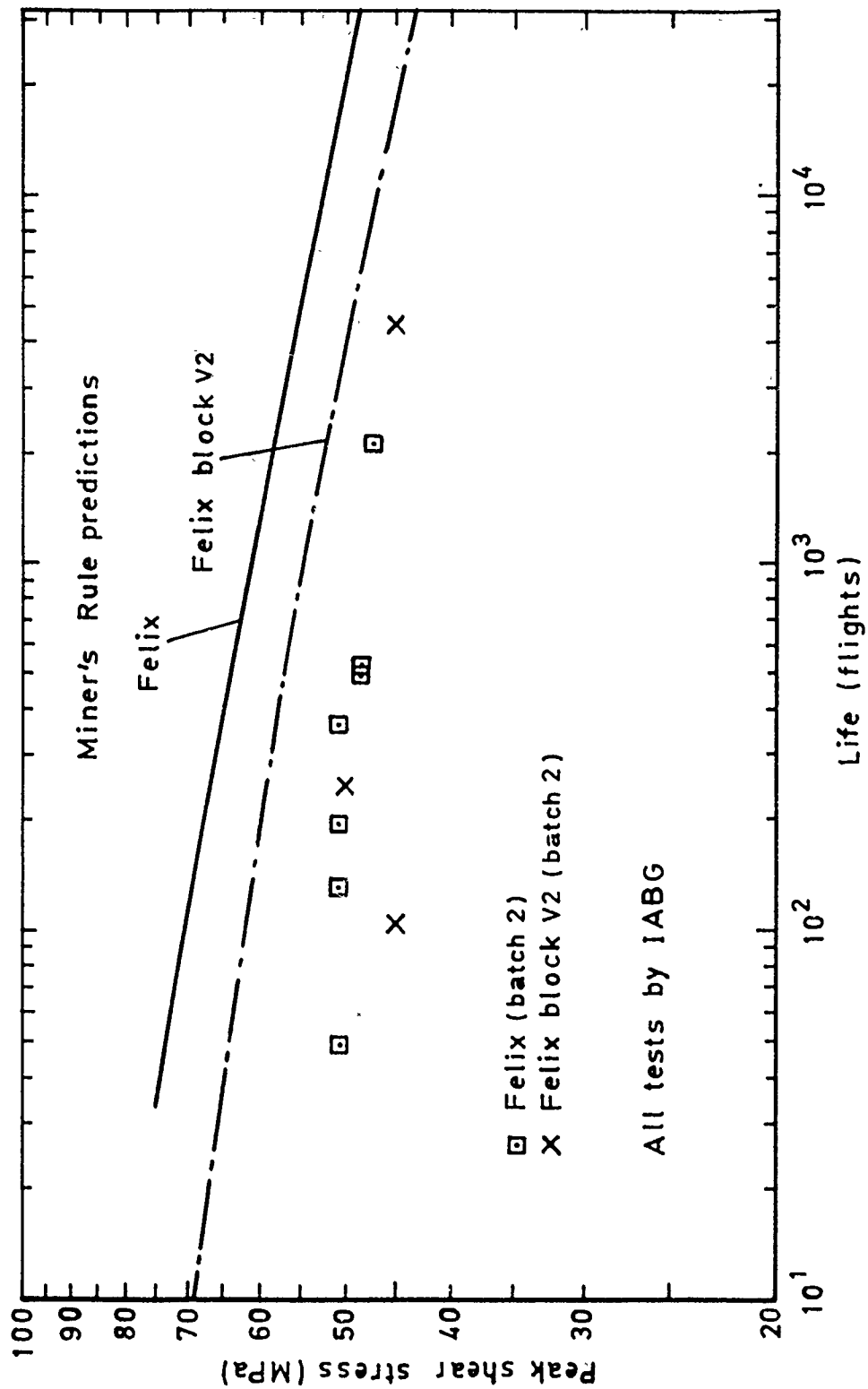


Fig 35 Felix and Felix block tests on unidirectional GRP bend specimens

Fig 36

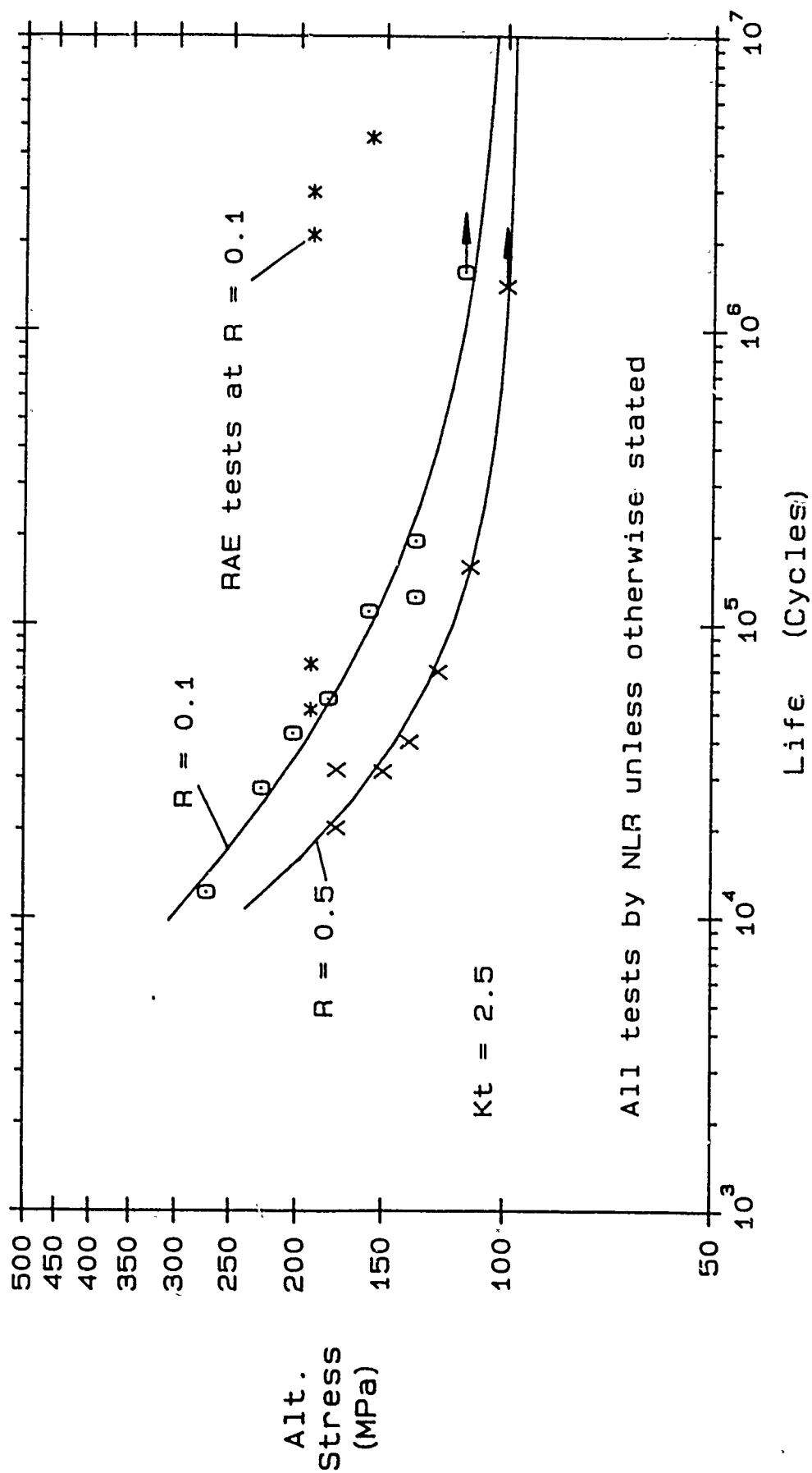


Fig 36 Constant amplitude tests on titanium alloy notched specimens

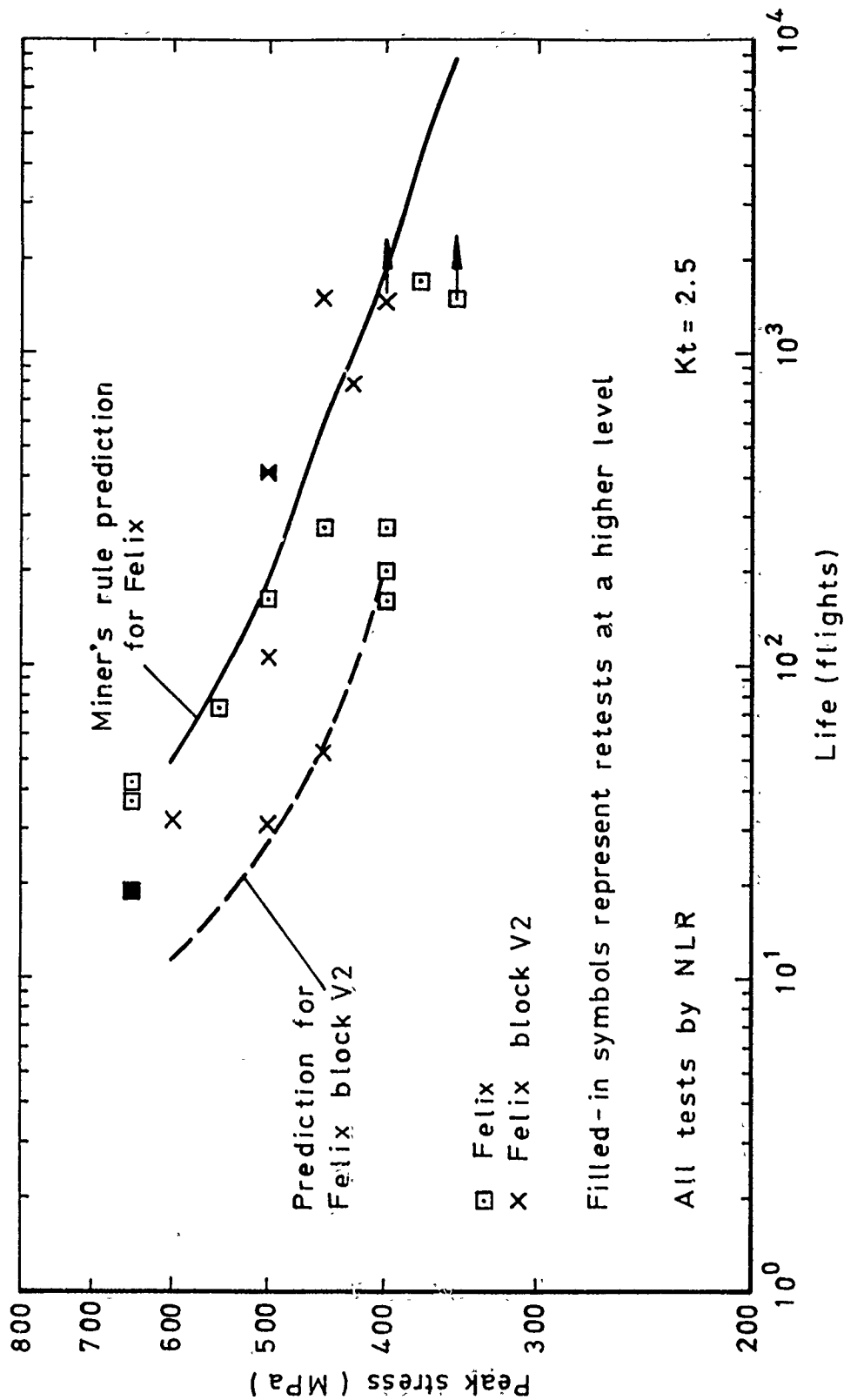


Fig 37 Felix and Felix block V2 tests on notched specimens of titanium alloy

Fig 38

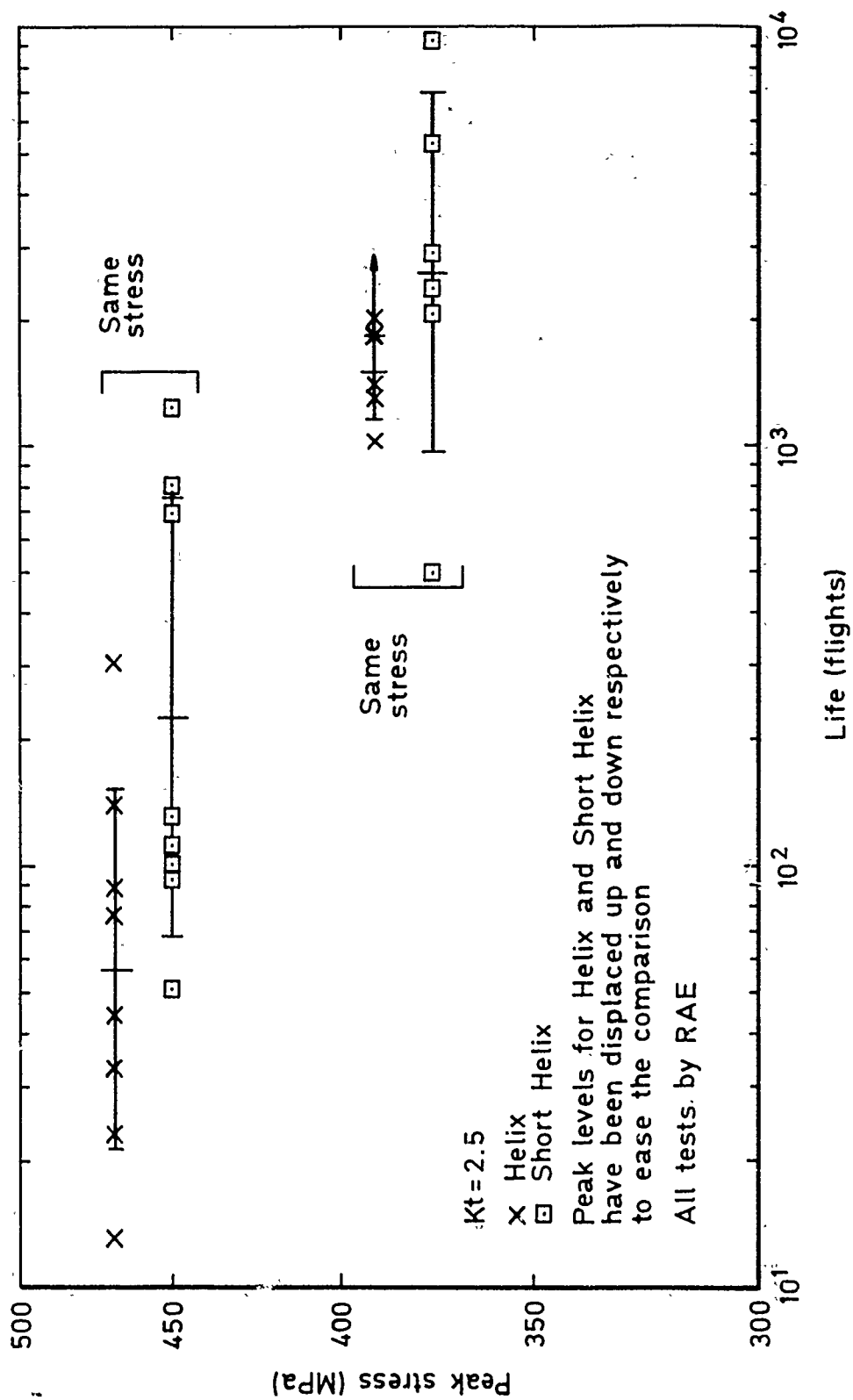
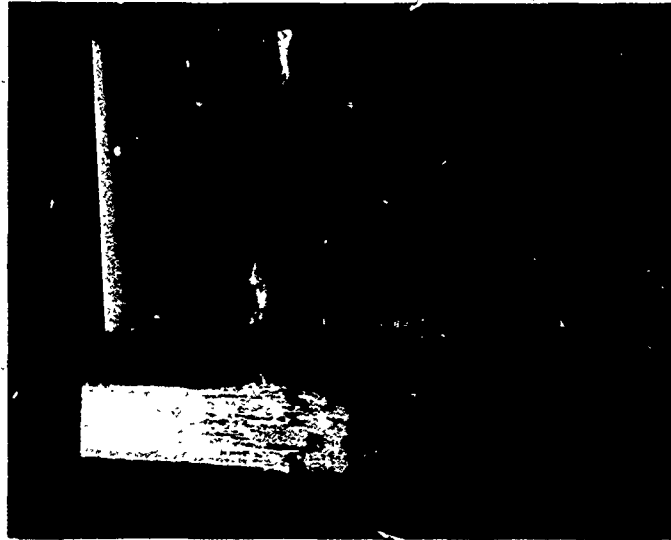


Fig 38 Helix and Short Helix tests on titanium alloy notched specimens

Fig 39a&b



a Lug



b Shear stress specimen

Fig 39a&b GFRP — fractures

Fig 40

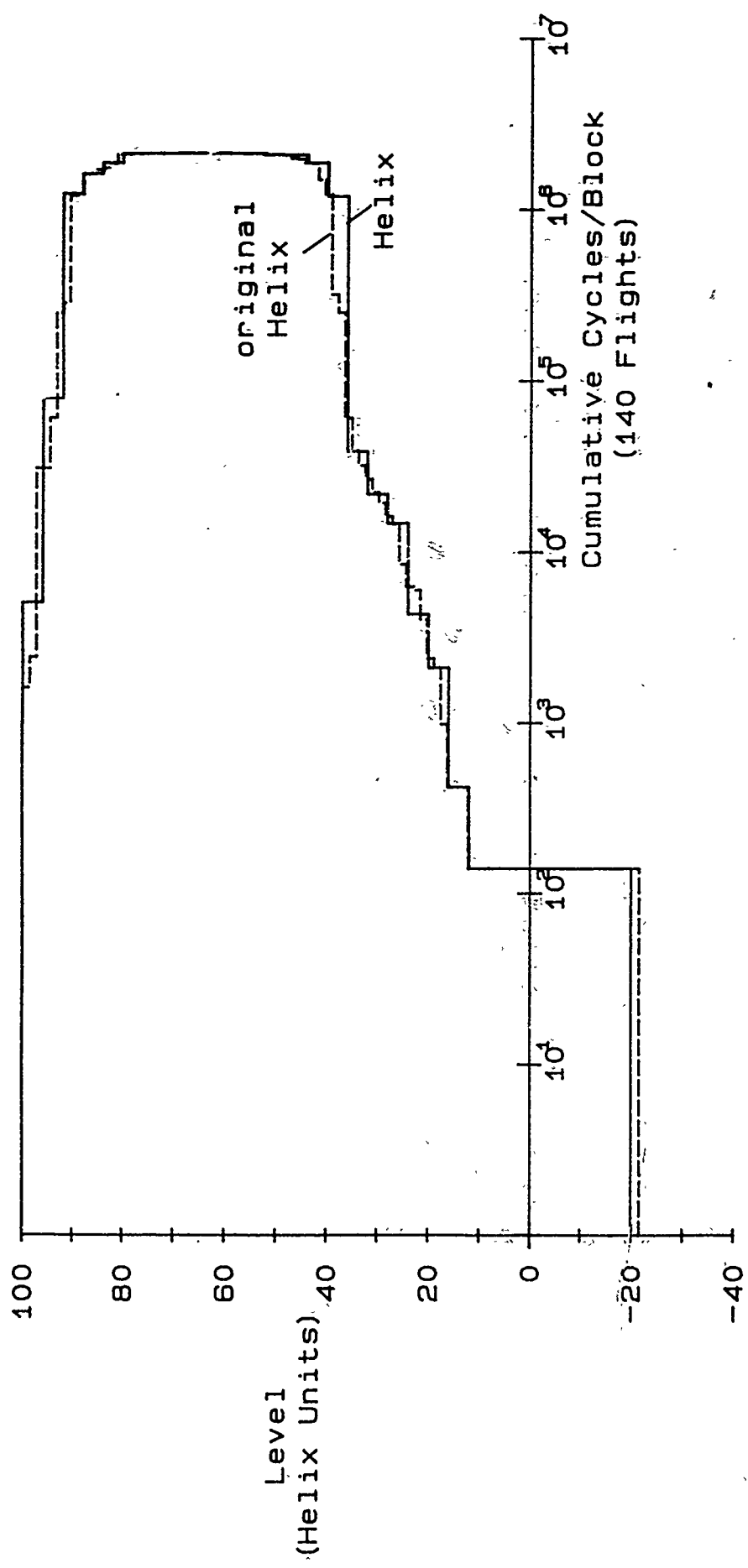


Fig 40 Comparison of Helix with original version of Helix — positive going levels crossed

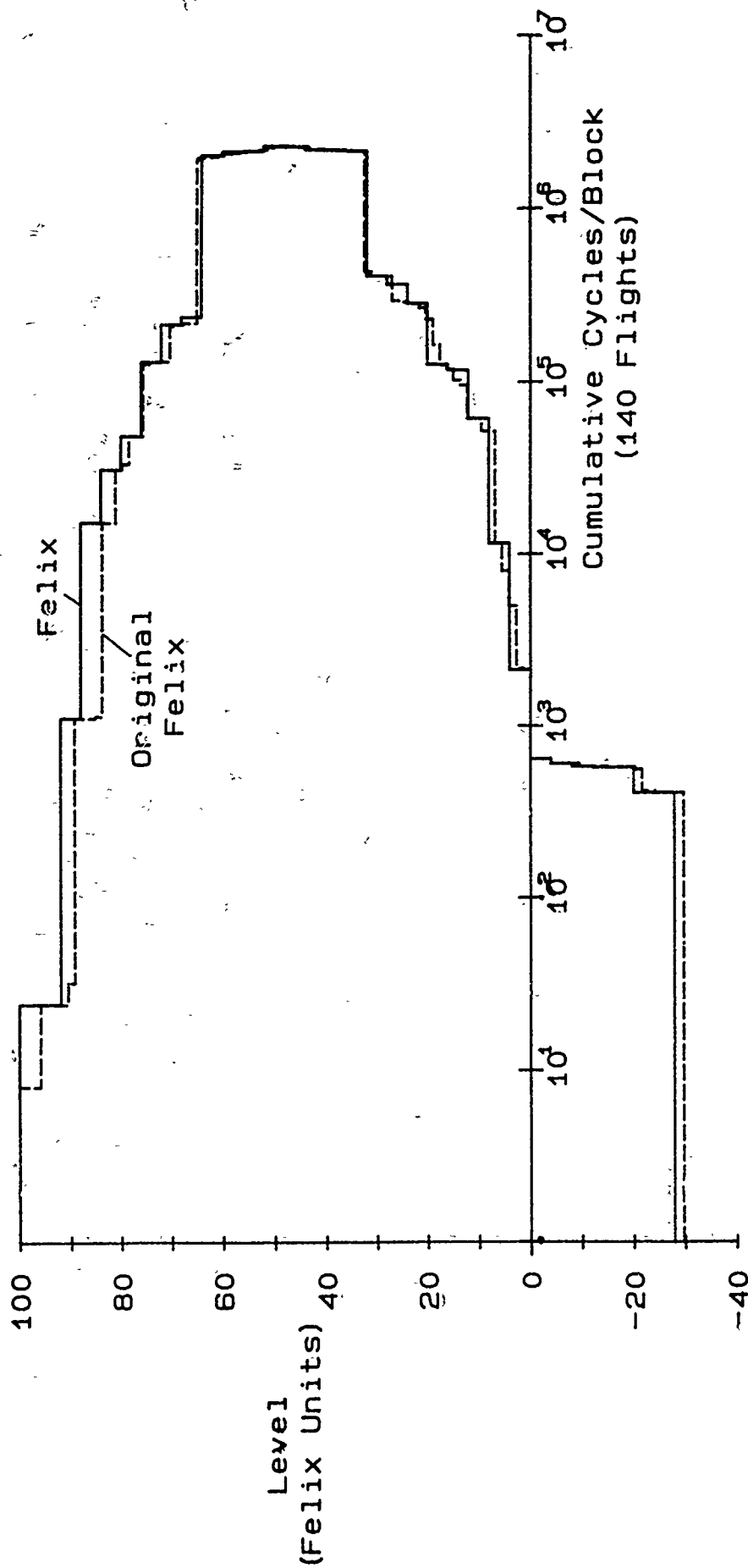


Fig 41 Comparison of Felix with original version of Felix — positive going levels crossed

## REPORT DOCUMENTATION PAGE

Overall security classification of this page

UNCLASSIFIED

As far as possible this page should contain only unclassified information. If it is necessary to enter classified information, the box above must be marked to indicate the classification, e.g. Restricted, Confidential or Secret.

1. DRIC Reference (to be added by DRIC)	2. Originator's Reference RAE TR 84084	3. Agency Reference N/A	4. Report Security Classification/Marking <b>UNLIMITED</b> UNCLASSIFIED		
5. DRIC Code for Originator 767300CW	6. Originator (Corporate Author) Name and Location Royal Aircraft Establishment, Farnborough, Hants, UK				
5a. Sponsoring Agency's Code N/A	6a. Sponsoring Agency (Contract Authority) Name and Location N/A				
7. Title Standardised fatigue loading sequences for helicopter rotors (Helix and Felix) Part 1: Background and fatigue evaluation					
7a. (For Translations) Title in Foreign Language					
7b. (For Conference Papers) Title, Place and Date of Conference					
8. Author 1 Surname, Initials Edwards, P.R.	9a. Author 2 Darts, J.	9b. Authors 3, 4 ....	10. Date August 1984	Pages 112	Refs. 24
11. Contract Number N/A	12. Period N/A	13. Project	14. Other Reference Nos. Materials & Structures 101		
15. Distribution statement (a) Controlled by –  (b) Special limitations (if any) –					
16. Descriptors (Keywords) (Descriptors marked * are selected from TEST)					
17. Abstract Helix and Felix are standard loading sequences which relate to the main rotors of helicopters with articulated and semi-rigid rotors respectively. The purpose of the loading standards is, first, to provide a convenient tool for providing fatigue data under realistic loading, which can immediately be compared with data obtained by other organisations. Second, loading standards can be used to provide design data. This Report is the first of the two final project reports and describes the background to the definition of Helix and Felix, statistical content according to different counting methods and the results of fatigue tests used to assess them. Full information on generating Helix and Felix is not given in this Report, but is provided in Part 2.  Also published as NLR Report No. TR 84043U Pt 1 LBF Report No. FB-167 Pt 1 IABG Report No. TF-1425/1					